THE ROLE OF PERILIPIN IN MURINE PERITONEAL MACROPHAGES

Mag.Eleonore Alexandra Rathke
Institute of Molecular Biology and Biochemistry
Center of Molecular Medicine, Medical University of Graz

Dissertation submitted at the Medical University of Graz
for the degree of Doctor of medical sciences (Dr.scient.med.)

Graz, December 2009

Acknowledgement

This doctoral thesis was performed at the Institute of Molecular Biology and Biochemistry at the Medical University of Graz and was supported by the Austrian Science Fund FWF (P19186). I would like to thank my supervisor Prof.Dr.Dagmar Kratky for the possibility of carrying out this thesis in her group and for my personal advancement thanks to her critical guidance. Furthermore I express my thanks Prof. Gerhard Kostner for his supporting encouragement and cooperation.

My special thanks go to Marlene Buchebner, Prakash Chandak and Jay Patankar for their amicable, mental support.
I would also like to say thank you to Anton Ibovnik and Silvia Povoden, Isabella and Fiona as well as Dagmar Silbert for their helpful assistance.

My innermost thanks go to my parents and my friends, who have been a very strong support in times of hard challenge.

For my parents and that challenging part of myself which is hopefully satisfied now

“Don’t hesitate in just that moment, when your way seems infinite and, suddenly, nothing seems to work out as you wish”

Dag Hammarskjöld

Affidavit

I thereby declare that this doctoral thesis has been written independently and completely on my own and without any assistance from third parties. Furthermore, I confirm that no sources have been used in the preparation of this thesis other than those indicated in the thesis itself.

Graz, December 2009

_____
Mag.Eleonore Alexandra Rathke

Summary

All eukaryotic cells exhibit the characteristic to store lipids in cytosolic lipid droplets (LD). Whereas the LD of adipocytes constitute the body's energy depot, the LD of other cells predominantly provide lipids for membrane synthesis. The management of cellular lipid storage is particularly important in non-adipose tissue with regard to the development of several metabolic diseases, in particular atherosclerosis. In this disease, macrophages take up lipids in an uncontrolled manner. Members of the perilipin/adipophilin/Tip47 (PAT) protein family manage the storage of lipids in cells of all tissues and many of the PAT proteins found in adipocytes were also detected in macrophages. While perilipin (Plin) is the predominant PAT protein in adipocytes, adipophilin (Adrp) is the predominant PAT protein in macrophages. The presence of Plin in foam cells of human atherosclerotic plaques has drawn new attention to a possible role for this protein also in macrophages. Therefore I investigated the consequences of Plin deficiency on lipid metabolism of mouse peritoneal macrophages.

One of the key findings of the current thesis was that loading of Plin (-/-) macrophages with VLDL for 24 hours, led to smaller LD compared to wild type cells. However this was not reflected by a different lipid content. Neutral as well as acidic triglyceride hydrolase activity or neutral cholesteryl ester hydrolase activities were also not different between wild type and Plin (-/-) macrophages and foam cells. Cpt-1α mRNA expression was significantly increased in Plin (-/-) foam cells but free fatty acid release was not different compared to wild type foam cells. FFA uptake as well as LPL activity were the same in wild type and Plin (-/-) foam cells and macrophages, respectively. The second key finding was that Plin deficiency was atheroprotective in female Plin(-/-)/apoE(-/-) mice after 8 weeks WTD, reflected by 42 % decreased atherosclerotic plaques compared to apoE (-/-) mice and a 50% decreased hepatic TG concentration. After 6 months WTD, Plin (-/-) mice had massive liver steatosis compared to wild type mice, whereas female Plin (-/-) mice were better protected from steatosis compared to male mice.

Although Plin is expressed to a low extent in macrophages, its deficiency impacts LD morphology in foam cells. In female apoE (-/-) mice, Plin deficiency was atheroprotective during 8 weeks WTD feeding but had no preventive effect with regard to the development of liver steatosis during 6 months WTD. To what extent Plin expression in macrophages contributes to foam cell formation and thus possibly to atherogenesis remains to be determined. However, its expression possibly depends on the inflammatory milieu and/or lipid mediators which are present in atherosclerotic plaques thereby restricting its expression to certain metabolic conditions.

Zusammenfassung

Alle eukaryontischen Zellen können Lipide in Form cytosolischer Lipidtröpfchen (LD) speichern. Während die LD von Adipozyten das Energiereservoir des gesamten Körpers darstellen, dienen die LD in den Zellen der meisten anderen Gewebe hauptsächlich dazu, Lipide für die laufende Membranbiosynthese zur Verfügung zu stellen. Im Hinblick auf die Entstehung von metabolischen Krankheiten, wie zum Beispiel Atheriosklerose, ist die Kontrolle über die zelluläre Lipidspeicherung in nicht-Fettgewebe von besonderer Bedeutung. Bei dieser Krankheit nehmen Makrophagen Lipide unkontrolliert auf. Mitglieder der Perilipin/Adipophilin/Tip47 (PAT) Protein Familie kontrollieren die Lipidspeicherung in Zellen aller Gewebe und viele der PAT Proteine, die man aus Adipozyten kennt, werden auch in Makrophagen exprimiert. Während Perilipin (Plin) das hauptsächlich vorkommende PAT Protein in Adipozyten ist, ist es adipophilin (Adrp) in Makrophagen. Die Tatsache dass Perilipin in Schaumzellen aus humanen atherosklerotischen Plaques gefunden wurde hat die Aufmerksamkeit auf eine mögliche Rolle des Proteins in Makrophagen gelenkt. Daher untersuchte ich die Auswirkungen des Fehlens von Perilipin auf den Lipidmetabolismus von murinen Peritonealmakrophagen.

Eines der key findings der vorliegenden Arbeit war, dass die Beladung von Plin (-/-) Makrophagen mit VLDL für 24 Stunden verglichen mit Wildtyp Schaumzellen in kleineren LD resultierte. Unterschiede im Lipidgehalt von Schaumzellen konnten aber nicht gefunden werden, auch nicht in der Aktivität neutraler und saurer Triglyceridhydrolasen oder neutraler Cholesterinesterhydrolasen. Plin (-/-) Schaumzellen zeigten zwar eine signifikant erhöhte expression der Cpt-1α mRNA, jedoch war die Freisetzung von freien Fettsäuren nicht unterschiedlich zu der von Wildtypzellen ebenso wie der uptake freier Fettsäuren oder die LPL-Aktivität. Das zweite key finding war, dass sich das Fehlen von Perilipin atheroprotektiv auswirkt. Weibliche Plin(-/-)/apoE(-/-) Mäuse hatten um 42% geringere atherosklerotische Plaques und 50% reduzierte hepatische Triglyceridwerte im Vergleich zu apoE (-/-) Mäusen nach 8 Wochen westlicher Diät (WTD). Nach 6 Monaten WTD konnte ich in Plin (-/-) Mäusen massive Lebersteatose im Vergleich zu Wildtypmäusen in beiden Geschlechtern beobachten. Weibliche Mäuse waren aber offensichtlich besser gegen Steatose geschützt als männliche.

Obwohl Plin nur in sehr geringem Ausmaß in Makrophagen exprimiert ist, beeinträchtigt sein Fehlen die LD Morphologie in Schaumzellen. Plin war atheroprotektiv nach 8 Wochen WTD. Keinen protektiven Effekt hatte das Fehlen von Plin hinisichtlich der Entstehung von Lebersteatose nach 6 Monaten WTD. In welchem Ausmaß Plin in Makrophagen die Schaumzellbildung und damit eventuell auch die Entstehung von Atheriosklerose beeinflusst, bleibt unklar. Seine Expression hängt möglicherweise von einem Entzündungsmilieu ab und/oder Entzündungsmediatoren, die in atheriosklerotischen Plaques vorhanden sind und die die Expression von Plin damit auf bestimmt metabolische Bedingungen beschränken.

Contents

Aim of the doctoral thesis

The aim of this thesis was to eludicate the role of Plin in murine peritoneal macrophages with regard to the effect of its deficiency on macrophage lipid metabolism.

Since foam cell formation is an initiating and ongoing event in all stages of atheriosclerosis, factors that affect macrophage lipid metabolism are of particular interest. The storage of lipids in LD is a hallmark of all eukaryotic cells. The current hypothesis is, that LD serve the exchange of lipids between different cellular organelles and thus cellular lipid homeostasis, which makes them very interesting especially with regard to macrophage foam cell formation. More and more evidence is accumulating that the same proteins which control LD metabolism in adipocytes fullfill a similar role in macrophages. The role of Plin in macrophages is still controversial and therefore I tried to elucidate it.

The following points were addressed:

Expression of the PAT protein family members during foam cell formation

Morphological analysis of LD in macrophage-derived wild type and Plin (-/-) foam cells

Investigation of pathways influencing LD formation and degradation

Influence of Plin deficiency on hepatic lipid metabolism

Effect of Plin deficiency on the development of atherosclerosis

1 Atherosclerosis – a multi-step inflammatory process

Atherosclerosis is still the most common reason of deaths in western societies causing stroke, myocardial infarction and high blood pressure (3, 4). Arteriosclerosis has to be separated from atherosclerosis. Arteriosclerosis refers to a chronic disease characterized by abnormal thickening and hardening of any arterial wall associated with loss of elasticity (5). Atherosclerosis in particular is the most common form of arteriosclerosis and is the deposition of lipids, cellular metabolites, cholesterol and various other substances within the arterial wall leading to atheromatous plaques. Atherosclerosis is an inflammatory process in which many factors are involved, namely retained modified lipoproteins, endothelial cells, monocyte-derived macrophages, vascular smooth muscle cells (VSMC) as well as T- and B-lymphocytes (5).

Stage 1: Fatty streak formation – the earliest stage of an atherosclerotic lesion

Under normal conditions the vascular environment (in particular tone and structure) is maintained by the balanced action of constricting and dilating substances that are secreted by endothelial cells. In this regard, the most important ones are nitric oxide, prostacyclin, tissue plasminogen activator and endothelin, which influence important physiological processes such as vasodilatation, the adhesion of leukocytes, the aggregation of thrombocytes and also the proliferation of smooth muscle cells (SMC) (6).
Endothelial dysfunction is induced by free radicals, infectious microorganisms, toxins after smoking or shear stress and hypertension following an altered rate or force of the blood flow as well as elevated and modified low-density lipoproteins (LDL) (3, 7, 8). It is reflected by an imbalance between vasodilatation and vasoconstriction in favor of the latter and leads to damage of the arterial wall. In dysfunctional endothelium, lipoproteins are more easily retained by the endothelial matrix and become more susceptible to modifications (6, 9).

In vivo, non-enzymatic (glycosylation, formation of immune complexes) and enzymatic (oxidation) modifications of LDL occur due to the interaction with arterial wall components, other blood cells or plasma constituents (10-12). LDL modification was shown to occur in vivo by oxidative lipid modification or its association with proteoglycans (13-15). Biochemical and morphological studies of human and animal lesions have shown that many of the retained lipoproteins occur in aggregated or fused form, in vitro being the most potent inducers of foam cell formation (16-18). Other modifications occur in parallel or in addition to lipoprotein oxidation whereas oxidation was shown increase the tendency to aggregate.

Significant acetylation of LDL (acLDL), one of the most studied forms of modified LDL in vitro, does not occur in vivo. The fatty acid composition and location as well as the content of anti-oxidative molecules (such as vitamin E or ubiquinol), which are bound to the lipoprotein, are all factors that influence lipid peroxidation (19, 20). Furthermore, extracellular occurring ions, the arterial matrix and cellular oxidative processes influence lipoprotein modification (21). Almost all lipids within lipoproteins are able to undergo modifications. The type of modification thereby changes the chemical nature of the lipoprotein and simultaneously determines its further uptake pathway (14).

Initially, the dysfunctional endothelium induces a compensatory response, which intentionally serves to neutralize the retained lipoproteins within the injured endothelium. The response includes the up-regulation of cell adhesion molecules for leukocytes (in particular monocytes, T-lymphocytes and B-lymphocytes), which subsequently transmigrate into the vessel wall, as well as the adhesion of paletelets (3).

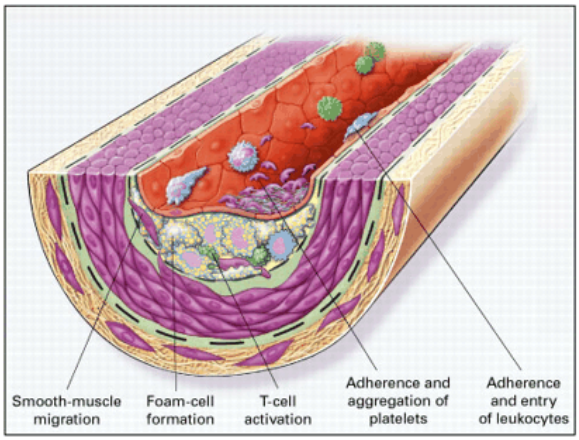

Fig.1: Fatty streak formation is the beginning of an atherosclerotic lesion. The initiating event in atherogenesis is endothelial dysfunction which is caused by several factors. As a consequence the endothelium expresses adhesion molecules and liberates cytokines by which leukocytes and platelets are recruited. The oxidative modification of lipoproteins through their interaction with components of the arterial wall (including cells and matrix components) is seen as an important driving force for fatty streak formation. The uptake of modified lipoproteins by macrophages turns them into foam cells, which is the major event in fatty streak formation (3).

Two subsets of monocytes are found in the circulation; classically activated (via Interferon γ (IFN-γ), pro-inflammatory cells (M1) and alternatively activated (via Interleukin 4 or 13 (IL-4, IL-13), anti-inflammatory cells (M2). These two subsets differ in their chemokine receptor expression and in antigen markers such as lymphocyte antigen complex 6c (Ly-6C) or granulocyte marker Gr-1 and give rise to either constitutively present, resident macrophages (M2) or to macrophages that are recruited to sites of infection or immunological injury (M1) (22-24). Classically activated monocytes promote inflammation, expand in hypercholesterolemia and develop to macrophages in atheromas. Alternatively activated monocytes attenuate inflammation, promote angiogenesis and can enter non-lymphoid tissue under homeostatic conditions.

The uptake of modified lipoproteins within the sub-endothelial space of the arterial wall by monocyte-derived macrophages turns them into foam cells. This is the major cellular event in fatty streak formation at early stages (19, 25) (Fig.1).

Stage 2 – Development of an advanced lesion and formation of a fibrous plaque

If the initial inflammatory response is not enough to neutralize the retained lipoproteins within the arterial wall, it stimulates the migration of smooth muscle cells resulting in the formation of an intermediate lesion. VSMC proliferate and secrete extracellular matrix proteins (such as collagen, elastin and proteoglycans) thereby forming fibrous tissue which walls off the fatty streak from the lumen (3). By taking up modified lipoproteins VSMC contribute to foam cell formation. The interaction of VSMC with macrophages and T-cells via various receptors (MHCII) and cytokines (IL-1, IL-12, IL-18, MIF, IFN-γ, TNF-α (reviewed in (26)) leads to an enhanced inflammatory response (5). However, some of the cytokines (IL-10, IL-6) released in this inflammatory process also have anti-atherogenic properties. A fibrous cap is formed as a consequence of the enduring recruitment of monocytes and the migration and proliferation of VSMC. The cap covers a mixture of leukocytes, cell debris, and accumulating lipids (Fig.2).

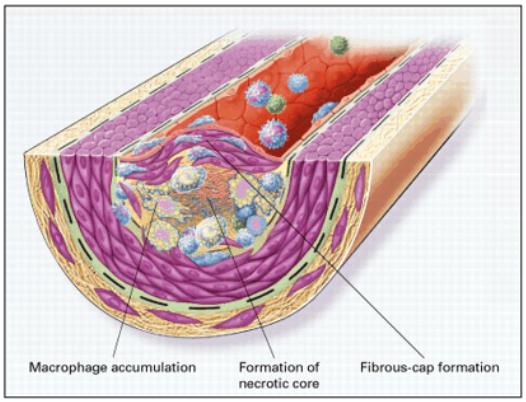

Fig.2: Development of an advanced lesion. With progressing lesion formation, smooth muscle cells are recruited and secrete fibrous tissue components to wall off the fatty streaks from the vascular lumen. With the ongoing inflammatory response and foam cell formation of leukocytes and smooth muscle cells, lipids and cell debris accumulate that are covered by a fibrous cap made up of smooth muscle cells, macrophages and their secretes (3).

The ongoing enhanced uptake of modified lipids finally leads to necrotic and apoptotic death of macrophages and VSMC leading to the development of an advanced lesion. Apoptotic cells are normally rapidly cleared by other macrophages. When phagocytic clearance is not assured, apoptotic macrophages release metalloproteinases that affect extracellular matrix proteins and neovascularisation. This favors plaque instability and potentially causes plaque rupture (27, 28). In addition, necrotic cell death of macrophages and VSMC liberates insoluble lipids and other cellular content that characteristically accumulates in advanced atherosclerotic lesions resulting in a necrotic core. Finally, blood and tissue factors activate the coagulation cascade together with fibrin deposition and platelet recruitment and activation thus enabling thrombus formation (29, 30).

To counter atherosclerosis drugs that regulate cellular lipid metabolism in metabolic important tissues already exist on the market or just undergo different stages of clinical trials. Statins are a group of 3-hydroxy-3-methyl-glutaryl-CoA reductase (HMGCR) inhibitors which target the rate limiting enzyme of the first step of cholesterol biosynthesis within the mevalonate pathway. They have lipid-lowering effects mainly by reducing hepatic cholesterol biosynthesis. This leads to increased uptake of LDL into peripheral cells and consequently lower plasma LDL-cholesterol levels (31). Statins slightly increase plasma high-density lipoprotein (HDL) (32) and they were shown to have anti-inflammatory properties by reducing the inflammatory cytokines TNF-α and IL-6 (33).

The exchange of lipids between triglyceride-rich lipoproteins and HDL is mediated via cholesteryl-ester transfer protein (CETP) and is one pathway for cholesterol delivery during reverse cholesterol transport (RCT) (34). CETP is present only in humans, but not in mice (35) .Elevation of plasma HDL levels in CETP-deficient humans has made this enzyme a possible target to counter atherosclerosis (reviewed in (36)). In theory it was thought that inhibiting CEPT would favor the direct cholesterol flux from the periphery to the liver. Experiments with LDL-receptor (-/-) mice over-expressing and lacking hepatic SR-BI have shown that the “net flux” of cholesterol through the RCT is probably of greater importance than the steady-state HDL-concentrations. As the ultimate step in RCT, the intestine plays a central role in cholesterol excretion. By inhibiting intestinal cholesterol absorption, ezetimibe was shown to promote cholesterol export from macrophages (37). CETP inhibition is currently seen as the most efficient strategy to raise plasma HDL levels. Nevertheless, the overall advantageous effect of CETP inhibitors on RCT and atherosclerosis in humans on the whole still remains an unresolved question (38).

Acyl-CoA:cholesterol acyltransferase (ACAT) mediates cellular esterification of cholesterol within the endoplasmatic reticulum (ER). Two genes, ACAT1 and ACAT2 exist. In humans ACAT1 is expressed in hepatocytes, adrenal glands, neurons, and macrophages and accounts for 80% of total ACAT activity measured in vivo (39, 40). ACAT2 is also expressed in human hepatocytes, but whether ACAT1 and/or ACAT2 are more important for CE synthesis and storage or packaging into very-low-density lipoprotein (VLDL) particles in humans remains to be determined (41). Hepatic ACAT2 expression in humans seems to be very heterogenous and its inhibition could effectively reduce CE content in LDL in subpopulations with elevated hepatic ACAT2. However non-specific ACAT inhibition in humans reduced VLDL and TG levels but failed to reduce LDL (42). In mice, ACAT2 is the predominant enzyme in the liver, delivering CE to VLDL particles (reviewed in (41)) and to

chylomicrons in the intestine (43, 44). ACAT2 (-/-) mice were shown to be resistant to diet-induced hypercholesterolemia. Liver specific silencing of ACAT2 within a hyperlipidemic mouse model (LDLR (-/-) mice) successfully reduced plasma cholesterol showing that hepatic ACAT2 inhibition has the potential to reduce atherosclerosis independent of dietary cholesterol absorption (45). In various animal models tested, non-selective ACAT inhibition alone significantly reduced plasma cholesterol (reviewed in (42)).

Deletion of ACAT1 in apoE (-/-) or LDL receptor (-/-) macrophages increased atherosclerotic plaque size. Moreover in vitro experiments with rodent macrophage cell lines showed that ACAT inhibition led to an increase in free cholesterol and macrophage apoptosis (46). Which was not observed in human macrophages (47). Regardless of the positive effects observed in animal models, which also seem to be species-dependent, the negative impact of ACAT inhibition on macrophages seems to be more disadvantageous than advantageous with regard to its potential as anti-atherogenic drug.

2 Whole body lipid metabolism

2.1. The different classes of plasma lipoproteins and their metabolism

Lipids cannot be transported in the blood due to their lipophilic nature. Therefore, they are bound within lipoproteins, water-soluble macromolecules which are made up of lipids (triglycerides (TG), cholesterol, phospholipids (PL)) and one or more specific apolipoprotein(s). Based on their density, particle size, electrophoretic mobility and affinity chromatography, lipoproteins with different metabolic functions may be classified as follows. (48).

Chylomicrons are the largest lipoproteins (>100nm in diameter). They are synthesized in the intestine and their physiological function is the transport of dietary TG and cholesterol to various cells of the body. After hydrolysis of TG by the vascular lipoprotein lipase (LPL), cholesterol-rich chylomicron remnants (β-VLDL) evolve and are rapidly cleared by the liver via the chylomicron remnant receptor (49) (50). β-VLDL accumulate within the plasma as a consequence of high fat diet feeding or hypertriglyceridemia and it was shown to be atherogenic due to its ability to cause massive cholesteryl ester accumulation in macrophages (51, 52). In the liver, dietary and endogenous lipids are packed into VLDL (30-90 nm in diameter) for redistribution to various tissues. The activity of plasma lipases (hepatic lipase (HL), LPL) converts VLDL particles into smaller, cholesterol-enriched intermediate density lipoproteins (IDL) as well as LDL (~20nm in diameter), the end product of VLDL catabolism (48).

High density lipoproteins (HDL) are the smallest lipoproteins and they arise from different sources like the liver and the intestine. HDL in the human plasma is very heterogenous with regard to its size, composition and surface charge. On a non-denaturing SDS-gradient gel, five different HDL subfractions between 7.6nm and 10.6nm in size are separated. On the basis of their surface charge, four subfractions (α, pre-α, pre-β or γ) can be separated on an agarose gel. By density, two major subfractions, HDL_2 (density range 1.063-1.125 g/ml) and HDL_3 (1.125-1.21 g/ml) can be distinguished. The two major apoproteins of human HDL are apoA-I and apoA-II. HDL particles either contain apoA-I, apoA-II or both. apoA-I/apoA-II containing particles can be found exclusively in the HDL_3 density range whereas apoA-I containing particles can be found in the HDL_2 but also in the HDL_3 density range. Spherical particles are the predominant subfraction within human plasma and they have α-mobility. Discoidal particles or monomolecular apoA-I can either have pre-α or pre-β mobility. A minor subfraction are discoidal particles containing apoE, which have γ–mobility (53).

The apoB lipoprotein metabolism includes two different pathways. The first is the chylomicron-chylomicron remnant pathway, which transports dietary lipids (mainly TG) from the intestine to peripheral cells and the remnants back to the liver. And the second is the VLDL-IDL-LDL pathway which transports endogenous, hepatic lipids (mainly TG) to peripheral tissues and returns cholesterol back to the liver (54). During LPL-mediated hydrolysis, chylomicrons and VLDL deliver their TG to peripheral tissues. Cholesterol, phospholipids and apolipoproteins are simultaneously delivered to lipid-poor apoA-I. The transfer of PL to HDL during the lipolysis of TG-rich lipoproteins is mediated via phospholipid transfer protein (PLTP). By delivering cholesterol to HDL, the TG-rich chylomicrons and VLDL participate in the formation of nascent pre-β HDL particles (55). The TG-depleted remnant particles are finally taken up by the liver via the apoE/apoB100 receptor (LDL receptor in the periphery) and are removed from the circulation. Alternatively, VLDL remnants can be hydrolyzed by HL converting them into IDL and LDL (56).

RCT is the physiological function of HDL. HDL metabolism begins with the secretion of lipid poor apoA-I mainly by the liver but also the intestine. Poorly lipidated apoA-I acquires additional cholesterol and phospholipids via ABCA1-mediated efflux from the liver (also the intestine) and from peripheral cells during RCT. Additionally, FC and PL are transferred to lipid-poor apoA-I during the LPL-mediated hydrolysis of VLDL and chylomicrons, giving rise to nascent HDL particles. The action of LCAT, which is bound to the lipoproteins, generates CE that are stored within the core of HDL particles resulting in the formation of large, mature, spherical HDL particles. With regard to atherosclerosis, cholesterol efflux from macrophages

during RCT is of particular importance. ABCA1, ABCG1 and scavenger receptor class B, type I (SR-BI) all mediate efflux of cholesterol from cells to extracellular acceptors. ABCA1 generally mediates cellular efflux of cholesterol to lipid-poor apoA-I, whereas ABCG1 and SR-BI deliver cholesterol to mature HDL. In macrophages ABCA1 and ABCG1 function cooperatively to mediate cholesterol efflux whereas SR-BI is in vivo of minor importance (57). Selective CE uptake from HDL via SR-BI by the liver during RCT represents a direct pathway of cholesterol delivery. Hepatic over-expression of SR-BI induces RCT and is thus suggested to be atheroprotective. An indirect pathway for CE uptake is the CETP mediated exchange of CE and TG between HDL and apoB containing lipoproteins (chylomicrons, VLDL, and their remnants, and LDL). CETP activity generates CE-depleted, TG-rich HDL particles (55). TG-enrichment of HDL occurs especially under hypertriglyceridemic conditions and favors HDL remodeling via hepatic lipase (HL), which plays an important role in the remodeling of all lipoproteins. HL activity promotes selective uptake of HDL and LDL via the hepatic SR-BI and apoB100/E receptor, respectively. There is in vivo evidence that endothelial lipase (EL) also plays an important role in HDL metabolism together with or in addition with HL (55).

2.2. Apolipoproteins determine the fate of plasma lipoproteins

The lipoprotein-associated apolipoproteins are involved in the redistribution of the different lipoproteins to their target tissue. The delivery of lipids from the lipoproteins to cells of a tissue is mediated via binding of the apolipoproteins to specific receptors. Additionally they act as cofactors for enzymes that mediate lipoprotein processing. They thus determine the unique role of each of the lipoproteins and are involved in the regulation of lipoprotein metabolism (48).

Apolipoprotein A-I (apoA-I) is the predominant apolipoprotein of HDL particles, is also constituent of chylomicrons, but not other lipoproteins, and is the main activator of LCAT. It can occur as a single, lipid-poor apoA-I molecule, with or without small amounts of PL attached. The existence of lipid-poor apoA-I in vivo is not definitively proven because these particles are rapidly excreted through the kidney or re-lipidated via direct incorporation into pre-existing HDL particles, by accepting PL and free cholesterol (FC) in exchange with other lipoproteins (mediated by CEPT) or from cells during RCT. The CEPT- and HL-mediated remodeling of spherical HDL particles or the LPL-mediated remodeling of TG-rich particles also produces lipid-poor apoA-I. Secondly it can be a constituent of discoidal HDL particles consisting of two or three apoA-I, PL, with or without FC. Thirdly, apoA-I can also be part of spherical HDL particles, consisting of two or more apoA-I (with or without apoA-II) molecules, PL, FC, CE and TG (53).

Apolipoprotein A-II: the human apoA-II is the second most abundant protein component of HDL and in lower amount also of other lipoproteins (48). It is mainly produced by the liver and it is believed to be an important structural component of HDL particles making them more stable. Displacement of apoA-I by apoA-II was shown to inhibit cholesterol esterification and to inhibit CE and PL transfer. The impact of apoA-II on HL activity is not definitively clear, both stimulatory and anti-stimulatory effects have been reported (58).

Apolipoprotein E is a constituent of chylomicrons, chylomicron remnants, VLDL and HDL. It is synthesized and secreted by the liver and also cells of peripheral tissues including macrophages. ApoE is necessary for hepatic uptake of all lipoprotein particles by the apoB100/E receptor. Hence apoE controls and regulates overall plasma cholesterol levels. Moreover it stimulates macrophage cholesterol efflux and it was shown to positively modulate the immune response. Thus apoE has several anti-atherogenic properties (59).
Together with apoCs, apoE is transferred to chylomicrons from HDL and during their hydrolysis, they are returned to HDL (60).

Apolipoprotein B is the primary apolipoprotein of chylomicrons, VLDL, and LDL particles. ApoB100 is synthesized by the liver and is an obligatory constituent of VLDL, IDL and LDL. ApoB48 is synthesized by the intestine and is found on chylomicrons and on chylomicron remnants (61). In contrast to all other apolipoproteins, apoBs are not exchanged between the different lipoproteins (62). The apoB100/E (LDL) receptor is present in hepatic as well as extrahepatic tissues, where it mediates the uptake of chylomicrons as well as VLDL-derived IDL and LDL.

Apolipoprotein A-IV is the most abundant apolipoprotein of chylomicrons (but not of chylomicron remnants, VLDL or LDL). In humans, it is primarily synthesized by enterocytes of the small intestine, whereas in rodents, it is produced by the liver and the small intestine. Active exchange of the apoA-IV apolipoprotein between chylomicrons and HDL occurs. ApoA-IV is able to influence LPL activity by facilitating transfer of apoC-II to TG-rich lipoproteins and variants of the apoA-IV gene correlated with modulated LPL activity. ApoA-IV is also involved in RCT by stimulating LCAT, facilitating cellular cholesterol efflux via its interaction with ABCA1 and by influencing CETP activity on HDL particles. All together these data indicate that apoA-IV could be beneficial with regard to atherogenesis. Nevertheless, the effects observed can for sure not solely be attributed to apoA-IV and the exact physiological role remains to be determined (63).

The C apolipoproteins are represented by three molecular weight apolipoproteins (apoCI-III) with apoC-III being the most abundant of all C apolipoproteins (48). They are surface components of chylomicrons, VLDL and HDL. ApoC-I, apoC-II and apoC-III are readily exchangeable between HDL and TG-rich lipoproteins as it is apoE. They were shown to indirectly influence the metabolism of TG-rich lipoproteins and to directly affect HDL metabolism. ApoC-I was demonstrated to activate LCAT and to inhibit HL and CETP (64). ApoC-II and apoC-III were shown to be important for efficient LPL activation (60). ApoC-III is expressed in the liver and intestine and under hypertriglyceridemic conditions, apoC-III containing TG-rich lipoproteins are elevated. ApoC-II could mask the apoE or apoB moiety on the TG-lipoproteins thereby negatively influencing their uptake via hepatic apoB100/E receptor resulting in their accumulation within the plasma.

2.3. Vascular lipases and their role in atherogenesis.

LPL, HL and endothelial lipase (EL) belong to the lipase family which involves lipases which sharing a common ancestral origin. The different lipases are expressed in a tissue specific manner indicating specific functions. The main site of lipase action is the endothelium. While lipolysis is generally anti-atherogenic because it reduces TG levels, the enduring exposure of endothelial and surrounding cells with lipolysis products can exhibit pro-atherogenic properties (65).

LPL is mainly responsible for TG hydrolysis from chylomicrons and VLDL. It is mainly synthesized by heart, skeletal muscle and adipose tissue, being secreted at the luminal surface of capillary endothelial cells, getting attached via highly charged heparin sulphate proteoglycans (HSPG). In addition to its catalytic activity it was also shown to act as a molecular bridge for lipoproteins promoting their binding and internalization by the apoB100/E receptor (LDLR) and LDL-receptor related protein (LRP) (65). In humans, macrophages in atherosclerotic plaques were found to be the predominant source of LPL attributing pro-atherogenic properties to LPL activity. Macrophages engulf remnant particles that arise through the activity of LPL thereby getting foam cells. Over-expression of LPL in macrophages of apoE (-/-) mice accelerated atherosclerosis, whereas deficiency of LPL in macrophages decelerated it, independent of the lipoprotein profile background (66). In vitro experiments have linked LPL activity also with SMC proliferation and disruption of vascular cell integrity (65).

HL is a glycoprotein, synthesized and secreted predominantly by the liver on the surface of sinusoidal endothelial cells and on the external surface of parenchymal cells. It has TG-

hydrolase as well as phospholipase activity and mediates the ultimate remodeling of all lipoproteins and their subsequent uptake by the liver. Like LPL, HL binds to HSPG and acts as a ligand for the cellular uptake of lipoproteins or, selectively, their lipids. Both pro- as well as anti-atherogenic properties are attributed to HL activity. The absence of HL in apoE (-/-) mice significantly reduced the formation of atherosclerotic lesions but total plasma as well as VLDL cholesterol levels were increased. The atherogenic potential of HL possibly lays in the retention of lipoproteins in the sub-endothelial arterial space, which drives foam cells formation (65).

EL is expressed in the liver, lung, endothelial cells as well as smooth muscle cells and macrophages in atherosclerotic plaques (65). It has predominantly phospholipase activity (67) and it was shown to substantially participate in HDL remodeling and to be up-regulated in vitro by pro-inflammatory signals (TNF-α and IL1-β) (68). In vivo, hepatic over-expression of EL significantly lowered HDL levels by increasing its catabolism (69). In EL (-/-) mice, the raise in plasma cholesterol was mainly due to an increase in HDL cholesterol (70). On the contrary, inhibition (71) and silencing (72) both increased plasma HDL levels.

3 How cells handle cholesterol

3.1. Endogenous cholesterol biosynthesis, its trafficking and compartmentalization

Cholesterol is an essential constituent of cell membranes, where it accounts for 20-25% of the lipid molecules. Phospholipids, sphingomyelin and glycolipids make up the remainder. Cholesterol not only helps to maintain membrane integrity and fluidity (73, 74) but it also participates in several trafficking and signaling processes. Moreover, the correct ratio between cholesterol and phospholipids establishes the according environment for the activity of certain critical plasma membrane enzymes (75-77). Cells of most organs satisfy their requirements for cholesterol via endogenous cholesterol biosynthesis. Cholesterol is synthesized in the ER, which generally has only a low cholesterol content of about 1% of total cell cholesterol. Newly synthesized cholesterol leaves the ER rapidly, predominantly by non-vesicular mechanisms that depend on ATP hydrolysis. This process probably involves sterol binding protein 2 (78) as well as caveolin (79) and bypasses the Golgi. Part of the newly synthesized cholesterol also ends up in the biosynthetic secretory pathway and takes its route via the Golgi to the cytoplasma membrane (80).

3.2. Uptake of cholesterol occurs at specialized membrane microdomains

Besides the capacity of endogenous cholesterol biosynthesis, many cell types (cells from steroidogenic tissues, hepatocytes, smooth muscle cells in atherosclerotic lesions and also macrophages) have evolved mechanisms to internalize cholesterol from exogenous sources, mostly plasma lipoproteins (81, 82).

Lipid uptake begins at the cytoplasma membrane at special microdomains. Lipid rafts are cholesterol and sphingolipid-enriched, plane areas in the outer cytoplasma membrane leaflet (Fig.3). Sphingolipids are tightly packed by cholesterol and thereby they form a liquid-ordered phase. This detergent-resistant, liquid-ordered phase is dispersed in the detergent-soluble, liquid-disordered phase, constituted of the more loosely packaged membrane matrix. Cholesterol was shown to keep preferred contact with sphingomyelin within the raft domains (reviewed in (83)) and the interaction between both lipids was shown to be important for the overall cholesterol distribution within the cell (84). Distinct classes of membrane proteins are concentrated in those lipid rafts. Examples include glycosylphosphatidylinositol (GPI) - anchored proteins, peripheral membrane proteins, cholesterol-linked proteins and trans-membrane proteins. Each raft harbors its own, limited set of proteins. This enables clustering of proteins in functional assemblies for diverse cellular processes such as signal transduction, membrane trafficking and cell adhesion (85, 86).

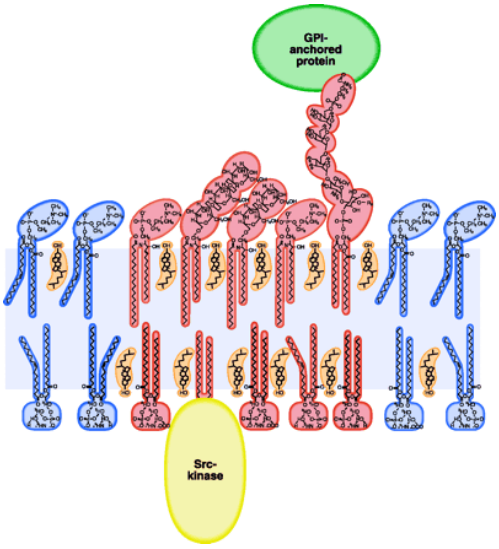

Fig.3: Architecture of a lipid raft. In lipid rafts (red) cholesterol (orange) and sphingolipids are tightly packed, thereby forming a liquid-ordered phase which is distributed in a liquid-disordered phase (blue). Each raft harbors ist own set of proteins (green and yellow). Cholesterol partitions preferentially into the liquid-ordered phase. The outer leaflet of the raft is enriched in glycosphingolipids and sphingomyelin and the corresponding inner leaflet contains glycerophospholipids with predominantly saturated fatty acid acyl side chains (1).

Caveolae are a subclass of lipid rafts. They are smooth-surfaced pits enriched in FC and caveolin, a cholesterol and fatty acid binding protein (87, 88). Caveolae contain all proteins which are necessary for vesicle formation, fission, docking, and fusion with target membranes, including ADP-ribosylation factor 6 (ARF6), ancyrin/spectrin and actin (87). Many peripheral cells such as adipocytes, muscle cells, endothelial cells and macrophages

contain caveloae (89, 90). Their formation is dependent on cellular cholesterol and through their association with receptors (like SR-BI) they likely serve as important regulators of cellular cholesterol content (91, 92).

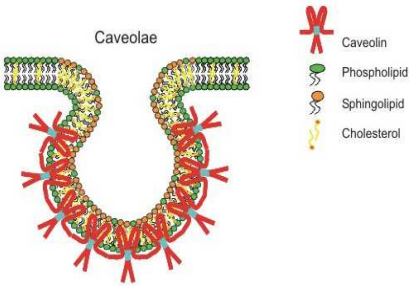

Fig.4: The structure of caveolae. Caveolae represent a subset of rafts, constituting caveolin-enriched flask-shaped invaginations of the plasma membrane. Like in rafts their formation depends on cholesterol and sphingolipids. (http://www.ruf.rice.edu/~rur/issue1_files/razani.html)

3.3. Macrophages take up cholesterol via different pathways

Lipid particles can be taken up by macrophages via different routes (Fig.5). One of them is endocytosis via the classical clathrin-dependent pathway, which is one of the best studied pathways (93). Examples for this pathway include endocytosis via the LDLR or the transferrin receptor, which were shown to be excluded from lipid rafts (86). Receptors which have bound their ligands are concentrated in clathrin-coated pits by their association with adaptor protein complexes. When numerous ligands have bound to their receptor, the large GTPase dynamin mediates the pinch-off of the clathrin-coated vesicle. The vesicle is uncoated by an uncoating ATPase. Receptors and their ligands are separated and the receptors are recycled back to the cytoplasma membrane. The ligand-containing vesicles fuse to early endosomes.

Two other endocytosis mechanisms exist that differ from the classical clathrin-dependent pathway in that they are both dependent on raft microdomains. One of them is a caveolin-dependent mechanism which leads to the formation of caveolin-coated vesicles and which is also dependent on dynamin. The other one is neither dependent on clathrin nor on caveolin (87). Examples for clathrin-independent endocytosis, like the uptake of IL-2 (94) and GPI-anchored receptors (for more examples see review (87)) exist. Clathrin-independent endocytosis requires actin polymerization driven by Rho GTPases, which dynamically regulate the actin skeleton in concert with Phosphoinositid-3-kinases (95). In addition to their role in endocytosis, the non-clathrin coated pathways are suggested to play a role in signal transduction (87) and the homeostasis of cholesterol (74, 89).

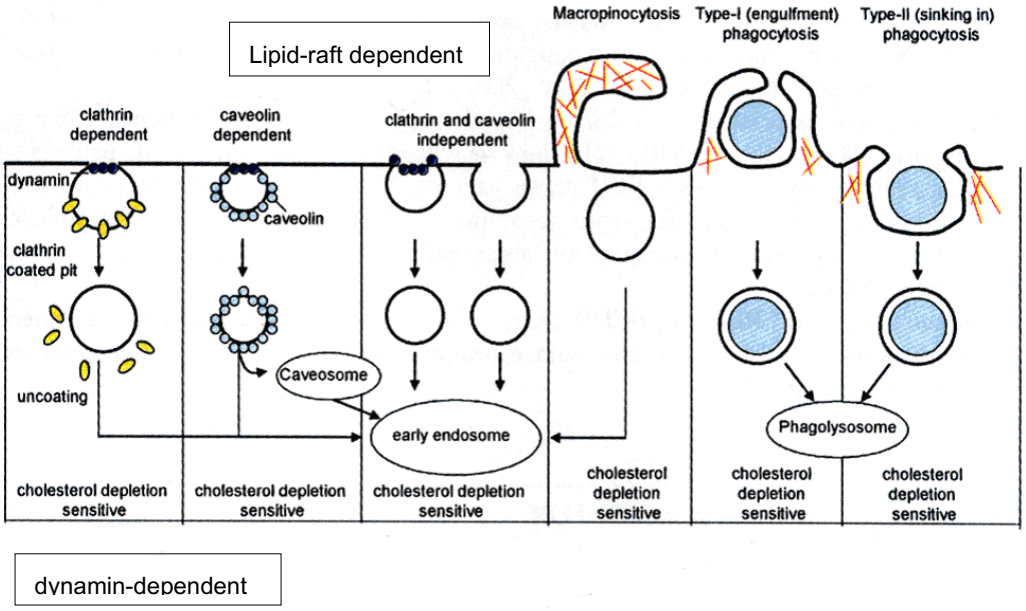

Fig.5: Different pathways exist for the uptake of lipoproteins into macrophages. Besides the classical endocytosis via clathrin-coated vesicles, clathrin-independent mechanisms exist. These include uptake via caveolin-containing vesicles or endocytosis mechanisms that are also independent of caveolin (83). Pinocytosis and phagocytosis belong to the clathrin-independent uptake pathways.

Phagocytosis and pinocytosis are other endocytic pathways by which large particles or small solutes are taken up in membrane-enclosed vesicles. Phagocytosis generally mediates the uptake of large particles into the cell. Like all clathrin-independent pathways, phagocytosis is also dependent on actin. Binding of a ligand to cell-surface receptors (Fc and complement receptors) thereby recruits Rho GTPases to mediate actin polymerization (96). Pseudopodes are extensed and wrap around the opsonized particle, leading to its engulfment. The resulting phagosome fuses with early/late endosomes as well as lysosomes, a process which is dependent on Rab GTP-binding proteins (97), which finally leads to the degradation of the engulfed particle (83).

Solid macromolecules can be taken up by cells also via fluid-phase endocytosis, called pinocytosis. The uptake occurs along with fluid within either micropinocytotic or macropinocytotic vesicles. The extracellular solute concentration thereby determines the extent of internalization and is proportional to the internalized fluid volume (98). Macropinocytosis can either be constitutive (as in dendritic cells) or can be induced (as in macrophages, lymphocytes, fibroblasts and endothelial cells) (99). In macropinocytosis, actin polymerization leads to ruffling of the plasma membrane thereby resulting in the formation of

large, irregular vesicles. In macrophages, macropinosomes are directed to the endolysosomal pathway for their degradation.

3.3.1. Several classes of receptors are involved in the uptake of modified lipoproteins by macrophages

Several receptors were shown to participate in the pathways by which macrophages take up native and modified lipoproteins. Uptake via these receptors occurs at different rates and each of the pathways participates to different extent in macrophage foam cell formation in vitro. Oxidized low-density lipoprotein (oxLDL) is taken up very fast via scavenger receptors, mainly SR-A, SR-BI, CD36 and lectin-like oxLDL receptor (LOX-1) (100, 101). These receptors are not feedback inhibited by the cellular cholesterol content, allowing massive foam cell formation. A number of alternative uptake pathways exists in macrophages (102). To what extent they contribute to foam cell formation in vivo is still a matter of debate. For example, aggLDL (103) and β-VLDL (104) are also taken up with a very fast rate by phagocytosis, maybe facilitated by the LDLR. Immune complexes with either native or modified LDL (glycated or oxidized) are also taken up very fast by phagocytosis, mediated via Fc receptors (105). Glycated end products (AGE) are taken up via the receptor for glycated end products (RAGE) (106) or, predominantly by A and B class scavenger receptors (107). Acetylated low-density lipoprotein (acLDL) is taken up mainly via SR-A (101).

3.3.2. The fate of endocytosed lipids

Endocytosed vesicles fuse with each other to form early endosomes after they have lost their clathrin-coat. Within the Golgi, early endosomes acquire numerous hydrolases and their lumen gets acidified during maturation into late endosomes/lysosomes. CE are hydrolysed within the lysosomes by an acidic hydrolase. FC is transported either back to the cytoplasma membrane or to the ER. Cholesterol is much more rapidly transported from the ER to the plasma membrane and the majority of endocytosed cholesterol probably ends up there (108). Excess sterols are conjugated with fatty acyl-CoA within the ER. Esterification is mediated by microsomal ACAT (109). The levels of FC and CE are additionally maintained by a neutral CE hydrolase that converts CE to FC (83). One of the earliest reactions following free cholesterol accumulation in macrophages is raising PL synthesis (75).

3.3.4. How macrophages balance foam cell formation: cellular cholesterol efflux during RCT

Excess cholesterol from peripheral cells, including macrophages, is rapidly delivered to HDL or its apolipoproteins to transport it to the liver for degradation. Key players in the exchange of cholesterol between cells and acceptors are the ATP-binding cassette transporter (ABC-) A1 and G1. Both transporters are distributed in rafts/caveolae of the plasma membrane as well as intracellular endolysosomal membranes (110). The proposed two-step process begins with a fast, initial efflux from rafts of the plasma membrane that subsequently mobilizes intracellular cholesterol from LD via the ER and Golgi (111). Alterations in the structure of membrane microdomains were shown to have an influence on cholesterol efflux from cells. Increased glycosphingolipid levels for example were shown to cause cholesterol accumulation in the endolysosomal pathway (112).

3.3.5. SREBPs and nuclear hormone receptors coordinately regulate enzymes of lipid synthesis and metabolism

The genes of many enzymes involved in cholesterol and fatty acid biosynthesis are regulated via sterol regulatory element-binding proteins (SREBPs). They are membrane-bound, basic helix loop helix leucine zipper transcription factors (81, 113). SREBP-2 regulates genes of the cholesterol biosynthesis pathway such as HMGCoA-synthase whereas SREBP-1c regulates genes of fatty acid metabolism such as fatty acid synthase or stearoyl-CoA desaturase (Fig.6).

SREBPs cycle between the ER and the Golgi. Their transport between the two compartments is regulated via a complexed co-factor, the SREBP cleavage-activating protein (SCAP) which has a sterol-sensing domain. Under normal conditions, sterols cause the SREBP-SCAP complex to bind to an ER-retention protein. However, when cellular cholesterol levels fall, the SREBP-SCAP complex moves from the ER to the Golgi, where it is cleaved twice releasing the active form of SREBPs to the nucleus, which regulates the expression of its target genes.

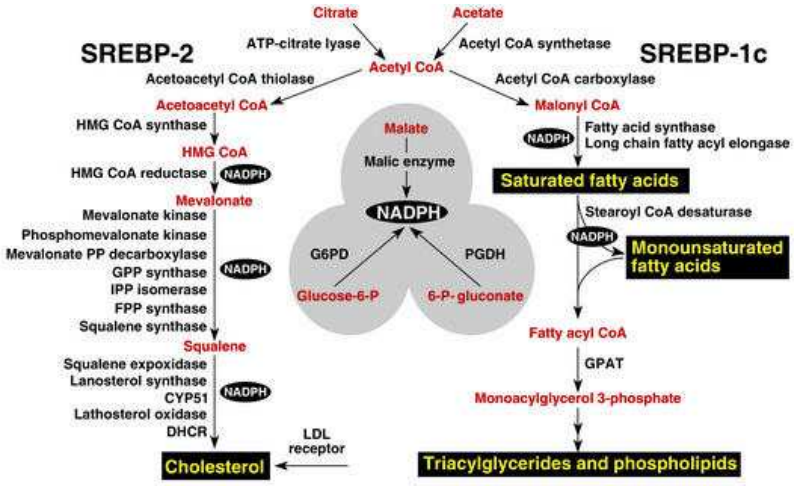

Fig.6: Regulation of cellular lipid metabolism by SREBPs. Different SREBPs regulate enzymes involved in cholesterol and fatty acid biosynthesis. SREBP-2 mainly regulates genes of cholesterol metabolism, whereas SREBP-1c regulates genes involved in fatty acid and phospholipid metabolism. (81).

3.3.6. PPARs, LXRs, RXRs

Peroxisome proliferator-activated receptors (PPARs) and liver X receptors (LXRs) are ligand-activated transcription factors which are activated by fatty acids and derivatives. In vascular endothelial cells, smooth muscle cells and monocytes/macrophages they regulate the expression of genes which are involved in lipid transport, storage and elimination (114). In hepatocytes, adipophilin (Adrp) expression is regulated by PPARα (115) as well as PPARγ (116). PPAR activation induces transcription of all perilipin/Adrp/Tip47 (PAT) proteins except for Tip47 (117, 118). Under non-lipolytic conditions, PAT proteins reduce cellular fatty acids by sequestering esterified fatty acids thereby reducing PPAR ligands.

PPARs and LXRs heterodimerize with the retinoid X receptor (RXR) and bind to specific response elements within the promoter region of their target genes. The formation of the PPAR, LXR/RXR heterodimer and the subsequent transcriptional activation of their target genes are ligand-dependent. LXR for example activate ABC-transporters and retinoids were identified as potent inducers of macrophage lipid efflux (119). PPARγ is highly expressed in adipocytes and macrophages and is involved in adipocyte differentiation, lipid storage and glucose homeostasis (120). PPARγ is activated by arachidonic acid metabolites that derive from the cyclooxygenase or lipoxygenase pathway, which also occurs in atherosclerotic lesions (121-123). Treatment of macrophages with oxLDL was shown to induce PPARγ and LXRα mRNA. The expression of many other genes in smooth muscle cells and macrophages are regulated by PPARγ that influence the atherogenic process. Examples include the

expression of cytokines (TNF-α) (124), enzymes (iNOS) (125) and the expression of several receptors (MMP-9 (126), MCP-1 (124), CD36 (122, 127) or SR-A (125)).

4. Lipid droplets are dynamic organelles with important cellular functions

4.1. LD resemble circulating lipoproteins

Lipid droplets (LD) have a similar structure as circulating lipoproteins. In most cells they have an apolar core of TG, diglycerides (DG) and CE (Fig.7). However, some types of cells may also contain retinol esters or ether lipids (128). The lipid core is surrounded by a PL monolayer in which phosphatidylcholine is the most abundant phospholipid followed by phosphatidylethanolamine and phosphatidylinositol. In this layer the relative content of specific PL and the acyl-chain composition differ from that of "classical" membranes, like the cytoplasma membrane or the membrane of peroxisomes, suggesting a different origin (128, 129).

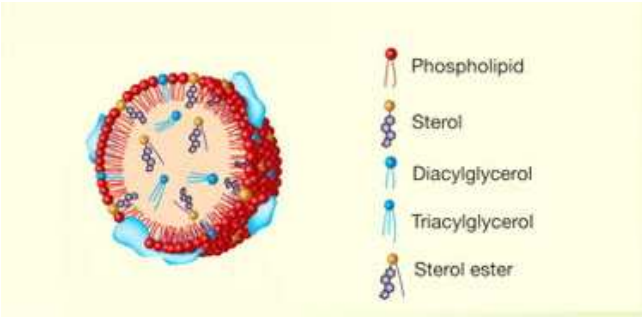

Fig.7: The constitution of LD: LD resemble circulating lipoproteins due to some shared features such as an apolar core of CE, DG and TG and a PL surface in which different proteins are embedded (2).

LD are very heterogenous with respect to their size, location and their protein-coat composition. This heterogeneity can be found between cells of different tissues and the different LD subpopulations likely have specialized functions (130).

4.2. LD originate from the ER membrane

Different models exist that try to explain LD formation (Fig.8). Phospholipase D and phosphatidic acid were shown to be essential for LD assembly in a cell-free system (131). The prevailing, accepted model for LD formation is that neutral lipids accumulate in a lense-like pool between the two membrane leaflets of the ER (130, 132). In this model, increasing lipid accumulation leads to budding of a droplet which is surrounded by the former cytoplasmic leaflet of the ER membrane. This model offers an explanation for the origin of

the PL monolayer that surrounds the LD. In addition, it also localizes LD formation to the organelle where the final steps of TG and cholesterol biosynthesis occur (130). From this model it was also concluded that at least a part of the LD-associated proteins derive from the ER membrane (132, 133). However, the pathway of LD formation proposed in this model has not been directly observed so far. Alternatively, LD might be seen as lipid-filled protrusions of the ER or specialized ER domains which keep sustained connection with the respective compartment. In the second model, the bicelle model, LD are excised from the ER membrane after they have accumulated lipids and the nascent LD are coated by PL from both ER membrane leaflets (134). The third existing model is the vesicular-budding model in which LD origin from small bilayer vesicles that remain bound to the ER. Newly synthesized lipids are subsequently pumped into the inter-membrane space of the vesicle bilayer (135).

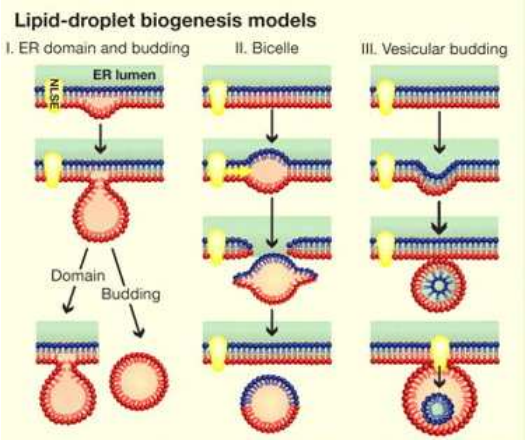

Fig.8: Different models try to explain the formation of LD. All models agree in the ER being the origin of LD. The models differ in whether PLs from both ER leaflets participate in LD formation or only one leaflet and whether the droplets remain attached to the ER or not (2).

In primary adipocytes, elevated TG levels within caveolae-like microdomains of the plasma membrane were shown to lead to cytosolic LD formation suggesting that LD can also emerge from the plasma membrane (136). It was shown in vitro that exogenous cholesterol or oleate stimulated caveolin recruitment to LD in HepG2 cells, rat kidney cells and human fibroblasts (137, 138). The association of caveolins with LD opens a possible role for this lipid raft protein in neutral lipid storage (137, 139, 140). In adipocytes from caveolin (-/-) mice, FC levels were dramatically reduced compared to wild type adipocytes. Caveolin-1 expression was also proposed to be important for efficient LD formation because lipid accumulation in caveolin-1 null embryonic fibroblasts, stably transfected with perilipin (Plin), was approximately 4.5-fold reduced compared to wild-type cells transfected with Plin (141).

4.3. How LD increase in size

Cytosolic LD are much larger than the vesicles formed at the ER membrane. This raises the question how LD grow. In one theory, LD expand as a single organelle by accepting lipids which are synthesized in the ER and enter the LD by passive diffusion (2). Also de novo synthesis of lipids is possible due to the recruitment of enzymes (such as diacylglycerol-acyltransferase (DGAT) to the LD surface. This would imply simultaneous increase of PL at the LD surface which has already been shown to occur (142). A third possibility is fusion of existing smaller LD to bigger ones (2).
Recently, Boström and colleagues have shown that LD can also grow by fusion in a process which is independent of TG biosynthesis, but depends on intact microtubules (143). Microtubules bring LD into close proximity so that fusion can occur. Fusion was proposed to be a quantitatively important mechanism for the formation of bigger LD and it can occur between droplets of any size (143). Proteomic analysis of LD of several cell types (CHO, 3T3 adipocytes, U937, Huh7, HepG2) has shown that LD contain a variety of proteins which are involved in membrane trafficking. Among them are (i) small GTPases (Rab GTPases), which regulate formation, transport, targeting and subsequent fusion of LD, (ii) motor proteins like myosin and kinesin, which mediate cytosceletal transport, (iii) N-ethylmaleimide sensitive factor (NSF) and its receptors (SNAREs), which drive membrane docking and fusion, (iv) vesicular trafficking proteins (Sec22, Arf1) which regulate budding and sorting and (v) membrane trafficking proteins of so far unknown function (Tip47) (144). The presence of membrane trafficking proteins on LD indicates that LD can move bi-directional and this is obviously important since disturbance of LSD2, a PAT protein family member that regulates microtubule motor proteins (145), reduces lipid accumulation (146). Moreover, LD interact with several cellular organelles like the ER, mitochondria, peroxisomes and endosomes (reviewed in (144)). This supports a role for LD as specialized organelles for the reciprocal exchange of lipids. Recently it was shown that LD can temporarily sequester proteins like histones or ApoB (147). It was proposed (148) that this sequestration serves to remove excess proteins from their original compartment for later reuse or to keep aggregation-prone proteins until their degradation.

LD are surrounded by a specific set of LD-associated proteins (133, 149). Among them are structural proteins (like the PAT proteins (150)) as well as enzymes that mediate lipid synthesis (like acetyl CoA carboxylase, acetyl CoA synthetase, DGAT 2) (151, 152). Two models exist that try to explain how LD-associated proteins are targeted and attached to LD. In the first model the proteins contain long membrane-embedded domains that enter and exit the PL monolayer of the LD on the same site. This mechanism was already shown for

caveolins (153) and DGAT 2 (151, 152). Alternatively, proteins could attach to the LD surface as peripheral proteins being embedded via amphiphatic α-helices (150).

4.4. PAT proteins organize TG storage

The existence and function of perilipins was first discovered in adipocytes (154). Since then four additional LD proteins with sequence similarity to the perilipins were discovered in vertebrates. These include adipophilin (adipose differentiation-related protein, Adrp) (Plin2), Tip47 (tail-interacting protein of 47 kDa) (Plin3), S3-12 (Plin4) and OXPAT (myocardial lipid droplet protein, LSDP5, MLDP1 or PAT-1) (Plin5). Based on their stability when not bound to LD, they can be divided into two groups: Plin and Adrp are constitutive LD-associated PAT-proteins (CPAT) (155). In adipocytes, Plin localizes exclusively and constantly to large central LD and is not found in any other cellular compartment (156). It is unstable in soluble form, being rapidly degraded, but stabilized by binding to LD (157). Plin plays a dual role in the regulation of adipocyte lipolysis. Under fed conditions, Plin A restricts the access of lipases to the LD in favor of TG storage (158-160) and under fasting conditions or exercise, phosphorylated Plin A facilitates hormonally regulated lipolysis (161). Three Plin isoforms exist which arise through alternative splicing of one mRNA giving rise to proteins with different C-terminal regions (162). The longest isoform is Plin A (517 amino acids), followed by Plin B (422 amino acids) and Plin C, which is the shortest isoform. A fourth isoform (Plin D) was predicted, displaying an in-frame stop codon in an unspliced intron (163). Plin A is the most abundant LD-associated protein in mature adipocytes and steroidogenic cells of the adrenal cortex, testis and ovaries (164). Plin B protein is expressed only to a minor extent in adipose tissue. Plin C is absent in adipose tissue, but it occurs in abundant amounts in steroidogenic cells, adrenal cortical and Leydig cells. Adrp is the CPAT in most other cell types but it is less protective against hydrolysis (165). Like Plin, Adrp is rapidly degraded within lysosomes after ubiquitination when not bound to LD (166, 167). The relative expression of the CPAT determines the amount of TG that can be stored by cells or tissues. Tip47, S3-12 and OXPAT are recruited from a pre-existing cytosolic pool (168) where they are also stable in soluble form when not bound to LD (168-170). As exchangeable proteins between the cytosol and LD they could ultimately deliver newly synthesized TG to CPAT-coated LD thereby maximizing their storing (155).

In adipocytes, the composition of the LD-associated PAT proteins changes during LD maturation. Large, Plin-coated LD represent the homeostatic LD architecture in adipocytes. Upon loading with long-chain fatty acids, TIP47, S3-12 and OXPAT are recruited from a pre-existing cytosolic pool to coat small, nascent LD which are found close to the periphery of adipocytes. New protein synthesis is not required for the formation of nascent LD. While

growing, LD move toward the centre thereby additionally acquiring Adrp. Further enlargement of the LD leads to the recruitment of Plin, which seems to replace all other PAT proteins (168, 169).

The specific coat of PAT proteins on LD determines how cells of different tissues manage their lipid stores. Cells which have a high turnover of lipids, such as adipocytes, hepatocytes, muscle cells and steroidogenic cells, express many different PAT proteins, whereas cells, which are basically not specialized for TG storage or management, express only Adrp and Tip47 (155). Very recently it has been observed in OP9 cells, that, under conditions which favor DG accumulation, the exchangeable PAT proteins Tip47 and S3-12 are recruited to DG-enriched membrane areas of the ER and also LD (171). This may be the branch point between lipid storage and membrane expansion thus linking LD formation to energy availability and cell growth.

4.5. PAT proteins also manage lipid homeostasis in macrophages

The time-dependent induction of Adrp mRNA in human macrophages after incubation with oxLDL was first shown in 1999 by Wang et al. (172). Adrp was found to be a key player in macrophage foam cell formation in vitro. It was shown to support the accumulation of TG and CE by stimulating TG biosynthesis and inhibiting β-oxidation after over-expressing Adrp and loading with acLDL (173). VLDL was also shown to be a strong inducer of Adrp protein expression. In vivo, Adrp was found to be the predominant PAT protein in atherosclerotic plaques (174). Consistent with the in vitro findings, silencing of Adrp expression resulted in reduced LD formation in macrophages of atherosclerotic plaques in apoE (-/-) mice, which was enough to prevent atherosclerosis in those mice (175).

Attention was drawn to a possible role also for Plin in atherosclerosis due to the finding that both Plin mRNA and protein were expressed in human atherosclerotic plaques and also in the arterial wall surrounding the atheromas (in particular in VSMC). Plin expression was found to be increased inside the plaques, in ruptured atherosclerotic plaques being located in cells surrounding cholesterol crystals and in foam cells (176, 177). Bearing in mind the regulatory role of Plin in LD metabolism in adipocytes, its increased expression might indicate reduced lipolysis leading to increased lipid retention and plaque destabilization. Together with modifications of key regulators of cholesterol metabolism, Plin over-expression in atherosclerotic plaques could further favor cholesterol accumulation. In human macrophages Plin expression was shown to be increased during differentiation from monocytes, but not by loading with oxLDL, acLDL or VLDL. Over-expression of Plin in THP-1

macrophages resulted in LD formation and TG accumulation, also when Adrp was silenced (178).

Tip47 was shown to be present in the plasma membrane and to form clusters when human macrophages were incubated with oleate. In the absence of Adrp, Tip47 was shown to be recruited to LD. The fact that Tip47 protein expression correlated with cellular TG levels, but not cholesterol levels, led to the conclusion that Tip47 could be a cargo protein for fatty acids (179).

4.6. Other proteins with similar functions to the PAT proteins

In vertebrates and insects, two additional members of the PAT protein family, LSD1 and LSD2, were found (Fig.9). Both proteins are expressed in fat bodies which resemble adipose tissue and the liver. The function of both proteins is controlled by phosphorylation indicating functional similarity with Plin A (180). Recently, members of the CIDE protein family were also shown to associate with LD (181). This family includes three members in mice (Cide a, b and c (Fsp27)) and in humans (CIDE a-c). Their N-terminus shows sequence similarity with the regulatory domains of apoptotic DNA fragmentation factors (182). Moreover Cidea and Cidec contain regions with low, but significant similarity to PAT protein family members: an N-terminal region which is similar to Adrp, a segment which is also found in Plin and thought to mediate the shielding of LD from lipases and two regions which are thought to be responsible for the binding of PAT proteins to LD (183). A similarity with the PAT domain was not observed (184). Cidea is highly expressed in brown adipose tissue in mice (185) and WAT in humans and was shown to co-localize with Plin (184). The current hypothesis is that CIDE proteins also promote TG storage in adipose tissue. As a consequence, FFA in the circulation decrease, saving muscle and liver from increased FA concentrations, thereby preventing the development of peripheral insulin resistance (184).

4.7. Structural and functional motifs of the PAT protein family

An N-terminal sequence of 100 amino acids (PAT1 region) is the most highly conserved region and is eponymous for this protein family (Fig.9). The PAT domain is shared between the Plins, Adrp, Tip47 and OXPAT, but not S3-12 and it can also be found in LSD1 and LSD2. The function of this sequence has not been established so far but it is obviously not necessary for targeting Plin to LDs (186, 187). Overlapping with this region, tandem repeats of an 11-mer sequence can be found in all members of the family, whereas it has its greatest extension in S3-12. This sequence is predicted to form amphipathic α-helices which may help in embedding the proteins into the LD phospholipid monolayer. It was shown that

deletion of a part or all of the 11-mer sequences leads to reduced targeting of OXPAT (188), but not Tip47 (189) or Plin (186), to the LDs. Furthermore, Adrp, Tip47 and OXPAT contain a 4-helix bundle of amphipathic α-helices (190) which has a similar sequence in Adrp and OXPAT. The same motif can also be found in lipid-free apoE in which opening of the bundle enables the hydrophobic surfaces of the helices to be embedded into the acyl-chains of the phospholipid monolayer (191, 192). In Plin this region is completely absent. Instead three sequences of moderate hydrophobicity and a highly acidic sequence can be found, the former being necessary for targeting and anchoring Plin to the LD (183). At the C-terminus Adrp, Tip47, OXPAT and S3-12 contain a highly conserved sequence of 14 amino acids that fold into hydrophobic clefts (190). Characteristic and unique for Plin A is a dispersed six consensus sequence for the phosphorylation of serine residues by protein kinase A (PKA). In humans, Plin A has 6 phosphorylation sites, Plin B and C have only the first two phosphorylation sites depending on the species (150).

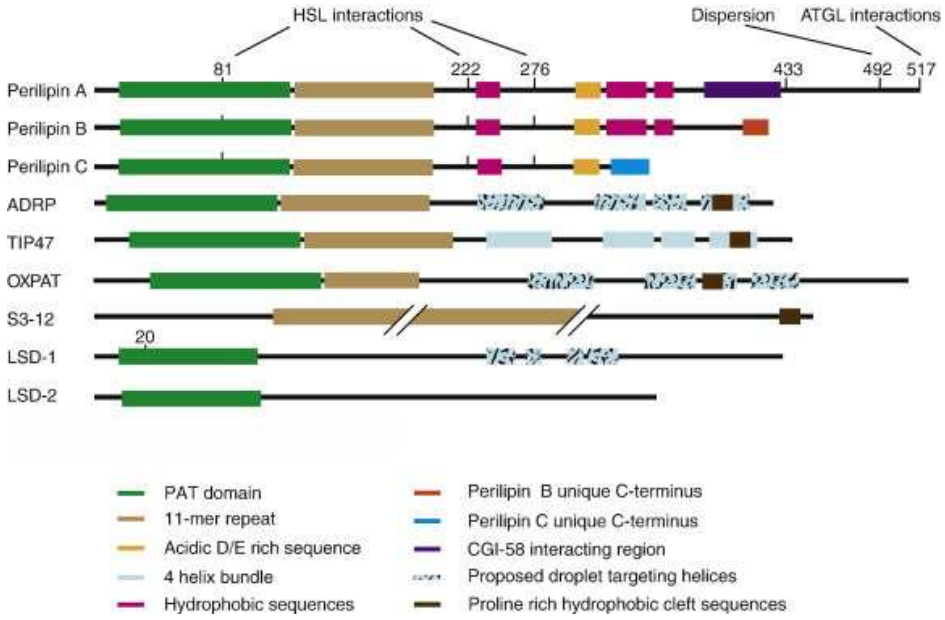

Fig.9: Structural motifs that characterize the members of the PAT protein family. The members of the PAT protein family partly share conserved motif regions (193).

The highest similarity in the amino acid sequence is shared between Adrp and Tip47 (43%). OXPAT shares 30% sequence similarity with Tip47 and 26% with Adrp. Plin and S3-12 have divergent amino acid sequence compared to Adrp, Tip47 and OXPAT and even to each other. A highly specialized function for Plin and S3-12 in adipocytes and a few other cell

types can therefore be suggested due to the divergence in their amino acid sequence and the restricted tissue expression pattern (150).

Leading scientists in the field of LD biology ruled that the current nomenclature for the PAT-proteins is insufficient to reflect the evolutionary relationship and shared functions between the different members of the PAT-protein family. Therefore a unifying nomenclature was recently established (194). PERILIPIN was selected as the founding root with Plin/PLIN as gene symbols for the murine and human genome. Following the Plin/PLIN gene symbol, each family member was numbered sequentially with PLIN1 for perilipin, PLIN2 for adipophilin, PLIN3 for Tip47, PLIN4 for S3-12 and PLIN5 for LSDP5. The four splice variants of PLIN1 were named PLIN1a-d (194).

5 MATERIALS

5.1. Chemicals and solutions used for cell culture experiments

Tab.1: Chemicals and solutions used for cell culture experiments

chemical/solution	Company
aggLDL	self made
Albumin, bovine serum, fraction V	Sigma-Aldrich
Albumin, bovine serum, fraction V, fatty acid free	Sigma-Aldrich
DMSO	Merck
DTT	Sigma-Aldrich
Dulbecco´s modified eagle´s (DMEM) medium	Gibco
EDTA	Roth
Fungizone	Gibco
Glucose	Sigma
Human serum extract	self made
KBr	Roth
KCl	Merck
KOH	Merck
LPDS	self made
L-cystein	Serva
NaOH	Roth
NaCl	Merck
Oleate	Sigma-Aldrich
PBS	self made
Penicillin/streptomycin	Cambrex
Peptone 140	Gibco
Peptone 110	Gerbu Biochemicals
Protease inhibitor cocktail (PIC)	Sigma-Aldrich
Sodium chloride	Roth
Sodium sulfite	Merck
Sodium thioglycollate	Sigma
3% thioglycollate medium	self made
Tris	Roth
Triton X100	Merck
Trypsin	PAA
VLDL	self made

3% thioglycollate medium

17g	Peptone 140
3g	Peptone 110
0.25g	L-cystein
6g	Glucose
2.5g	Sodium chloride
0.5g	Sodium thioglycollate
0.1g	Sodium sulfite
0.7g	Agar

components were dissolved in 1l ddH_2O and sterile filtrated.

5.2. Chemicals and solutions used for molecular biological techniques

Tab.2: Chemicals and solutions used for molecular biological techniques

Chemical/solution	**company**
Agarose	Gibco
Bromo phenol blue	Merck
Chloroform	Fluka
ddH_2O	Fresenius
Diethylpyrocarbonate (DEPC)	Sigma.Aldrich
DNA 100bp latter	Fermentas
Ethanol	Merck
Ethidium bromide	Sigma-Aldrich
Formaldehyde	Sigma-Aldrich
High-Capacity cDNA reverse transcription Kit	Applied Biosystems
Isopropanol	Merck
β-Mercaptoethanol	Merck
Morpholinopropansulfonicacid (Roth)	Roth
Primer	Invitrogen
QuantiFast SYBR green Kit	Qiagen
RNAse Inhibitor	Qiagen
TAE Buffer	self made
TRI-Reagent	PeqLab

DEPC water:

400µl DEPC were added to 400ml ddH_2O. The mixture was leaved under the hood overnight and autoclaved on the next day.

10x MOPS buffer:

10.5g	MOPS
1.7g	Na-acetate
5ml	0.5M EDTA
200ml	DEPC-water

pH was set to 7 with 10N NaOH and finally the volume was filled up to 250ml with DEPC water.

RNA sample buffer:

1.44 ml	99.5% formamide
280µl	10x MOPS buffer
520µl	37% formaldehyde
400µl	dEPC water
s200µl	80% sterile glycerol
10µl	ethidium bromide

5.3. Chemicals and solutions used for biochemical methods

Tab.3: Chemicals and solutions used for biochemical methods

chemical/solution	**Company**
Acrylamid/bisacrylamid	Sigma Aldrich
Ammonium persulfate (APS)	BioRad
BioRad protein reagent	BioRad
10x Blotting Buffer	self made
Boric Acid	Riedel de Haen
Butanol	Merck
$CaCl_2$	Merck
^{14}C-cholesteryl oleate	Amersham
Sodium Desoxycholate	Fluka
ECL Western Blotting detection reagents	Amersham
Fast Green	Serva
Glycerin	Merck
Glycerol Trioleate	Sigma-Aldrich
Glycerol tri [9,10(n)-^{3}H]oleate	Amersham
Glycin	Roth
Hexane	Roth
Isopropanol	Merck
K_2CO_3	Sigma
KH_2PO_4	Merck
Lysis Buffer	self made
Methanol	Roth
$MgCl_2$	Merck
Nile red	Sigma
[9,10(n)-^{3}H] oleic acid	Amersham
PAGE Ruler™	Fermentas
Phosphatidylcholine	Sigma-Aldrich
Phosphatidylinositol	Sigma-Aldrich
RIPA Buffer	self made
SDS	Serva
10xSDS running buffer	self made
SDS sample buffer	self made
Separating gel buffer	self made
Skim Milk	Interspar
Stacking gel buffer	self made
TEMED	Sigma Aldrich

Composition of the separating gel

Reagent	**8%**	**10%**
Acrylamid	2293µl	2867µl
Buffer 1	2170µl	2170µl
ddH_2O	4137µl	3563µl
10% SDS	100µl	100µl
TEMED	4.4µl	4.4µl
10% APS	76µl	76µl
Final volume	87804.4µl	87804.4µl

Composition of the stacking gel

reagent	**volume**
Acrylamid	326µl
Buffer 2	500µl
50% Glycerin	1650µl
10% SDS	21.5µl
TEMED	1.25µl
10% APS	19µl
Final volume	2517.75µl

All components of the separating and the stacking gel were mixed (except for TEMED and APS) and liquid gels were vented for 10-15 minutes under vacuum to allow a better movement and separation of the proteins loaded.

10x SDS running buffer:

30.3g	Tris
150.1g	Glycin
10g	SDS

volume was made up to 1l with ddH_2O.

Separating gel buffer (Buffer 1) 1.75M Tris/HCl pH 8.8:

18.2g	Tris
4ml	10% SDS
80ml	ddH_2O

pH was set to 8.8 with HCl and the volume was filled up to 1l.

Stacking gel buffer (Buffer 2), 0.5M Tris/HCl pH 6.8:

6g Tris were dissolved in 90ml ddH_2O, pH was adjusted to 6.8 with HCl and the volume was filled up to 100ml.

SDS sample buffer:

2.15g	SDS
0.76g	Tris
45ml	ddH_2O

pH was set to 6.8 with HCl and 10ml glycerol (80%) and some granules of bromphenolblue were added.

10x Blotting buffer:

12.1g	Tris
30g	Glycin
1mg/ml	EDTA

volume was made up at 1l with ddH_2O.

10x Blot washing buffer:

5g	Tween
90g	NaCl
100ml	1M TrisHCl pH 7.4

volume was made with 1l up with ddH_2O.

100mM Potassium phosphate lysis buffer

0.1M	KH_2PO_4
1mM	EDTA
0.25m	Saccharose
1M	DTT
1:2000	PIC

PIC (proteinase inhibitor cocktail) was always freshly added before use, pH was set with KOH to 7 (for neutral hydrolase activity assay) or 3.2 (for acidic hydrolase activity assay).

RIPA Buffer

50 mM	KH_2PO_4
150 mM	NaCl
1%	Triton X100
0.5%	Desoxycholate
1:2000	PIC

PIC was always freshly added

6 METHODS

6.1. Animals and diets

Animal experiments were performed in accordance with the standards established by the Austrian Federal Ministry of Science and Research, Division of Genetic Engineering and Animal Experiments (Vienna, Austria). C57Bl/6 (Himberg, Austria) and Plin (-/-) mice as well as apoE-deficient mice on a C57Bl/6 background (Charles River WIGA GesmbH, Sulzfeld, Germany) were maintained in a clean environment on a regular light-dark cycle (14 hours light, 10 hours dark) receiving a standard chow diet (Ssniff R/M H; Soest, Germany). For certain experiments, mice were fed with western type diet (WTD; TD88137 mod. containing 21% fat and 0.2% cholesterol, (Ssniff R/M H; Soest, Germany) for 2 or 6 month. Plin(-/-)/apoE(-/-) mice were obtained by crossbreeding Plin (-/-) and apoE (-/-) mice in our own animal facility.

6.2. Cell culture

All cells were cultivated in DMEM (25mM glucose, glutamin) supplemented with 1% streptomycin/penicillin and grown in a humidified incubator with 5% CO_2 at 37°C. Before use, media were pre-warmed to 37°C in a water bath.

6.2.1. Isolation of LDL and VLDL

LDL was isolated by gradient ultracentrifugation of human plasma. 1mg/ml sodium acide was added to the plasma to avoid bacterial contamination. Density of the plasma was adjusted to δ = 1.06g/l by adding ~10g/200ml plasma NaCl. Then, 1g EDTA and 1g sodium acide per l were added. 40ml plasma were put into beckman centrifugation tubes and centrifuged in the ultracentrifuge using a fixed angle rotor (Ti 60 or Ti 70.2) at 48000 rpm at 15°C for 24 hours. Two phases built up during this centrifugation: the upper containing VLDL and LDL and the lower containing Lp(a) as well as HDL. Both phases were dialysed versus distilled water for 30 minutes. Thereafter density of the LDL/VLDL phase was set again to δ =1.027g/l with NaCl. Separation of VLDL from LDL was performed by centrifugation at 48000 rpm and 15°C for 24 hours. After centrifugation, VLDL was found in the upper phase, LDL in the lower phase. Approximately 18ml of the LDL fraction were taken and density was adjusted to δ =1.063g/l. 3ml LDL fraction were put into high-speed centrifugation tubes and centrifuged for 24 hours at 48000 rpm at 15°C in a swing-up (SW-41) rotor. After centrifugation, the LDL fraction, which appeared as a yellow band of about 5 mm wide in the middle of the tube, was

aspirated and filtered through a crude filter into a shot on which a 40µm acetate sterile filter (Iwaki, Willich, Germany) was attached.

6.2.2. Preparation of aggregated LDL (aggLDL):

Native LDL was loaded on a PD10 column to get rid of salts. Cholesterol content of LDL was determined spectrophotometrically. Thereafter, native LDL was vortexed vigorously for 2 minutes, which yielded aggLDL.

6.2.3. Isolation of primary mouse peritoneal macrophages (Mpm)

Mice were injected intraperitoneally with 3ml of sterile 3% thioglycollate medium. After three days, mice were killed by cervical dislocation and Mpm were washed from the peritoneal cavity with 10ml of sterile PBS. Cells were harvested by centrifugation for 5 minutes at 800 rpm at 4°C. Mpm were resuspended in DMEM medium and seeded in 6-well plates or chamber slides. After 2 to 3 hours, cells were washed twice with PBS to remove non-adherent and dead cells. Mpms were immediately used for experiments.

6.3. MOLECULAR BIOLOGICAL METHODS

6.3.1. RNA isolation from cell lines with the Qiagen RNeasy Kit

In order to isolate RNA from cells, medium was aspirated and cells were washed once with PBS. Thereafter, the cells were lysed with 600µl RLT buffer supplemented with 10µl β-mercaptoethanol per ml RLT buffer. Cells were scraped off and the cell lysate was applied to Qia shredders to get rid of cell debris and proteins. After centrifugation for 2 minutes at 12000xg the eluate was diluted with the same volume (600µl) of 70% EtOH (diluted with DEPC water), mixed by pipetting up and down and transferred to RNeasy Mini Spin columns. After centrifugation at 10000xg for 30 seconds the flow-through was discarded and 700µl RW 1 buffer were added to the column. The flow-through was discarded and the column was washed two times with 500µl RPE buffer. Thereafter, the column was dried by centrifugation at 12000xg for one minute to get rid of the EtOH. RNA was eluted into 1.5ml RNase free tubes by adding 50µl RNase-free water, incubating for 1 minute and centrifugation at 10000xg for 1 minute. Elution was repeated with 25µl RNase-free water. The volume was concentrated to approximately 20µl using the SpeedVac and RNA concentration was measured photometrically (Nano drop spectrophotometer, Peqlab, Erlangen, Germany). RNA was stored at -70°C.

6.3.2. RNA isolation from murine tissues with peqGold TriFast^{Tm} reagent

Mice were killed by cervical dislocation and tissues were removed surgically as fast as possible. Tissues were immediately frozen in liquid nitrogen and stored at -70°C. 50-100 mg tissue were weighed and put into homogenization tubes (Precellys Peqlab, Erlangen, Germany) vials containing 1.44mm ceramic globes and 1ml TriFast (PeqLab, Erlangen, Germany) reagent. Samples were always kept on ice. Homogenization was performed with a homogenizer (Precellys 24, Peqlab; Erlangen; Germany) for 1x20 sec. at 5000 rpm. After 5 minutes incubation at room temperature, 0.2 ml chloroform per ml TriFast reagent were added for phase separation and vials were shortly vortexed. Incubation for 10 minutes at room temperature followed and centrifugation at 8500 rpm for 15 minutes at 4°C. The aqueous (upper) phase was transferred to a fresh tube and 0.5 ml isopropanol per ml TriFast reagent were added to precipitate the RNA. Incubation for 10 minutes at room temperature followed and centrifugation at 8500 rpm for 10 minutes at 4°C. The supernatant was removed and the pellet was washed with 1 ml 75% ethanol (diluted with DEPC water) per ml TriFast reagent. Centrifugation at 8500 rpm for 5 minutes at 4°C followed. Ethanol was removed and the pellet was air-dried for about 10 minutes. RNA was dissolved in 50 to 200 µl DEPC-water depending on the pellet size.

6.3.3. RNA quantification and quality control

RNA concentration was measured photometrically (Nano drop spectrophotometer, Peqlab, Erlangen, Germany) in 2 µl of the eluate. $C_{(ngRNA/\mu l)}=\lambda_{260nm}x40$.
RNA quality was controlled by applying 2µg RNA on an RNA gel. The RNA was mixed with 4µl 5x RNA sample buffer prior to loading on the gel in a total volume of 20µl. For the RNA gel 1.1g agarose were dissolved in 11 ml 10xMOPS and 81.9 ml DEPC-water by boiling in the microwave. 17.1 ml formaldehyd was added after cooling of the gel to approximately 60°C. The RNA gel was run at a voltage of 150 V for 45 minutes.

6.3.4. Reverse Transcription

Reverse transcription of RNA into cDNA was performed using the High capacity cDNA reverse transcription kit. 1 or 2µg RNA were diluted in 10µl nuclease free water for reverse transcription.

Tab.4: Components of the Master Mix for reverse transcription

Component	µl/reaction
10xRT Buffer	2.0
25xdNTP Mix (100mM)	0.8
10xRT random primers	2.0
MultiScribe™ Reverse Transcriptase	1.0
RNase Inhibitor	0.7
Nuclease free water	3.5
total per reaction	10µl
Final volume	20µl

Tab.5: Cycling conditions for reverse transcription

	Step1 primer extension	Step2 cDNA synthesis	Step3 Termination	Step4
Temperature	25℃	37℃	85℃	4℃
Time	10 min	120min	5sec	Infinite

6.3.5. Real time PCR using SYBR Green I

Real time PCR is a very sensitive method to quantify mRNA transcripts and small changes in their expression. The use of SYBR Green I, a fluorescent dye, enables analysis of different targets without the need to synthesize target-specific labeled probes. It binds all double-stranded DNA molecules, its excitation wavelength is at 521nm and a fluorescent signal is emitted at 494nm while binding. The M-MLV RT reverse transcriptase, which is used for extension, has to be activated in the first minutes of the PCR program thereby preventing miss-primed PCR products and primer dimers. PCR was performed with the Light Cycler 480 (Roche) using 96-multiwell plates.

Cycler conditions were:

Step 1: Initial activation of the M-MLV RT reverse transcriptase for 5 minutes at 95℃
Two-step cycling: 40 cycles

Step2: Denaturation of target cDNA for 10 seconds at 95℃.

Step3: combined annealing/extension for 30 seconds at 60℃ for both, annealing and extension

Step4: Cooling of the instrument

Melting curve analysis: for product analysis, a melting curve was performed at 95°C, 10 seconds (ramp rate 4.4°C/sec), 60°C for 20 seconds (ramp rate 2.2°C/sec) and 95°C continuous (ramp rate 0.11°C/sec). For the generation of the melting curve, temperature was increased from low (65°C) (where all PCR products are double-stranded and fluorescence was high) to high (95°C) (where PCR products are denatured) and fluorescence is measured continuously and plotted against temperature. Curves with peaks at Tm lower than that of the specific PCR product indicate primer-dimers. The design of optimal primer pairs is inevitable when performing real time PCR. Primers used were 18-24 nucleotides in length with about 50% GC-content and a melting temperature between 55-65°C. It was paid attention to that primer pairs had a similar melting temperature and GC-content for optimal annealing of both primers. The products amplified were below 500 base pairs. Tab.6 shows the primer sequences and amplicon sizes of genes analyzed by real time PCR. The primer sequences for Real time PCR were taken from the Harvard Primer Bank (http://pga.mgh.harvard.edu/primerbank/index.html) and all primers used had an annealing temperature of 60°C. For each primer pair the efficiency was calculated. For that purpose a pool of all original cDNAs (containing ~200ng of each cDNA) was diluted 1:5, 1:25, 1:125 and 1:625 with ddH_2O. The efficiency should be between 1.8 and 2.

Tab.6: Sequence of the forward and reverse primers used for real time PCR. Shown are the sequences, annealing temperatures and the amplicon size of the primer pairs.

Gene	forward primer sequence	reverse primer sequence	T(a)	amplicon size
mCylophilin	TTCCAGGATTCATGTGCCAG	CCATCCAGCCATTCAGTCTT	**60°C**	**202**
mPbgd	CTTGGACCTAGTGAGTGTGTTG	CTGAGCCATCTAGACTCCATAC	**60°C**	**172**
mTIP47	CTTCTCAGTCGGCTGCTGGA	GGACTGTGTGCGATGTGGCT	**60°C**	**179**
mS3-12	CGGCCCTTGTCGGAACTAAG	TCCTTCGTATTGGTGAGGACATT	**60°C**	**121**
mAdfp	GCAGCAGTAGTGGATCCGCA	TCTCGGCCATCTCACACACG	**60°C**	**148**
mPat-1	TGTCCAGTGCTTACAACTCGG	CAGGGCACAGGTAGTCACAC	**60°C**	**155**
mPlin	GGTGGCCTCTGTGTGCAATG	GATGCTGTTCCTGGCGCTTC	**60°C**	**244**
HSL-RT	GCTGGTGACACTCGCAGAAG	TGGCTGGTGTCTCTGTGTCC	**60°C**	**182**
ATGL-RT	GCCACTCACATCTACGGAGC	GACAGCCACGGATGGTCTTC	**60°C**	**175**

Total reaction volume for PCR was 10µl consisting of 5µl SybrGreenI Master Mix, 1µl forward primer, 1µl reverse primer and 3µl cDNA. Original cDNA was diluted 1:25 (when 1µg mRNA was reversely transcribed) or 1:50 (when 2µg mRNA was reversely transcribed). 6ng cDNA were used for all real time PCRs to be able to compare the crossing points of genes in different experiments and mRNAs. For PCR with the Plin primers, 5% DMSO was added to the reaction to avoid the formation of secondary structures. PBGD was used as internal normalization standard. Evaluation of the real time PCR data was performed using the REST program which has already included tools for statistical analysis (195, 196)

6.4. Biochemical methods

6.4.1. Preparation of cell lysates

Cells were plated in 6-wells and were allowed to adhere for 2-3 hours in DMEM+1% P/S. Cells were washed twice with ice-cold PBS and lysed with 120µl 100mM potassium phosphate lysis buffer (pH 7 (for acidic TGH activity) or pH 3.2 (for hydrolase activity assays)) or 100µl RIPA buffer (for Western Blotting) and were sonicated twice for 10 seconds on ice. Protein concentrations were determined according to the Bradford method (6.4.2.).

6.4.2. Protein quantification according to Bradford

The Bradford Assay is a common method to determine protein concentrations. It is based on Coomassie Brillant Blue (Bradford Reagent), which shifts its absorbance from 465nm to 595nm having bound to protein. For the assay, 200µl distilled water and 60µl Bradford reagent per sample were mixed and added. 15µl of the samples were put into a 96 multi-well plate. 260 µl of the diluted Bradford reagent were added, the plate was shaken vigorously and the reaction was allowed to proceed for 5 minutes. Protein content was measured photometrically at 595nm. A standard curve with BSA was prepared to calculate the protein concentration of the samples.

6.4.3 Extraction of lipids from tissues and cells

Extraction of lipids from tissue was performed following the protocol of Folch (197) with some variations. About 100 mg tissues were put into vials containing 1.44mm ceramic globes (Precellys, Peqlab; Erlangen; Germany). 1ml $CHCl_3$:MeOH (2:1) (v:v) was added and tissues were homogenized 2x20 seconds at 6500rpm in a homogenizer (Precellys, Peqlab, Erlangen, Germany). The homogenate was put into polypropylen vials and the vials were rinsed once with 1ml $CHCl_3$:MeOH (2:1). The lipids were extracted for 20 minutes on a spinning wheel at room temperature. Centrifugation followed for 10 minutes at 4000rpm (RT). The upper phase was taken off carefully and 1ml CHCl3:MeOH (2:1) was added to the rest of the homogenate and was centrifuged for 5 minutes at 4000 rpm (RT). Again the upper phase was carefully taken off. Non-lipid components were then removed from the homogenate by adding 0.2 volumes (600µl) of 50mM sodium chloride. After short vortexing and centrifugation for 2 minutes at 4000 rpm, the upper phase (which contains the non-lipid components) was discarded and the lower phase was transferred into pyrex glass vials. The $CHCl_3$:MeOH solvent was evaporated with nitrogen gas and lipids were dissolved in 1ml $CHCl_3$:MeOH (2:1) and stored at -20°C. 300µl of the lipid extracts were used for the

determination of the lipid concentration. The solvent was evaporated and 100µl 1% TritonX-100 (dissolved in chloroform) were added. Chloroform was evaporated and lipids were dissolved in 100µl distilled water for 15 min at 37°C in a water bath. Two to 5 µl of the extract were user for lipid determination and values obtained were referred to the tissue weight.

Lipids from MPMs were extracted with 2ml hexan:isopropanol (3:2, v:v) for one hour at 4°C. The solvent was evaporated with nitrogen and lipid extracts were re-dissolved in 100µl 1% Triton X-100, which was dissolved in chloroform. Chloroform was evaporated again and the lipids were dissolved in 100µl distilled water for 15 min at 37°C in a water bath. 50µl of the extract were used for TG determination, 15µl for TC and 15µl for FC determination. Lipid values were standardized to the protein content. Therefore the extracted cells were lysed for 2-3 hours in 1m NaOH at RT and the protein content was measured using Bradford Assay (6.4.2.).

6.4.4. Determination of lipid parameters from plasma and cell extracts

Lipid parameters were determined enzymatically using standard kits. The kits for FC and TG determination were from DiaSys (Holzheim, Germany), for TC measurement from Greiner Diagnostics (Langenthal, Switzerland) and for FFA determination from WAKO Chemicals GesmbH (Neuss, Germany). Five µl plasma were used for the measurement. The CE content was calculated by subtracting free cholesterol from total cholesterol and multiplying the value with the factor 1.7253 for esters.

6.4.5. Thin layer chromatography (TLC)

TLC is a method to separate different lipid classes. Chromatography was performed on Silica Gel 60 plates (Merck, Darmstadt, Germany) as stationary phase. Extracted lipids were evaporated and suspended in 100 µl human serum extract. 50µl of the lipid sample were applied on the silica gel plate which was run for 30 minutes in a chamber containing 50ml hexan:diethylether:acetic acid (65:35:1, v:v:v) as mobile phase. Lipids were visualized by incubation of the plate with iodine vapor for 5 minutes. The different bands corresponding to PL, FFA, TG, FC and CE were labeled with a pencil. On the next day, the bands were cut out and radioactivity was measured by scintillation counting.

6.4.6. Separation of plasma lipoproteins by fast protein liquid chromatography (FPLC)

200µl pooled plasma of overnight fasted mice were separated on a Pharmacia FPLC System (Karlsruhe, Germany) using a Superose 6 column (Amersham Biosciences, Piscataway, USA) as stationary phase. The different lipoprotein fractions were eluted with 10mM Tris in PBS, pH 7.4, 1mM EDTA, 0.9% NaCl and 0.02% NaN_3 with a flow of 0.5 ml/min. Sixty fractions of 0.5 ml were collected and 50µl of each fraction were used for lipid determination. Lipid determination was performed enzymatically (6.4.4.). Sodium-3,5-dichloro-2-hydroxybenzenesulfonate (DHBS) (Sigma-Aldrich) was added to the respective reagents to enhance sensitivity.

6.4.7. Fatty acid uptake

The fatty acid/BSA complex solution contained finally 500µM oleic acid and 700nM [9, 10 (n)-^{3}H] oleic acid. For example 2.8µl non radioactive oleic acid (dissolved in EtOH, 3.543M solution) and 20µl [9, 10 (n)-^{3}H] oleic acid were mixed and solvents were evaporated under the hood with N_2. 0.5ml 0.01M NaOH and 1,66ml 5%BSA (fatty acid free, dissolved in PBS) solution were added. After short vortexing the solution was incubated for 30 minutes at 70°C in a water bath. Finally 17.84ml DMEM+1%P/S were added to a final volume of 20ml.
Cells were kept overnight in DMEM+2%BSA (fatty acid free). On the next day, cells were washed twice with PBS and loaded with 2 ml of the complex-containing medium. Cells were incubated for 6 or 24 hours with 1ml of the "loading medium". After that, cells were washed twice with PBS and lipids were extracted as described (6.4.3.). 10µl of the lipid extracts were pipetted into a scintillation vial containing 4ml Scintillation cocktail and radioactivity was measured in a β-counter. Extracted cells were lysed with 1ml 0.3M NaOH and protein concentration was determined (6.4.2).

6.4.8. Assays for TG (neutral and acidic) and CE (neutral) hydrolase activities

As substrates, micelles of specific content were always freshly prepared:

Tab.7: Substrate components per sample.

Substrate (per sample)	**TGH**	**Substrate (per sample)**	**CEH**
non radioactive triolein	0.073µl	**non radioactive CO**	0.1087µl
PC/PI (3:1, w:w)	0.75µl (15µg)	**PC/PI**	1.775µl (35.5µg)
^{3}H-triolein [0.5µCi/µl] (tracer)	2µl	**^{14}C-cholesteryl oleate (tracer)**	2µl
final concentration	25nmol	**final concentration**	20nmol

Non radioactive triolein or cholesteryl oleate, PC/PI and radioactively labeled triolein or cholesteryl oleate were mixed and solvents were evaporated with N_2. After adding 50µl 0.1M potassium dihydrogenphosphate buffer (pH 7 (for neutral TGH activity) or pH3.2 (for acidic

TGH activity) per sample, the substrate was sonicated (Virsonic 475) twice for 1 minute with 1 minute on ice between. Thereafter 25µl 5% BSA (fatty acid free) per sample were added. The substrate was again sonicated two times with for 30 seconds with 1 minute on ice between. Finally 25µl 20% BSA (fatty acid free), were added. BSA was also dissolved either in 100mM potassium phosphate lysis buffer pH 7 (for neutral TGH activity) or pH 3.2 (for acidic TGH activity).

100µl substrate were incubated with 100µg cell homogenate (preparation see 2.4.1.). The tubes were put on 37°C in the water bath for 1 hour. After this, 3.25ml Stop solution (n-heptane:MeOH:$CHCl_3$ (10:9:7, v:v:v)) and 1ml 0.1M K_2CO_3-boric acid buffer (2,73g K_2CO_3/200ml; pH 10.5) were added per sample. Samples were vortexed for 5 seconds and centrifuged for 10 minutes at 3200 rpm and 4°C. 1ml of the upper, aqueous, phase was put into scintillation vials and radioactivity was measured with a β-counter.

Calculation of specific hydrolase activities

Lipase activity (nmol FFA/h*mg protein) =

$$(cpm_{(sample)} - cpm_{(spontaneous\ hydrolysis)} * FactorA) / cpm_{(100\mu l substrate)} =$$

Factor A=

$$\frac{\text{total volume of the upper phase x nmol total FFA/sample x correction protein to 1 mg}}{\text{extraction coefficient (0.76)}}$$

6.4.9. LPL activity assay

Cells were isolated, plated in 12-well plates and allowed to adhere in DMEM+1% P/S for 2-3 hours. After washing cells twice with PBS 300µl cells were incubated with DMEM +1% P/S + 2% BSA + 2U/ml Heparin for 1 hour at 37°C. WAT (positive control) was surgically removed, washed in PBS, weighed, minced with scissors and transferred to ice cold tubes. 1ml medium containing 2%BSA and 2 units heparin per ml were added and tissue was incubated for 1 hour at 37°C on a shaking incubator.

Substrate per sample was prepared by mixing 920ng non-radioactive glycerol trioleat, 0.6 µCi [^{3}H] triolein and 0.1% Triton X-100. Solvents were evaporated under the hood with N_2. Forty µl of Tris (1M, pH 8.6) and 80µl distilled water were added and the mixture was sonicated 3 times for 1 min with 1 min on ice between. Finally, 40µl heat-inactivated human

activator serum (containing apoCII as activator, obtained from different donors, inactivated for 60 min at 50°C, stored at -20°C) and 40µl 10% BSA (FFA free) were added.
For the assay, 200µl ice cold substrate were incubated with 100µl sample for 1 hour at 37°C in a water bath. After incubation samples were put on ice and 3,25 ml stop solution (n-heptane:MeOH:$CHCl_3$ (1.41:1.25:1,v:v:v)) per sample and 1ml 0.1M K_2CO_3-boric acid and 100mM potassium carbonate (pH 10.5) per sample were added. NEFA were extracted by vortexing for 10 seconds and phases were separated by centrifugation for 10 min at 4000 rpm, 4°C. One ml of the upper phase (aqueous) phase was put into scintillation vials containing 4ml Ultima Gold Scintillation cocktail and radioactivity was counted with a β-counter. Extracted cells were lysed with 1ml 0.3M NaOH and protein was quantified using the Bradford Assay (6.4.2.).

Calculation of Lipase activity

Lipase activity (µmol FFA/h/mg protein) =

$$\frac{cpm_{(sample)} - cpm_{(spontaneous\ hydrolysis)} \times Factor\ A}{cpm_{(200\mu l\ substrate)}}$$

Factor A=

$$\frac{\text{volume of the upper phase x µmol total FFA/ sample x2}}{\text{extraction coefficient (0.76)}}$$

2= correction for volume sample to volume substrate

6.4.10. Free fatty acid release

Cells were plated in 12-well plates in DMEM+1%P/S. After 2-3 hours, cells were loaded with a complex of BSA, 500µM non-radioactive oleic acid and 7nmol 9, 10 n [^{3}H] oleic acid (as tracer) in DMEM+1%P/S+10%LPDS for 24 hours. On the next day the medium was changed to DMEM+1%P/S+10%LPDS and 1% BSA as acceptor. 2.5µM triacsin C, a long chain fatty acyl CoA synthetase inhibitor were additionally added to avoid re-incorporation of the fatty acids into TG. Fatty acid release was followed over 6 hours. After 30 minutes, 1hour, 2, 3, 4 and 5 hours, 100µl medium were put in 4ml scintillation cocktail and radioactivity was measured with a β-counter. At each time point, 100µl removed medium were substituted with fresh “BSA acceptor medium”. In all experiments, fractional FFA release was corrected for

the radioactivity released into the medium without an acceptor. FFA release was expressed as the percentage of the radioactivity released from cells into the medium relative to the total radioactivity in cells and medium. Values were normalized to cell protein.

6.4.11. SDS-Polyacrylamid gel electrophoresis (SDS-PAGE)

SDS is a common method used to separate proteins according to their molecular weight. The SDS gel used was a discontinuous consisting of a separating and a stacking gel on the top. SDS on the one hand denatures proteins and also equalizes the charge of all proteins by binding in equal amounts. Due to their negative charge, the proteins move through the gel with large proteins moving slower than smaller ones.
After washing the cells twice with ice cold PBS proteins were harvested by lysing the cells with 120µl RIPA Buffer (50mM Tris·HCl pH 8.0 (0.605g/100ml), 150mM NaCl (0,876g/100ml), 1% Triton X-100 (1ml/100ml) and 0.5% desoxycholat sodium salt (0.5g/100ml)) and scraping them off on ice with a cell scraper. For total cell lysis, lysates were sonicated twice (on ice!) for 10 seconds with a sonication bar. Protein concentrations were determined using Bradford assay (198). Before loading onto the gel, samples were diluted with the same volume of SDS sample buffer (2.15g SDS, 0.76g Tris 10ml 80% glycerol and some granules of bromophenolblue). 60µl/ml β-mercaptoethanol were freshly added to the sample buffer and samples were boiled at 95° in a thermo block for 2 minutes for complete protein denaturation. Thereafter, samples were centrifuged at 12000 rpm to get rid of cell debris. Having applied the samples onto the gel proteins were separated by applying a voltage of 150V.

6.4.12. Immunoblotting

Proteins separated by SDS-PAGE were transferred onto a nitrocellulose membrane. Blotting components were thereby commonly assembled as shown in Fig.10.

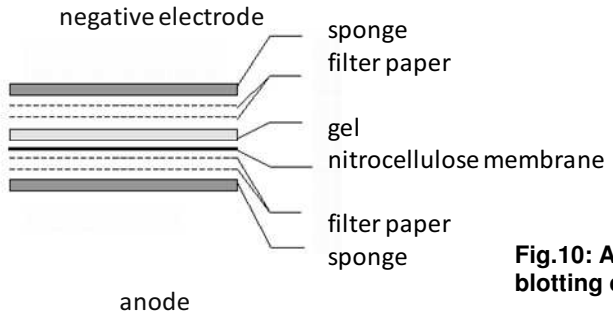

Fig.10: Assembly of the Western blotting components.

Proteins were transferred onto the membrane by applying a current of 150mA for 45 minutes. After the transfer the membrane was washed shortly with distilled water and proteins were visualized by incubating the membrane with FastGreen (100mg/100ml FastGreen, 100ml distilled water, 1ml acetic acid) for some seconds. Thereafter the membrane was neutralized with 0.01M NaOH. Finally unspecific binding sites of the membrane were blocked with 15ml 5% milkpowder or 3% BSA (both dissolved in 1x washing buffer) per blot for 1 hour at room temperature. After that the membrane was incubated with 10ml of the primary antibody (Tab.8) overnight at 4℃ on a shaker. On the next day the membrane was washed three times for 10 minutes with ~20ml blot-washing buffer. Then the membrane was incubated with the secondary antibody (Tab.8) for 2 hours at room temperature on a shaker. Afterwards, the membrane was washed with blot-washing buffer five times for 15 minutes. Detection of the proteins was performed by chemiluminescence using the ECL Western Blotting Substrate (Amersham Bioscience, Piscataway, NJ). The membrane was incubated with a mixture of peroxide solution (solution1) and luminal enhancer solution (solution2) (1:1 ratio) for 3 minute and then wrapped into a cling film. The wrapped blot was placed into a film cassette and an x-ray autoradiography film was applied on the top of the membrane. Exposure times varied from 1 minute to 1 hour depending on the antibody used.

Tab.8: Dilutions of primary and secondary antibodies

Primary antibody	**Dilution**	**Company**
Adrp (mouse,human) (sc-32448)	1:500	Santa Cruz
Plin (mouse, human) (GP29)	1:1000	Progen
Tip47 (mouse,human) (sc-14723)	1:500	Santa Cruz
S3-12 (human) (GP34)		Progen
PAT-1 (mouse,human)	1:1000	Progen
β-Actin	1:2000	Santa Cruz
ATGL	1:1000	Cell signaling
Secondary antibody	**Dilution**	**Company**
Polyclonal Rabbit-Anti-Goat IgG-HRP	1:2000	Dako Chemicals
Polyclonal-Goat-Anti-Guinea Pig IgG-HRP	1:10000	Dianova
Polyclonal Goat-Anti-Rabbit IgG-HRP	1:2000	Calbiochem
Polyclonal-Rabbit-Anti-Mouse IgG-HRP	1:1000	Dako Chemicals

6.4.13. Nile red staining

Cells were washed twice with PBS and were fixed with 1ml 4% formaldehyd for 20–30 minutes. Thereafter cells were washed three times with 1 ml PBS and were incubated with 1ml nile red (2.5µg/ml) for 3 minutes. Cells were again washed twice with PBS. Two drops of

mounting medium vectorshield with DAPI (Vector Laboratories, Burlingame, CA, USA) were added onto the cells. Slides were kept at 4°C in the fridge. LD were visualized by confocal laser scanning microscopy using an LSM 510 META microscope (Carl Zeiss GmbH, Vienna, Austria).

6.4.14. Glucose tolerance test

Before performing the tolerance test, mice were fasted overnight. A glucose solution (2g glucose monohydrate/10ml water) was prepared. Mice were gavaged with 2g/kg glucose. After 0 (before gavaging), 15, 30, 60 and 120 minutes, blood glucose concentration was measured using “AccuCheck active” (Roche, Vienna, Austria) and the according test stripes. Blood was taken from the tail of the mice. Therefore, mice were anesthesized for a short time with isofuran and tail tipped.

6.4.15. Preparation of histological sections and atheroassays

Mice were euthanized using approximately 100 µl of nembutal (1g/50ml) and the heart was perfused for about 10 min with PBS. The upper two-thirds of the heart were fixed in 4% formaldehyd and kept at 4°C. One day before cutting cryosections with a freeze-microtome (Microm HM 500, Fisher Scientific, Walldorf, Germany), tissues were put into Tissue-Tek O.C.T (Sanova Pharma GesmbH Diagnostik, Vienna, Austria) in eppendorf vials and kept at 4°C. After approximately 600 µm, 8 µm cryosections of the aortic root were cut.

6.4.16. Oil red staining

Cryosections were stained with oil red O (Sigma, Vienna, Austria) and counterstained with hemotoxylin (Richard-Allen Scientific, Kalamazoo, MI).

Oil red stock solution (150ml): 0.75g Oil red (Merck, Vienna, Austria) in 150ml isopropanol, kept overnight at RT

Oil red working solution (200ml):
135 ml oil red stock solution
90 ml distilled water

The immunohistochemical sections were fixed in 60% isopropanol for 5 minutes at RT. Thereafter they were stained for 10 minutes in oil red (working solution) and destained in 60% isopropanol. After short washing with distilled water, sections were counterstained with

hemotoxylin (Richard-Allen Scientific, Waltham MA, USA) for 3 minutes. Bluecoloration was performed using NH_4-water (4,375ml 20% NH_4/ 1000ml water). Finally, sections were fixed by adding two drops of glycerin gelatine (Merck, Vienna, Austria) and covered with coverslips.

6.4.17. Statistics

Statistical analyses were performed with GraphPad Prism 5.0 using the Student's t-test. Significance levels were set * ($p<0.05$), ** (0.01), *** (0.001)

7 RESULTS

7.1 Expression profile of Plin in murine tissues, macrophages and foam cells

First, Plin mRNA expression in tissues, macrophages and foam cells was examined by Real-time PCR. Highest Plin mRNA levels were found in WAT. To a much lower extent, Plin mRNA was detected in skeletal muscle (SM) and the brain. In macrophages and foam cells, the amount of Plin mRNA was about one twentieth of that in WAT. There was no difference in Plin mRNA expression between macrophages and foam cells (Fig.11).

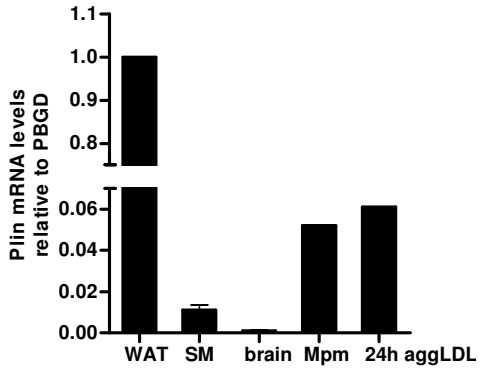

Fig.11: Plin mRNA expression in WAT,SM, macrophages and foam cells. Peritoneal macrophages from male wild type and Plin (-/-) mice were cultivated in the absence or presence of aggLDL for 24 hours. Total RNA from macrophages and tissues was isolated and Plin mRNA concentrations were determined by real time PCR 5% DMSO were added to the PCR reaction to avoid the formation of secondary structures. Plin mRNA quantities were normalized to PBGD as housekeeping gene and mRNA levels shown were set in relation to the expression in WAT (arbitrarily set to 1)

7.2. THE ROLE OF PLIN IN MACROPHAGES

7.2.1. The impact of Plin deficiency on LD morphology in foam cells.

In adipocytes, Plin is a structural component of LD and there is evidence that it also plays an important role in foam cell formation in vivo since it was found to be highly expressed in macrophages of atherosclerotic lesions. Therefore the first question I wanted to answer was whether Plin deficiency had an impact on LD morphology in foam cells with regard to their size or total number. I loaded macrophages from wild type and Plin deficient mice with VLDL for 6 and 24 hours. Each condition was performed in triplicate. Nile red staining was performed and LD within the cells were visualized with a laser scanning microscope. Virtual 0.31µm sections were evaluated along the z-axis. Depending on cell dimensions, 20 to 30 sections were recorded and LD were counted in each z-stack. Five pictures of each well were taken and evaluation was performed using ImageJ. The average number of LD was referred to the average cell number and the average area of the LD was referred to the area covered by the cell bodies.

Wt 6h VLDL

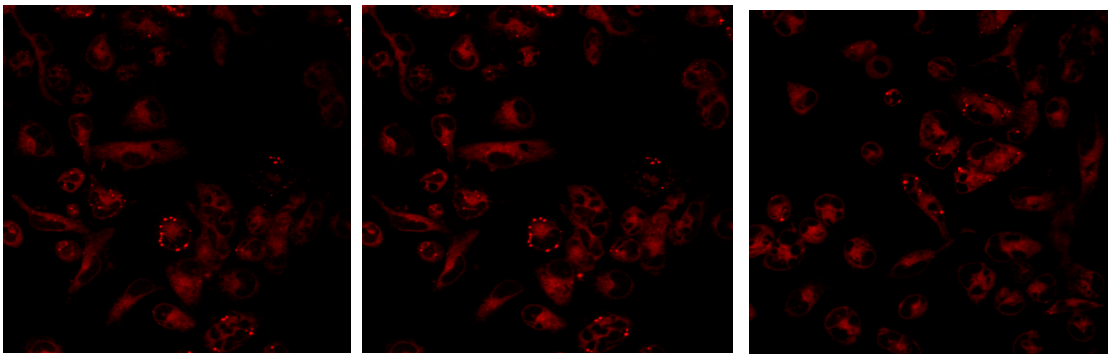

Plin (-/-) 6h VLDL

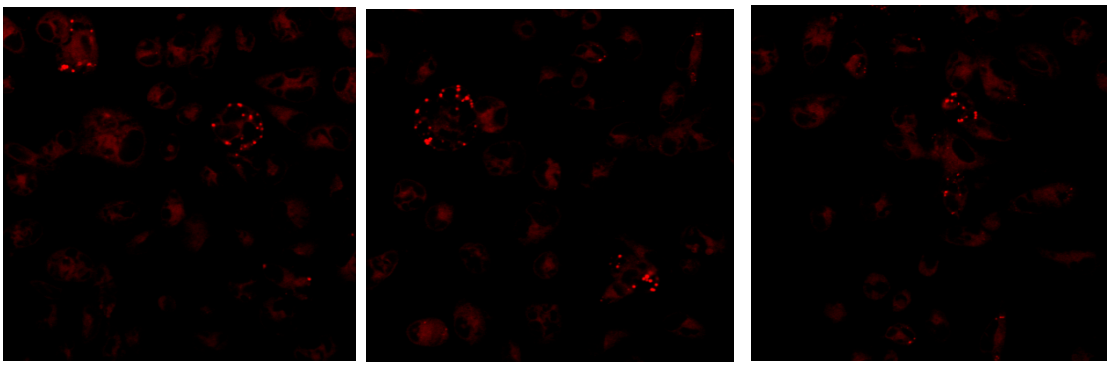

Wt 24h VLDL

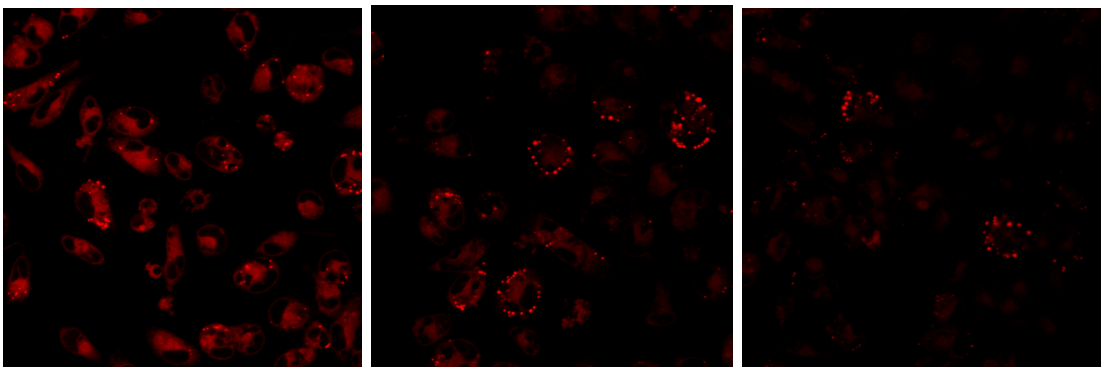

Plin (-/-) 24 VLDL

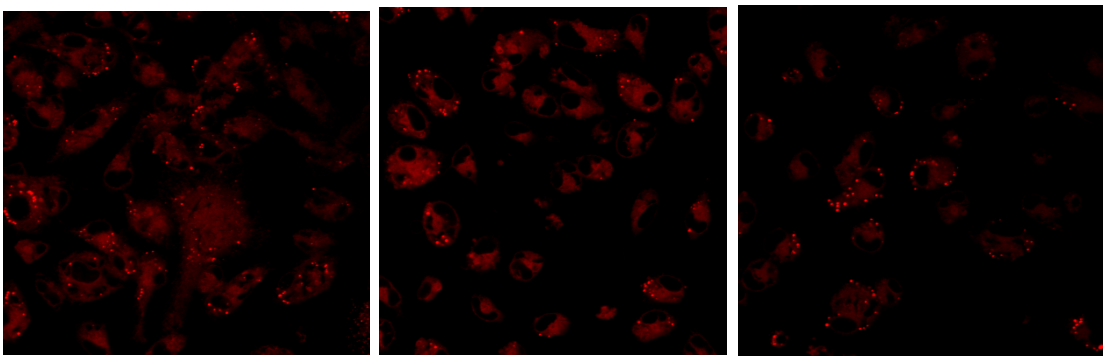

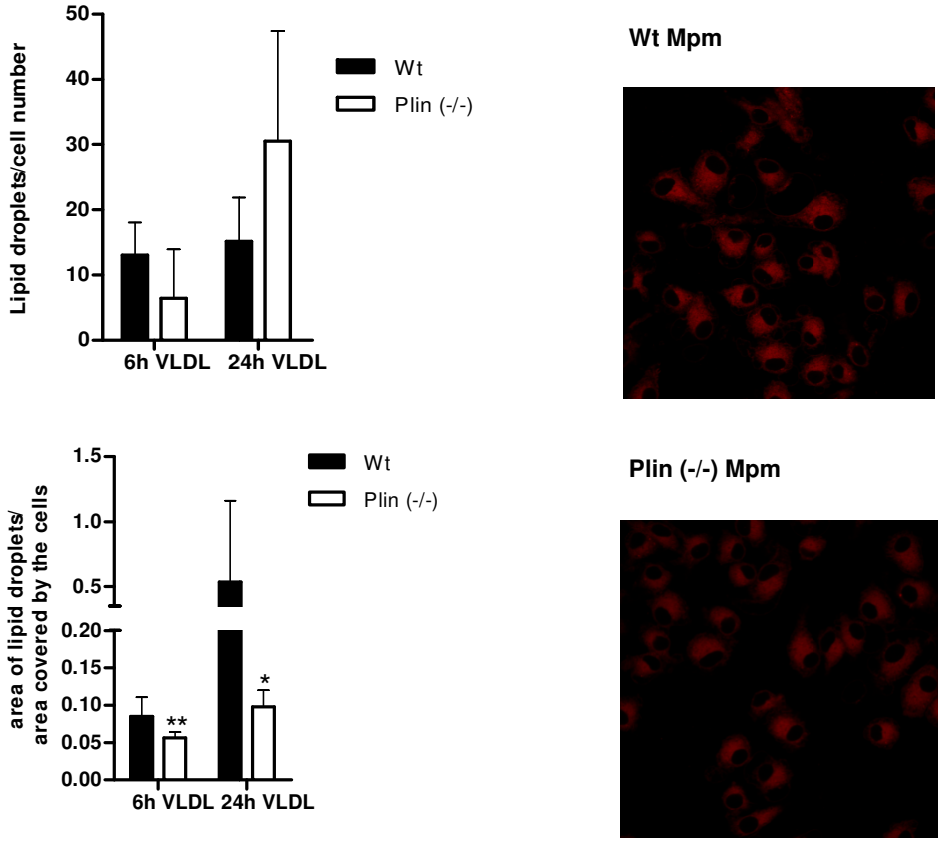

Fig.12: Microscopy of nile red stained wild type and Plin (-/-) macrophages and foam cells. Peritoneal macrophages from wild type and Plin (-/-) mice were cultivated in DMEM containing 10% LPDS, 1% P/S in chamber slides in the absence or presence of VLDL (100µg/ml) for 6 or 24 hours. After the incubation for 6 or 24 hours, cells were stained with nile red. Each condition was performed in triplicate. From each triplicate, 5 pictures were taken, showing 20-40 cells. Virtual 0.31µm sections were evaluated from each picture along the z-axis. Depending on cell dimensions, 12 to 30 sections were recorded and LDs were counted in each z-stack. Data were evaluated using ImageJ. Values represent mean ± SD. * ($p<0.05$), ** ($p<0.01$).

No LD could be found in wild type and Plin (-/-) macrophages (Fig.12). Wild type foam cells had on average more LD per cell at earlier time points (after 6 hours) but this was inverted after longer loading (after 24 hours) when Plin (-/-) foam cells had more LD, however, the differences did not reach statistical significance. LD were constantly smaller in Plin (-/-) foam cells ranging from 29% smaller LD after short time loading (6 hours) to 82% after longer loading (24 hours) (Fig.12).

7.2.2. Plin deficiency and its influence on macrophage lipid content

Since Plin deficiency obviously has an impact on the size of LD in macrophages I investigated whether this was also reflected in the lipid content of macrophages and foam cells. To achieve foam cell formation, cells were loaded with aggLDL or VLDL.

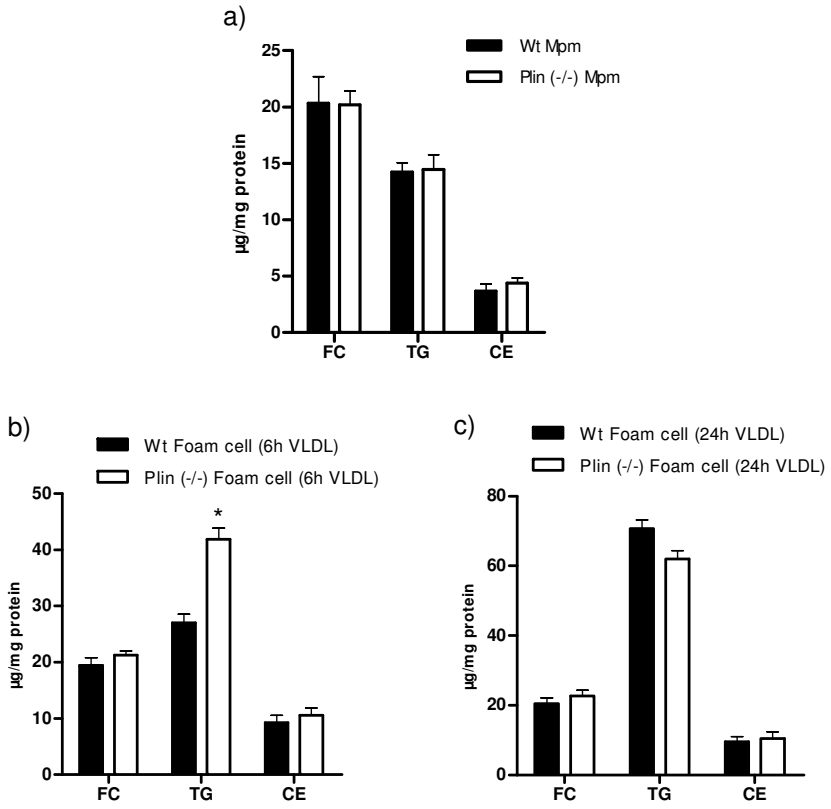

Fig.13: TC, FC, TG and CE concentrations of female wild type and Plin (-/-) macrophages and foam cells. (a) Peritoneal macrophages from wild type and Plin (-/-) mice were cultivated in FFDMEM+10%LPDS in (a) the absence or (back) presence of VLDL (100µg/ml) for 6 or 24 hours. Lipids were extracted and lipid parameters were determined enzymatically. Values represent mean of two representative experiments performed in triplicate ± SD. * ($p<0.05$).

No differences were observed in FC, TG or CE concentrations between female wild type and Plin (-/-) macrophages (Fig 13a). After loading with VLDL for 6 hours, TG concentrations were increased 1.5-fold in Plin (-/-) foam cells compared to wild type cells, while FC and CE concentrations were the same (Fig.13b). After 24 hours loading with VLDL, no difference between FC, TG or CE concentrations could be observed comparing both genotypes (Fig.13c).

After 48 hours loading with aggLDL, male Plin (-/-) macrophages had 17% decreased TG and slightly increased CE concentrations compared to wild type foam cells, while both had equal FC concentrations (Fig.14a). After 48 hours loading with VLDL male Plin (-/-) macrophages had reduced FC and TG concentrations (29% and 12%, respectively) compared to wild type foam cells while showing equal CE concentrations (Fig.14b).

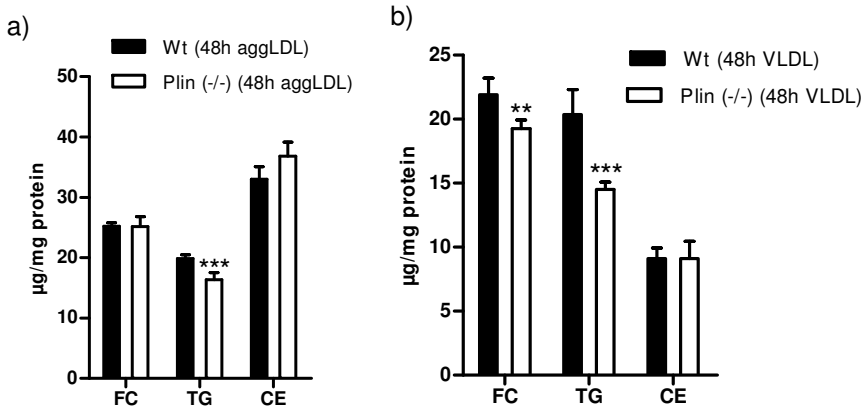

Fig.14: TC, FC, TG and CE concentrations of male wild type and Plin (-/-) foam cells. Peritoneal macrophages from wild type and Plin (-/-) mice were cultivated in the presence of (a) aggLDL (50µg/ml) or (b) VLDL (100µg/ml) for 48 hours. Lipids were extracted and lipid parameters were determined enzymatically. Values represent mean of one experiment performed in triplicate ± SD. * ($p<0.05$), ** (0.01), *** (0.001).

7.2.3. Effect of Plin deficiency on neutral TG and CE hydrolase activities in macrophages

The phenotype of smaller LD can either arise from an increased lipase activity, or other processes that drive the degradation of LD, or from an impaired formation. Thus, I wanted to find out whether the absence of Plin possibly has an impact on the overall activity of TG or CE hydrolases and consequently on LD degradation. Activity assays for neutral TG and CE hydrolases were performed with macrophages isolated from male and female wild type and Plin (-/-) mice.

Neutral TG and CE hydrolase activities were identical in female Plin (-/-) foam cells compared to control cells (Fig.15a, b). Plin deficiency in male macrophages reduced neutral TG hydrolase activity by 31% compared to wild type cells (Fig.15c), while no difference could be found in the neutral CE hydrolase activity (Fig.15d).

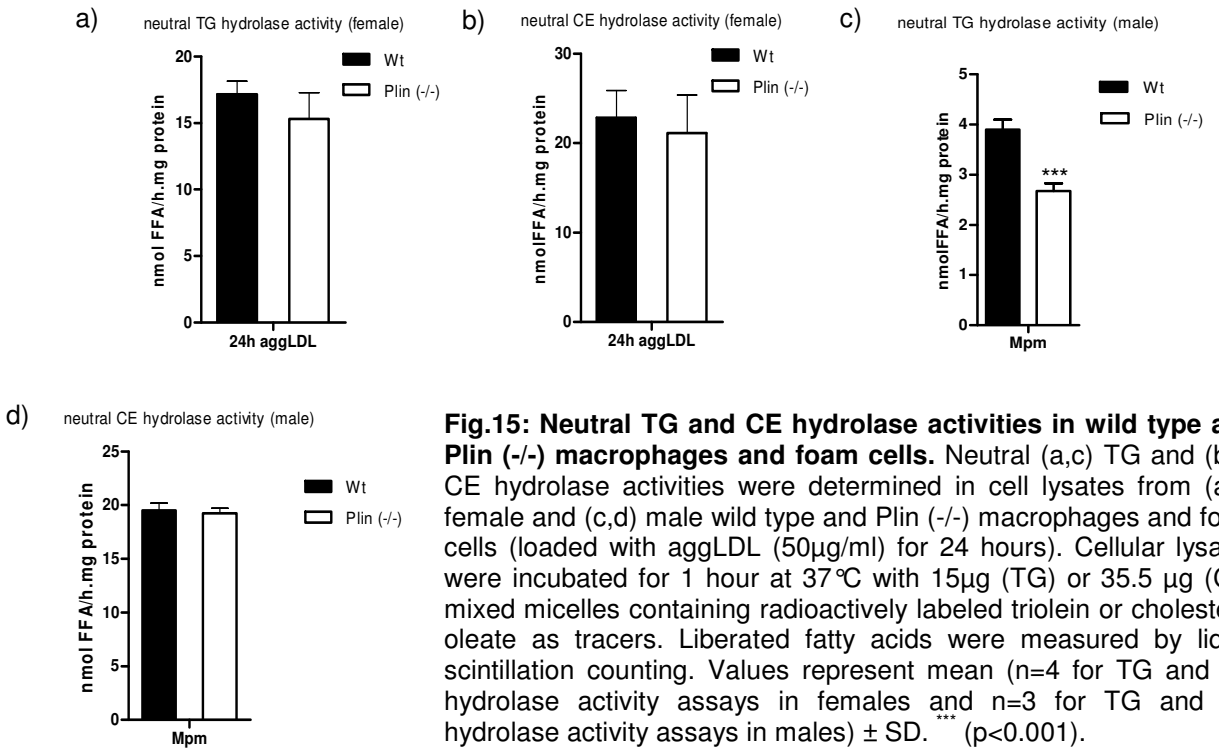

Fig.15: Neutral TG and CE hydrolase activities in wild type and Plin (-/-) macrophages and foam cells. Neutral (a,c) TG and (b,d) CE hydrolase activities were determined in cell lysates from (a,b) female and (c,d) male wild type and Plin (-/-) macrophages and foam cells (loaded with aggLDL (50µg/ml) for 24 hours). Cellular lysates were incubated for 1 hour at 37°C with 15µg (TG) or 35.5 µg (CE) mixed micelles containing radioactively labeled triolein or cholesteryl oleate as tracers. Liberated fatty acids were measured by liquid scintillation counting. Values represent mean (n=4 for TG and CE hydrolase activity assays in females and n=3 for TG and CE hydrolase activity assays in males) ± SD. *** ($p<0.001$).

7.2.4. ATGL and HSL mRNA expression in wild type and Plin (-/-) macrophages and foam cells.

In addition to the neutral hydrolase activities, I investigated mRNA and protein expression of ATGL and HSL in macrophages and foam cells.

While ATGL mRNA quantities were increased 1.6-fold after 6 hours loading, they were lower (22%, without statistical significance) after 24 hours loading with VLDL in Plin (-/-) foam cells compared to wild type cells (Fig.16a). After 48 hours loading with aggLDL equal amounts of ATGL mRNA were found in wild type and Plin (-/-) foam cells (Fig.16b). ATGL protein content was by tendency lower in Plin (-/-) macrophages and foam cells (18% and 16%, respectively) but these differences are negligible (Fig.16c). Plin deficiency did not show a significant effect on ATGL protein content when Western blot analysis was performed once with protein from macrophages pooled from three mice. Therefore it was not repeated and subsequently no statistical evaluation was indicated.

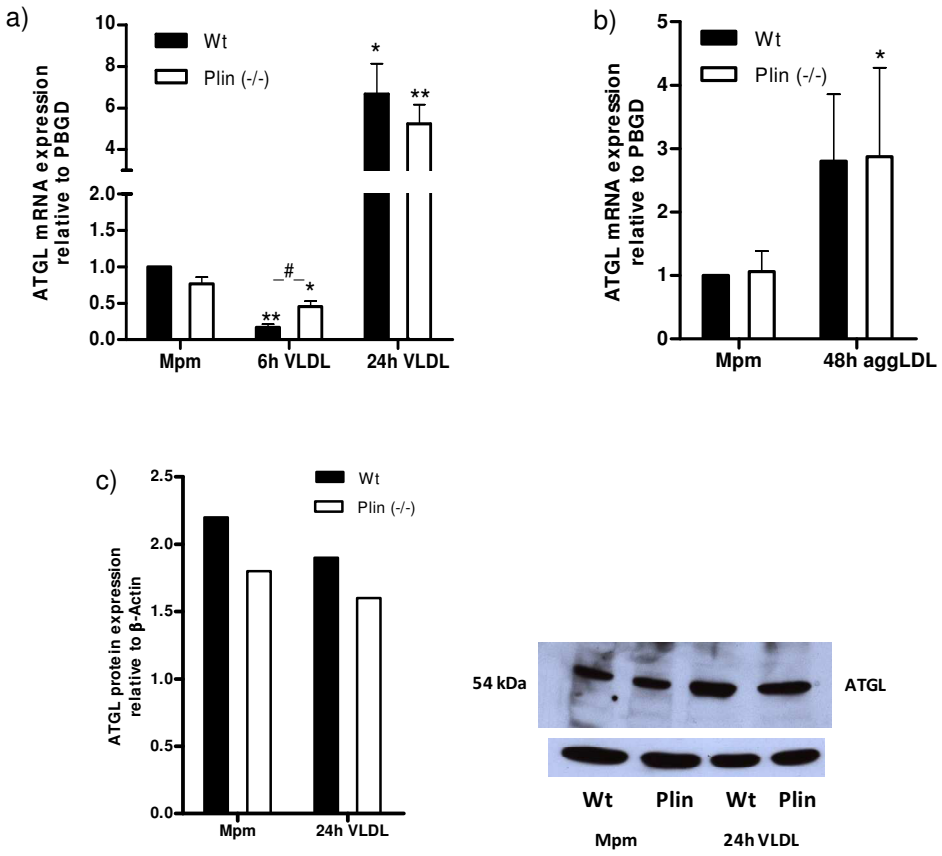

Fig.16: ATGL mRNA and protein expression in wild type and Plin (-/-) macrophages and foam cells. Peritoneal macrophages from wild type and Plin (-/-) mice were cultivated in the absence or presence of (a) VLDL (100µg/ml) or (b) aggLDL (50µg/ml) for 6, 24 or 48 hours. Total RNA was isolated and ATGL mRNA concentrations were determined by real time PCR. mRNA quantities of ATGL were normalized to PBGD as housekeeping gene and mRNA levels shown were set in relation to the expression in wild type macrophages (arbitrarily set to 1). Data were evaluated with the REST program. Values represent mean (n=3) ± SEM. * ($p<0.05$), ** ($p<0.01$). (c) Peritoneal macrophages from 3 wild type and Plin (-/-) mice were pooled. After cultivation in the absence or presence of VLDL (100µg/ml) for 24 hours, macrophages were lysed in RIPA buffer. 50µg protein were separated on a 10% SDS gel and Western Blot analysis was performed using an specific anti-ATGL antibody.

Negligible lower (26%) HSL mRNA concentrations were found in Plin (-/-) foam cells after 24 hours loading with VLDL but this difference was without statistical significance. After loading with aggLDL for 48 hours there was no difference in the HSL mRNA quantities comparing wild type and Plin (-/-) foam cells (Fig.17b).

HSL protein content was identical comparing macrophages and foam cells as well as wild type and Plin (-/-) cells. Due to lack of differences in the HSL protein content in wild type and Plin (-/-) foam cells, Western blot analysis was only performed once and therefore no statistical evaluation was indicated.

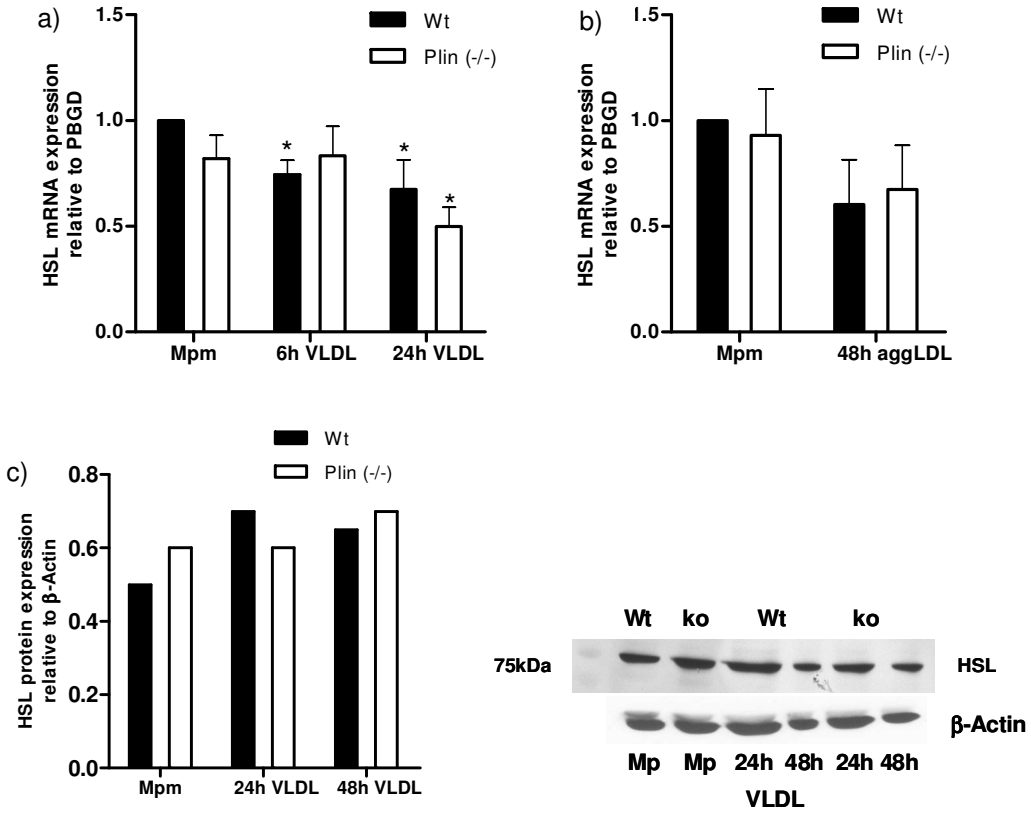

Fig.17: HSL mRNA and protein expression in wild type and Plin (-/-) macrophages and foam cells. Peritoneal macrophages from wild type and Plin (-/-) mice were cultivated in the absence or presence of (a) VLDL (100µg/ml) or (b) aggLDL (50µg/ml) for 6, 24 or 48 hours. Total RNA was isolated and HSL mRNA concentrations were determined by real time PCR. mRNA quantities of HSL were normalized to PBGD as housekeeping gene and mRNA levels shown were set in relation to the expression in wild type macrophages (arbitrarily set to 1). Data were evaluated with the REST program. Values represent mean (n=3) ± SEM. * ($p<0.05$), ** ($p<0.01$). (c) Peritoneal macrophages from 3 wild type and Plin (-/-) mice were pooled. After cultivation in the absence or presence of VLDL (100µg/ml) for 24 or 48 hours, macrophages were lysed in RIPA buffer. 50µg protein were separated on a 10% SDS gel and Western Blot analysis was performed using an specific anti-HSL antibody.

7.2.5 Effect of Plin deficiency on acidic lipase activity in macrophages and foam cells

LAL mediates hydrolysis of lipoprotein-derived, endocytosed CE and TG in the endolysosomal compartment, where they are degraded into FC and FFA. When leaving the lysosome, FC reduces LDL-receptor gene expression and enzymes of the cholesterol biosynthetic pathway. In this way LAL activity is preventive with regard to cellular lipid overload and a possible influence of Plin deficiency on its activity was therefore examined. Acidic TG hydrolase activity was the same in male Plin (-/-) foam cells compared to wild type cells (Fig.18).

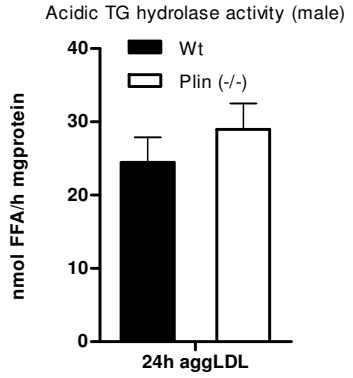

Fig.18: Acidic TG hydrolase activity in male macrophages and foam cells. Acidic TG hydrolase activity assay was performed in cell lysates from wild type and Plin (-/-) foam cells, loaded with aggLDL (50µg/ml) for 24 hours. Cellular lysates were incubated for 1 hour at 37°C with 15 µg mixed micelles containing radioactively labeled triolein as tracer. Liberated free fatty acids were measured by liquid scintillation counting. Values represent mean (n=4) ± SD.

7.2.6. Potential effect of Plin deficiency on β-oxidation in foam cells

CPT 1α transfers long-chain fatty acids from CoA to carnitine, activating them for their entry into mitochondria. The enzyme thus controls the rate-limiting step in mitochondrial FA oxidation. An increased metabolic rate in muscle, liver and adipose tissue of Plin (-/-) mice was published and an increased metabolic rate in macrophages could result in smaller LD in Plin (-/-) foam cells. To get evidence pro or against this theory, Cpt-1α mRNA levels were investigated in macrophages and foam cells of Plin deficient mice and control littermates.

Indications for an increasing effect of Plin deficiency on β-oxidation in foam cells come from the observation that CPT-1α mRNA concentrations were increased in Plin (-/-) foam cells (1.6-fold after 6 hours and 1.5-fold (without statistical significance) after 24 hours VLDL loading) compared to wild type cells (Fig.19). On the contrary, CPT-1α mRNA quantities were decreased by 49% in Plin (-/-) macrophages compared to wild type macrophages.

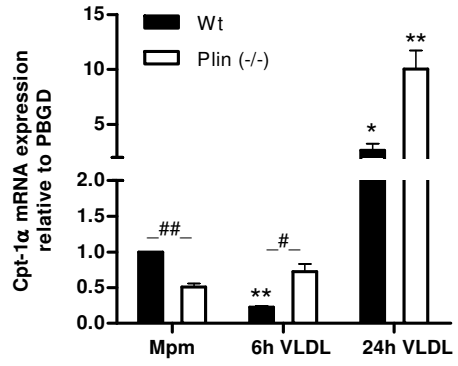

Fig.19: CPT-1α mRNA expression in macrophages and foam cells. Peritoneal macrophages from wild type and Plin (-/-) mice were cultivated in the absence or presence of VLDL (100µg/ml) for 6 or 24 hours. Total RNA was isolated and Cpt-1α mRNA concentrations were determined by real time PCR. mRNA quantities of Cpt-1 α were normalized to PBGD as housekeeping gene and mRNA levels shown were set in relation to the expression in wild type macrophages (arbitrarily set to 1). Data were evaluated with the REST program. Values represent mean (n=3) ± SEM. *(p<0.05), ** (p<0.01), $^{\#}$ (p<0.05).

7.2.7. Effect of Plin deficiency on free fatty acid release from macrophages

Next I determined the release of free fatty acids in wild type and Plin (-/-) macrophages. Wild type macrophages released 12% of total loaded [^{3}H] oleic acid after 1 hour, 16% after 3 hours, 24% after 6 hours and 27% after 8 hours. Plin (-/-) macrophages released 8% of total loaded [^{3}H] oleic acid after 1 hour, 15 % after 3 hours, 27% after 6 hours and 30% after 8 hours (Fig.20). Overall, oleic acid release was the same Plin (-/-) macrophages and control littermates after 1, 3, 6 and 8 hours.

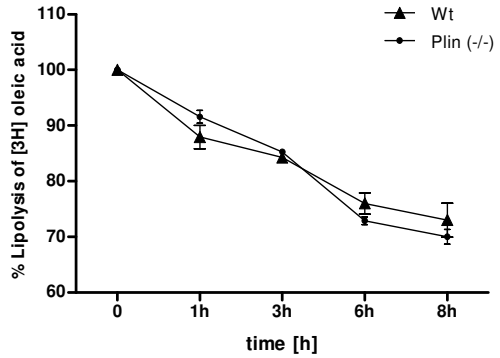

Fig.20: Fatty acid release from wild type and Plin (-/-) macrophages. Peritoneal macrophages from wild type and Plin (-/-) mice were labeled with [^{3}H] oleic acid provided as a complex with BSA. Fatty acid release was followed over 8 hours in the presence of triacsin C, to avoid reincorporation of the free fatty acids into TG, and was expressed as the percentage of [^{3}H] oleic acid released from cells into the medium relative to the total radioactivity in cells and medium. In all experiments, fractional FFA release was corrected for the radioactivity released into the medium without an acceptor and values were normalized to total cell protein. Values were normalized to total cell protein. Values represent mean (n=3) ± SD.

7.2.8. Potential effect of Plin deficiency on macrophage cholesterol efflux

ABCA1 is the most important cholesterol transporter in macrophages mediating cholesterol efflux to HDL_3. To reveal a potential effect of Plin deficiency on ABCA1-mediated reverse cholesterol transport, ABCA1 mRNA expression was determined in macrophages and foam cells.

At earlier time points during foam cell formation (after 6 hours), ABCA1 mRNA concentrations were up-regulated 1.9-fold in Plin (-/-) foam cells compared to wild type cells. whereas at later time points (after 24 hours) they were decreased by 30% in Plin (-/-) foam cells, however the difference did not reach statistical significance (Fig.21).

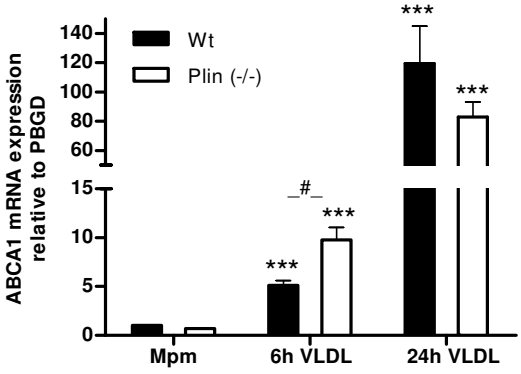

Fig.21: ABCA1 mRNA expression in macrophages and foam cells. Peritoneal macrophages from wild type and Plin (-/-) mice were cultivated in the absence or presence of VLDL (100µg/ml) for 6 or 24 hours. Total RNA was isolated and ABCA1 mRNA concentrations were determined by real time PCR. ABCA1 mRNA quantities were normalized to PBGD as housekeeping gene and ABCA1 mRNA levels shown were set in relation to the expression in wild type macrophages (arbitrarily set to 1). Data were evaluated with the REST program. Values represent mean (n=3) ± SEM. *** ($p<0.001$), # ($p<0.05$).

7.3. Effect of Plin deficiency on macrophage free fatty acid uptake

The smaller LD in Plin (-/-) foam cells could also be the result of impaired lipid uptake. To address this point, cells were loaded with [^{3}H]-labeled oleic acid/BSA complex and uptake of free fatty acids was followed over 24 hours. After 6 and 24 hours, lipids were extracted and radioactivity was counted. An aliquot of the extracts was applied to thin layer chromatography to determine FFA incorporation into the different lipid fractions.

After 6 and 24 hours, wild type and Plin (-/-) macrophages had taken up identical amounts of total FFA (Fig.22a,b).After 6 hours loading, the major part of FFA was incorporated into PL (79% (wild type), and 100% (Plin (-/-)). Lower amounts were incorporated into FFA (11% (wild type and Plin (-/-)) and TG (8% (wild type) and 12% (Plin (-/-)). Only 1% (wild type and Plin (-/-)) was found in the CE fraction (Fig.22c). 20% and 44% more FA.were found in the PL and TG fraction of Plin (-/-) cells, respectively, whereas no difference was found in the FFA or CE fractions (Fig.22c). After 24 hours most of the incorporated oleic acid was found in the PL and, to lower extent, in the TG fraction, in which FA were increased by 42% in Plin (-/-) cells. No difference was found in the FFA content of the other lipid fractions (Fig.22d).

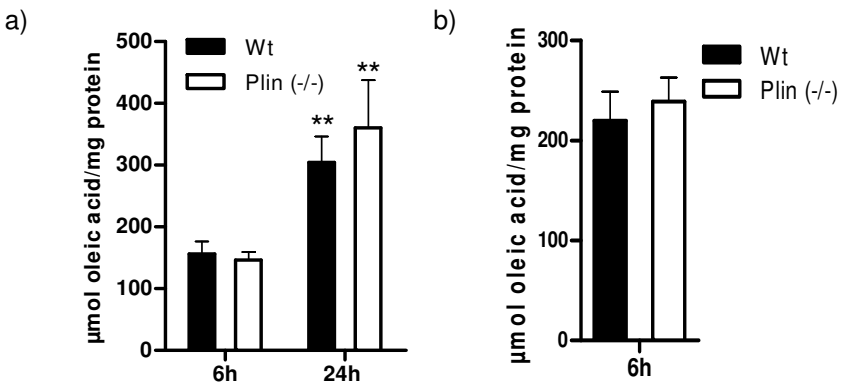

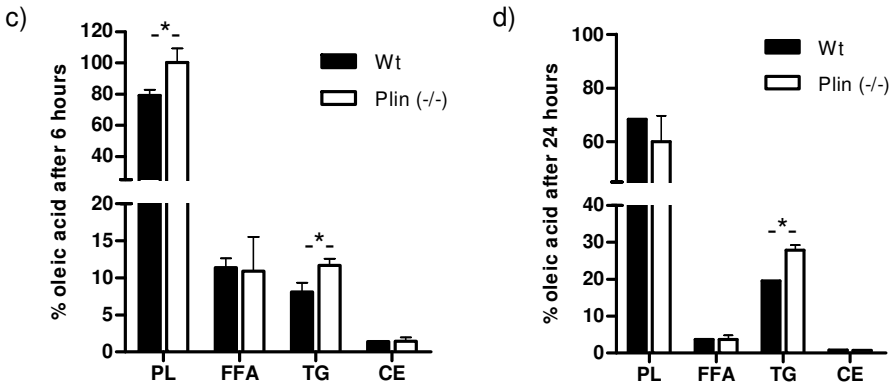

Fig.22 Free fatty acid uptake in wild type and Plin (-/-) macrophages. Peritoneal macrophages from female and male wild type and Plin (-/-) mice were loaded with [^{3}H] oleic acid/BSA complex. At the indicated time points, lipids were extracted. with hexan:isopropanol (3:2,v:v) and were either (a, b) directly measured or (c, d) were separated by thin layer chromatography. The respective lipid fractions were cut out and radioactivity was measured. In both cases, lipid parameters were normalized to the cellular protein content. Values represent mean of one experiment performed in triplicate ± SD. * ($p<0.05$), ** ($p<0.01$).

7.3.1. Effect of Plin deficiency on macrophage LPL activity

The secretion of LPL supports the degradation of TG-rich lipoproteins by hydrolyzing TG from chylomicrons and VLDL particles, thereby facilitating lipid uptake in macrophages. Macrophage LPL activity thus participates in the process of foam cell formation. LPL activity was lowered by 38% in Plin (-/-) macrophages but without statistical significance. LPL activity was 0.5% of that found in WAT in wild type macrophages and 0.3% in Plin (-/-) macrophages (Fig.23).

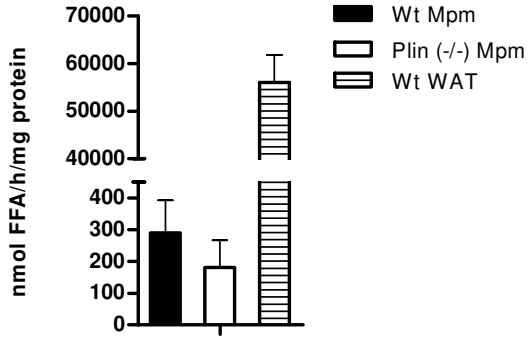

Fig.23: LPL-activity of female wild type and Plin (-/-) macrophages. LPL activity was measured in whole cell lysates from wild type and Plin (-/-) macrophages. Lysates were incubated for 1 hour at 37°C with a substrate containing radioactively labeled triolein and apoCII as activator of LPL activity. Liberated fatty acids were measured by liquid scintillation counting. Activity of LPL in WAT of wild type mice was determined as positive control Values represent mean (n=3) ± SD.

7.3.2. Effect of Plin deficiency on the mRNA expression of DGAT1 in macrophages and foam cells

To target later steps in the formation of LD, mRNA levels of DGAT1 were examined in wild type and Plin (-/-) macrophages and foam cells. DGAT1 mediates the conversion of diglycerides to TG thereby supporting LD formation.

DGAT1 mRNA levels were down-regulated by 39% in Plin (-/-) macrophages compared to wild type macrophages (Fig.24). Plin (-/-) foam cells had 2-fold increased DGAT1 mRNA quantities compared to wild type cells after 6 hours loading with VLDL. No difference was observed comparing wild type and Plin (-/-) foam cells after 24 hours VLDL loading.

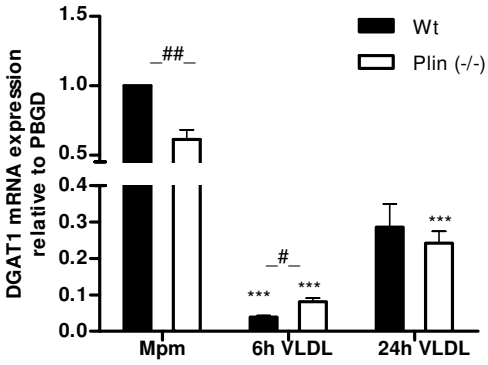

Fig.24: mRNA expression of DGAT1 in wild type and Plin (-/-) macrophages and foam cells. Peritoneal macrophages from wild type and Plin (-/-) mice were cultivated in the absence or presence of VLDL (100µg/ml) for 6 or 24 hours. Total RNA was isolated and DGAT1 mRNA levels were determined.by real time PCR. DGAT1 mRNA quantities were normalized to PBGD as houskeeping gene and DGAT1 mRNA levels shown were set in relation to the expression in wild type macrophages (arbitrarily set to 1). Data were evaluated with the REST program. Values represent mean (n=3) ± SEM. * ($p<0.05$), ** ($p<0.01$), *** ($p<0.001$), $^{\#}$ ($p<0.05$), $^{\#\#}$ ($p<0.01$).

7.3.3. Caveolin-1 mRNA expression in macrophages and foam cells

Since caveolins play a role in LD formation and since they are suggested to play a role in cellular cholesterol homeostasis, I determined caveolin-1 mRNA expression in wild type and Plin (-/-) macrophages and foam cells.

Caveolin-1 mRNA levels were lowered by 33% in Plin (-/-) macrophages compared to Plin (-/-) macrophages, however the difference did not reach statistical significance (Fig.25). Plin (-/-) foam cells had 3.7-fold increased caveolin-1 mRNA quantities after 6 hours VLDL loading. After 24 hours caveolin-1 mRNA concentrations were still increased 1.3-fold in Plin (-/-) foam cells, but without reaching statistical significance (Fig.25).

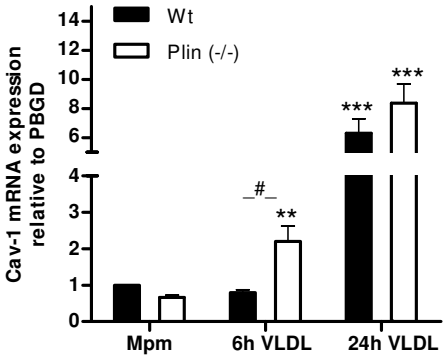

Fig.25: Caveolin-1 mRNA expression in macrophages and foam cells. Peritoneal macrophages from wild type and Plin (-/-) mice were cultivated in the absence or presence of VLDL (100µg/ml) for 6 or 24 hours. Total RNA was isolated and caveolin-1 mRNA concentrations were determined by real time PCR Caveolin-1 mRNA quantities were normalized to PBGD as houskeepig gene and caveolin-1 mRNA levels were set in relation to the expression in wild type macrophages (arbitrarily set to 1). Data were evaluated with the REST program. Values represent mean (n=3) ± SEM. * ($p<0.05$), ** ($p<0.01$), *** ($p<0.001$), $^{\#}$ ($p<0.05$).

7.3.4. Snap23 and VAMP4 mRNA expression in macrophages and foam cells

Snap23 and VAMP4 are proteins that are implicated in the fusion of LD leading to their enlargement. Therefore I investigated the mRNA concentrations of both proteins in wild type and Plin (-/-) macrophages and VLDL loaded cells. Snap23 mRNA levels were increased 1.5-fold in Plin (-/-) foam cell compared to wild type foam cells after 6 hours loading with VLDL, but no difference was observed after 24 hours (Fig.26a). VAMP4 mRNA concentrations were increased 2.4-fold in Plin (-/-) foam cells after 6 hours and were insignificantly decreased by 30% in Plin (-/-) foam cells after 24 hours loading with VLDL (Fig.26b).

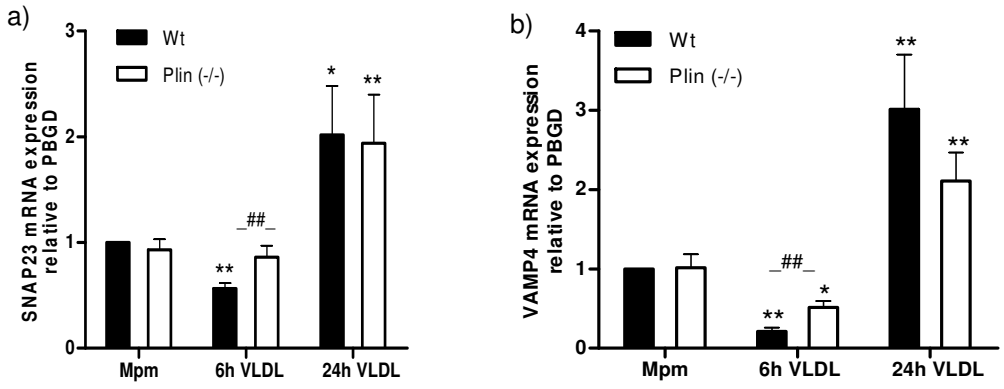

Fig.26: Snap23 and VAMP4 mRNA expression in macrophages and foam cells. Peritoneal macrophages from wild type and Plin (-/-) mice were cultivated in the absence or presence of VLDL (100µg/ml) for 6 or 24 hours. Total RNA was isolated and Snap23 and VAMP4 mRNA concentrations were determined by real time PCR. mRNA quantities were normalized to PBGD as housekeeping gene and mRNA levels shown were set in relation to the expression in wild type macrophages (arbitrarily set to 1). Data were evaluated with the REST program. Values represent mean (n=3) ± SEM. *($p<0.05$), ** ($p<0.01$), $^{\#\#}$ ($p<0.01$).

7.4. THE EFFECT OF PLIN DEFICIENCY ON THE EXPRESSION OF OTHER PAT FAMILY MEMBERS

To answer the question how the expression of other PAT protein family members changes in the absence of Plin, mRNA and protein expression of the other PAT protein family members was evaluated by real time PCR and Western blotting.

7.4.1. Protein expression of Plin in macrophages and foam cells

First the expression of Plin during foam cell formation was determined in wild type macrophages. No significant changes were observed in the Plin protein content after 48 and 72 hours loading with aggLDL compared to macrophages (Fig.27).

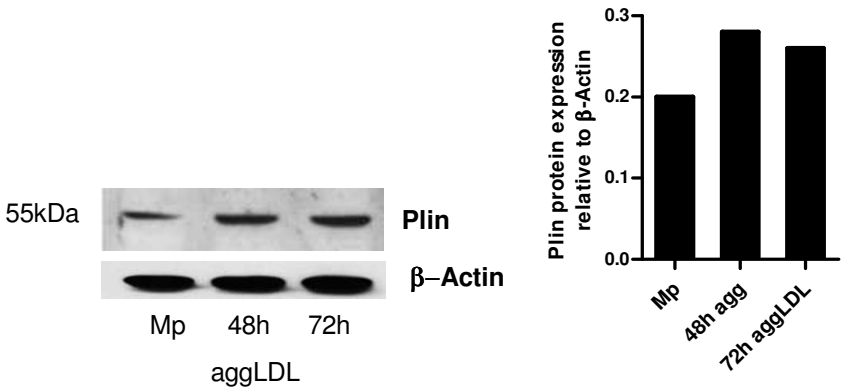

Fig.27: Plin protein expression in wild type macrophages and foam cells. Peritoneal macrophages from wild type and Plin (-/-) mice were were cultivated in the absence or presence of aggLDL (50µg/ml) or VLDL (100µg/ml) for 48 and 72 hours. Cells were lysed in RIPA buffer. 50µg protein were separated on a 10% SDS gel. Western Blot analysis was performed using a specific anti-Plin antibody.

7.4.2. mRNA and protein expression of Adrp in macrophages and foam cells

In female wild type foam cells, Adrp mRNA levels were the same as in macrophages after 48 hours and were up-regulated 3.3-fold after 72 hours loading with aggLDL. VLDL loaded foam cells showed 42% decreased and 1.6-fold increased Adrp mRNA levels after 48 and 72 hours compared to macrophages (Fig.28a).

In males, loading with aggLDL for 24 and 48 hours increased Adrp mRNA levels (2.4-fold and 2.7-fold in wild type and 3.1-fold and 3.4 fold in Plin (-/-)) compared to macrophages but Adrp mRNA levels were not different comparing wild type and Plin (-/-) foam cells (Fig.28b). VLDL loading for 24 and 48 hours increased Adrp mRNA levels 3.8-fold and 4.2-fold in wild

type foam cells and 2.8-fold and 4.5-fold in Plin (-/-) foam cells. After 24 hours VLDL loading, Adrp mRNA levels were decreased by 37% in Plin (-/-) foam cells compared to wild type foam cells but no differences were observed after 48 hours VLDL loading comparing wild type and Plin (-/-) foam cells (Fig.28b). Adrp protein content was lower in Plin (-/-) macrophages (33%) and foam cells (64% after 6 hours and 48% after 48 hours loading with aggLDL and 40% after 24 hours and 33% after 48 hours loading with VLDL) compared to wild type cells (not statistically different).

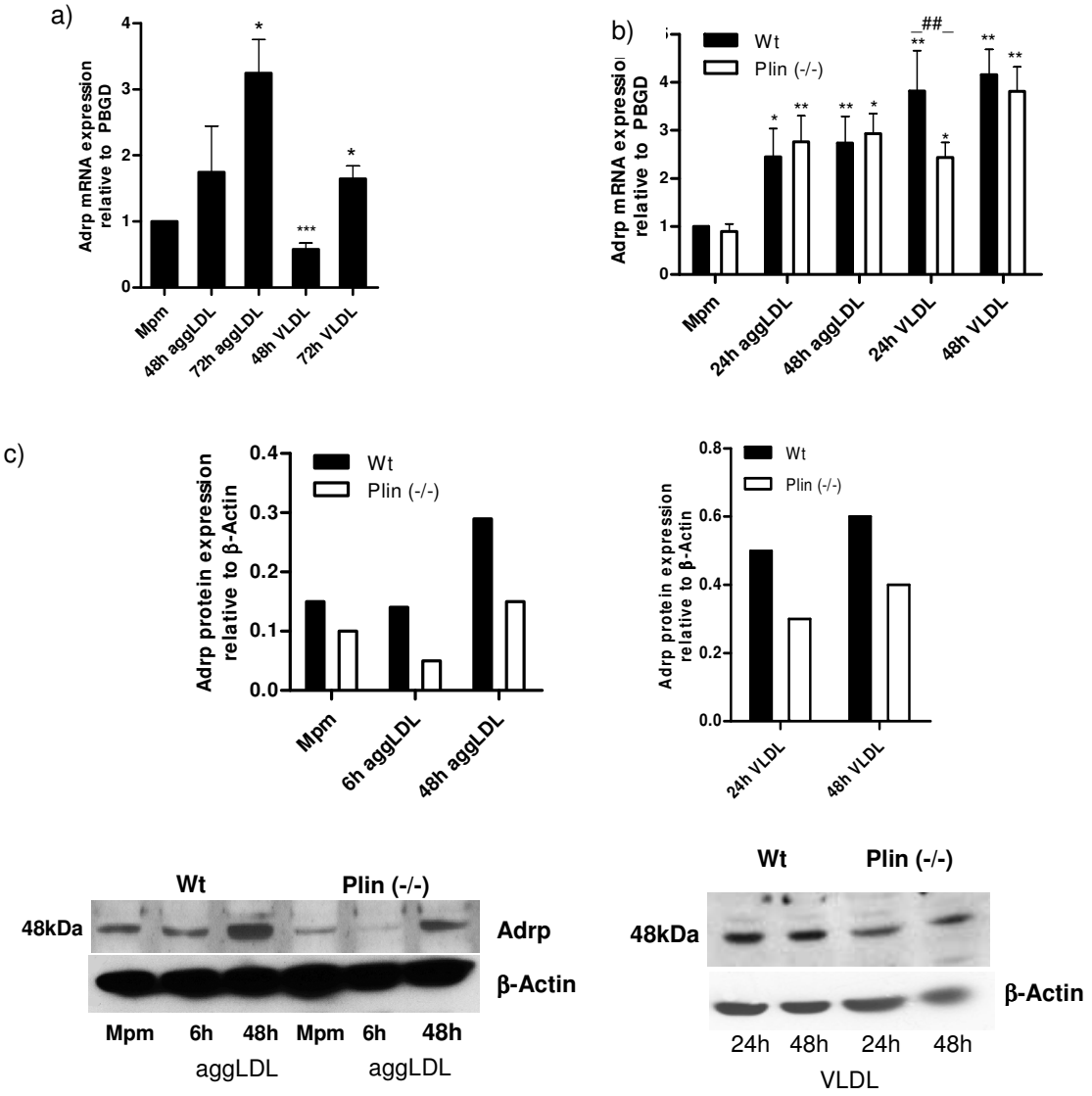

Fig.28: Adrp mRNA and protein expression in wild type and Plin (-/-) macrophages and foam cells. (a, b) Peritoneal macrophages from wild type and Plin (-/-) mice were cultivated in the absence or presence of aggLDL (50µg/ml) or VLDL (100µg/ml) for 6, 24, 48 or 72 hours. Total RNA was isolated and Adrp mRNA concentrations were determined by real time PCR. Adrp mRNA quantities were normalized to PBGD as housekeeping gene and mRNA levels shown were set in relation to the expression in wild type macrophages (arbitrarily set to 1). Data were evaluated with the REST program. Values represent mean (n=3) ± SEM. * ($p<0.05$), ** ($p<0.01$), *** ($p< 0,001$), $^{\#\#}$ ($p<0.01$). (c) Peritoneal macrophages from 3 mice were pooled. After incubation with aggLDL or VLDL, cells were lysed in RIPA buffer. 50µg protein were separated on a 10% SDS gel. Western Blot analysis was performed using a specific anti-Adrp antibody.

7.4.3. mRNA and protein expression of Tip47 in macrophages and foam cells

Equal Tip47 mRNA quantities were found in female wild type foam cells after 48 and 72 hours loading with aggLDL compared to macrophages. After 48 loading with VLDL, Tip47 mRNA concentrations were down-regulated by 33% but they were identical after 72 hours compared to macrophages (Fig.29a).
In males, incubation with aggLDL did not increase or decrease Tip47 mRNA levels in wild type or Plin (-/-) foam cells compared to macrophages and similar Tip47 mRNA concentrations were detected in wild type and Plin (-/-) foam cells (Fig.29b). After loading with VLDL for 24 hours, Tip47 mRNA levels were decreased by 21% in wild type and by 42% in Plin (-/-) foam cells compared to macrophages and Tip47 mRNA concentrations were 39% lower in Plin (-/-) foam cells compared to wild type foam cells (Fig.29b). After 48 hours loading with VLDL, Tip47 mRNA levels were similar to that of macrophages in both genotypes, but Tip47 mRNA levels were decreased by 28% in Plin (-/-) foam cells compared to wild type foam cells. Tip47 protein content was decreased in Plin (-/-) foam cells by 37% and 27% after 48 hours loading with aggLDL and VLDL, respectively, but without statistical significance (Fig.29c).

Since no significant differences were observed in the protein content of Plin, Adrp and Tip47, Western blot analysis was only performed once and therefore data shown are presented without statistical significance

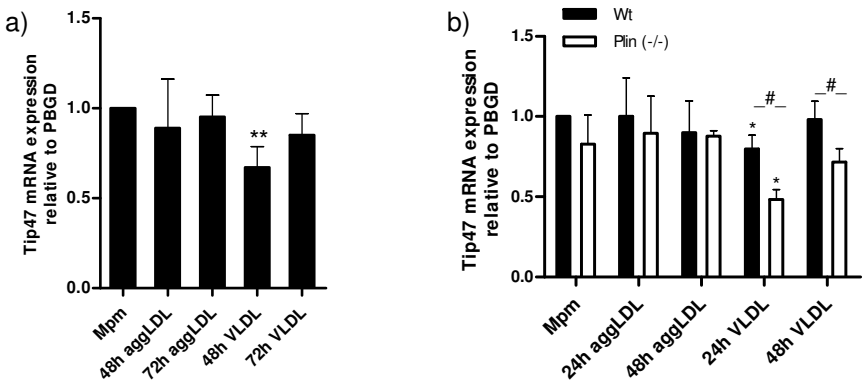

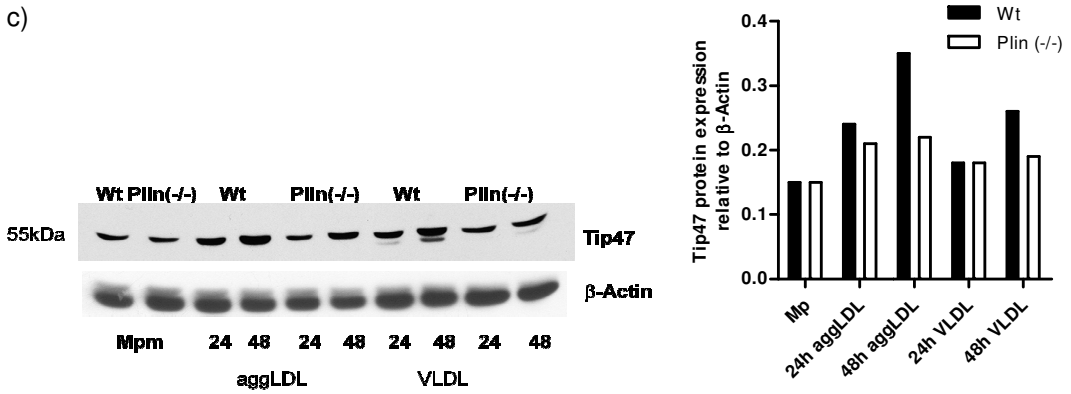

Fig.29: Tip47 mRNA (a, b) and (c) protein expression in macrophages and foam cells. (a, b) Peritoneal macrophages from wild type and Plin (-/-) mice were cultivated in the absence or presence of aggLDL (50µg/ml) or VLDL (100µg/ml) for 24, 48 or 72 hours. Total RNA was isolated and Tip47 mRNA concentrations were determined by real time PCR. Tip47 mRNA quantities were normalized to PBGD as housekeeping gene and mRNA levels shown were set in relation to the expression in wild type macrophages (arbitrarily set to 1). Data were evaluated with the REST program. Values represent mean (n=3) ± SEM. * ($p<0.05$), ** ($p<0.01$), $^{\#}$ ($p<0.05$). (c) Peritoneal macrophages from 3 mice were pooled. After incubation with aggLDL (50µg/ml) or VLDL (100µg/ml) for 24 or 48 hours, cells were lysed in RIPA buffer. 50µg protein were separated on a 10% SDS gel. Western Blot analysis was performed using a specific anti-Tip47 antibody.

7.4.4. mRNA expression of S3-12 and PAT-1 in macrophages and foam cells

In female wild type macrophages, S3-12 mRNA levels were not different after 48 hours and were down-regulated by 43% after 72 hours loading with aggLDL.compared to macrophages (Fig.30a). After 48 hours loading with VLDL, S3-12 mRNA concentrations were increased 1.4-fold but were unaltered after 72 hours loading. In males, S3-12 mRNA levels were increased 1.6-fold and 1.8-fold in wild type foam cells after 48 hours loading with aggLDL and VLDL, respectively whereas in comparison, Plin (-/-) foam cells had 39% and 50% reduced S3-12 mRNA quantities under the same conditions (Fig.30b).

Neither aggLDL nor VLDL loading showed an effect on PAT-1 mRNA quantities in female wild type foam cells compared to macrophages (Fig.31a). After 72 hours loading with VLDL, PAT-1 mRNA concentrations were lowered by 38%, however without being statistical significant. In males, PAT-1 mRNA concentrations were increased 2.5-fold and 2.2-fold in wild type cells after 48 hours loading with aggLDL and VLDL, respectively (Fig.31b), whereas Plin (-/-) had 60% and 56% reduced PAT1 mRNA concentrations compared to wild type cells compared to wild type cells

There was no according S3-12 antibody available and the PAT-1 antibody, raised only against the human epitop, did not work for WB in our hands. Therefore the protein expression of S3-12 and PAT-1 could not be investigated.

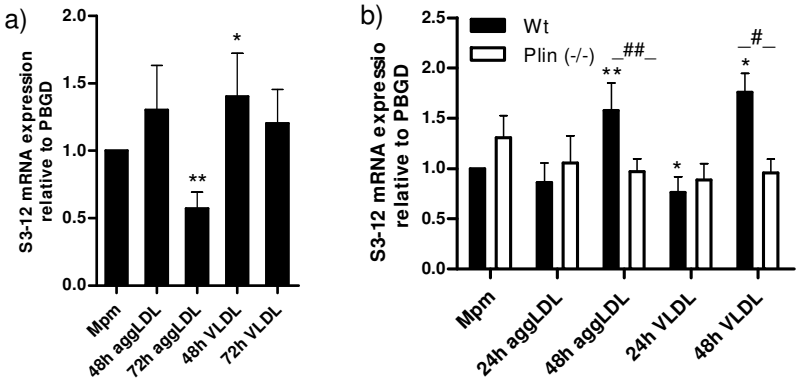

Fig.30: mRNA expression of S3-12 in macrophages and foam cells. Peritoneal macrophages were cultivated in the absence or presence of aggLDL (50µg/ml) or VLDL (100µg/ml) for 24, 48 or 72 hours Total RNA was isolated and S3-12 mRNA concentrations were determined by real time PCR. S3-12 mRNA quantities were normalized to PBGD as housekeeping gene and mRNA levels shown were set in relation to the expression in wild type macrophages (arbitrarily set to 1) Data were evaluated with the REST program. Values represent mean (n=3) ± SEM. * ($p<0.05$), ** ($p<0.01$), $^{\#}$ ($p<0.05$), $^{\#\#}$ ($p<0.01$). Cells were lysed in RIPA buffer. 50µg protein were separated on a 10% SDS gel. Western Blot analysis was performed using a specific anti-S3-12 antibody.

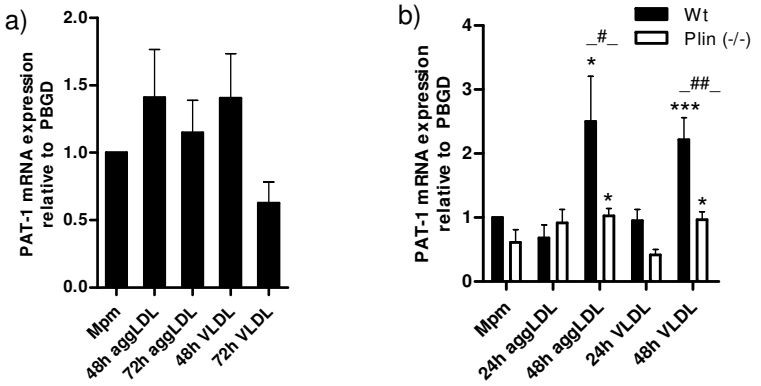

Fig.31: mRNA expression of PAT-1 in macrophages and foam cells. Peritoneal macrophages were cultivated in the absence or presence of aggLDL (50µg/ml) or VLDL (100µg/ml) for 24, 48 or 72 hours Total RNA was isolated and PAT-1 mRNA concentrations were determined by real time PCR. PAT-1 mRNA quantities were normalized to PBGD as housekeeping gene and mRNA levels shown were set in relation to the expression in wild type macrophages (arbitrarily set to 1). Data were evaluated with the REST program. Values represent mean (n=3) ± SEM. * ($p<0.05$), *** ($p< 0,001$), $^{\#}$ ($p<0.05$), $^{\#\#}$ ($p<0.01$)

7.4.5. The effect of fatty acid loading on Plin protein expression

To determine the effect of FFA loading on the expression of Plin, cells were loaded with oleic acid and Western blotting analysis of Plin protein expression was performed.
Loading with oleic acid/BSA complex down-regulated Plin protein levels in wild type foam cells (1.3-fold and 1.6-fold, respectively, without statistical significance) after 24 and 48 hours loading with oleic acid (Fig.32).

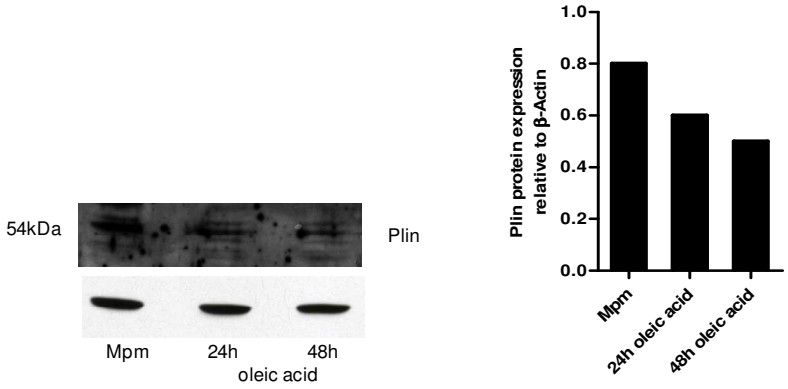

Fig.32: Plin protein expression in foam cells after loading with oleic acid. Peritoneal macrophages were cultivated in the absence or presence of oleic acid/BSA complex (molar ratio 8:1) for 24 or 48 hours. Cells were lysed in RIPA buffer. 70µg protein were separated on a 10% SDS gel. Western blot analysis was performed using a specific anti-Plin antibody.

7.5. EFFECT OF PLIN DEFICIENCY ON PLASMA LIPID PARAMETERS

7.5.1. Plasma lipid parameters in wild type and Plin (-/-) mice

Due to its regulatory function on lipolysis in adipose tissue, Plin has an important impact on the whole body lipid metabolism. Therefore the influence of Plin deficiency on plasma lipid parameters of female and male mice on chow diet was determined in the 4 hours fasted and overnight fasted state. In the 4 hours fasted state, TC, FC and TG concentrations were the same in female and male wild type and Plin (-/-) mice (Fig.33a, Fig 34a). Plasma FFA concentrations were reduced by 25.2% in female Plin (-/-) mice (Fig.33.b) and were decreased by 32.4% in male Plin (-/-) mice compared to wild type littermates, however without statistical significance (Fig.34b). In the overnight fasted state, female Plin (-/-) mice had 66.3% reduced TG concentrations compared to female wild type mice, TC and FC concentrations were not different. (Fig.33c), Male Plin (-/-) mice had 15.5% reduced plasma TG and 10.5% reduced FC concentrations while TC concentrations were unaltered (Fig 34c). Plasma FFA concentrations were reduced to 35.0% in female Plin (-/-) mice compared to

female wild type mice (Fig.35d), but FFA concentrations were not different in male Plin (-/-) mice (Fig.34d).

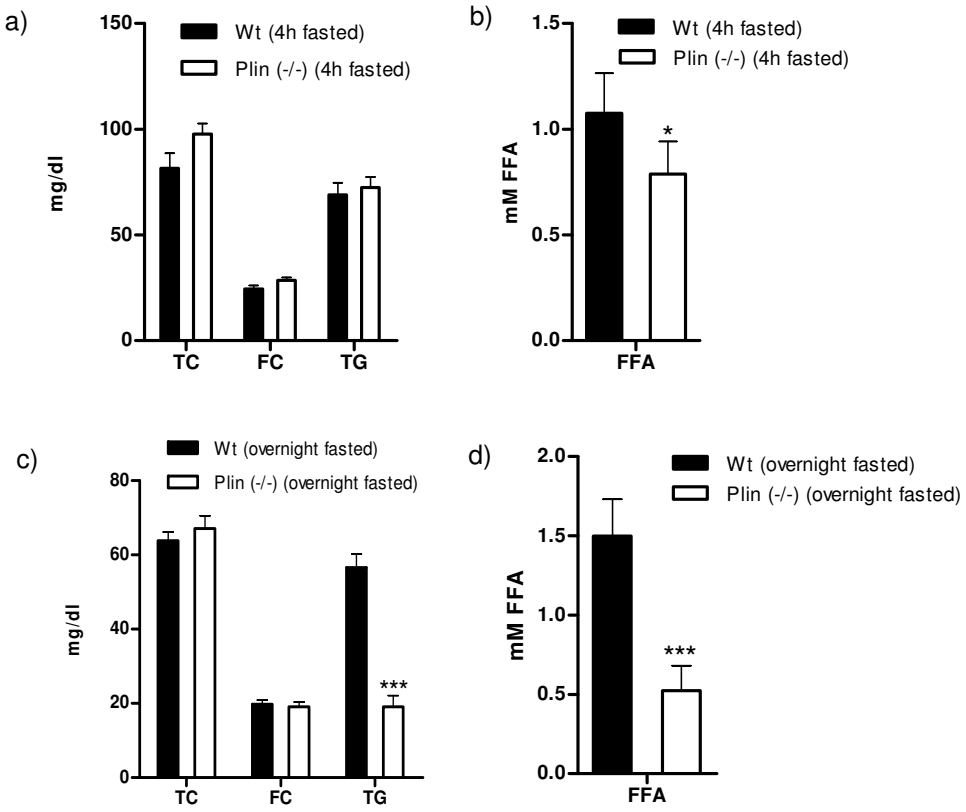

Fig.33: Plasma lipid parameters of female mice after (a, b) 4 hours and (c, d) overnight fasting. Blood was taken from female wild type (n=6) and Plin (-/-) (n=10) mice on chow diet. Lipid parameters were determined enzymatically. Values represent mean ± SD. *** ($p<0.001$).

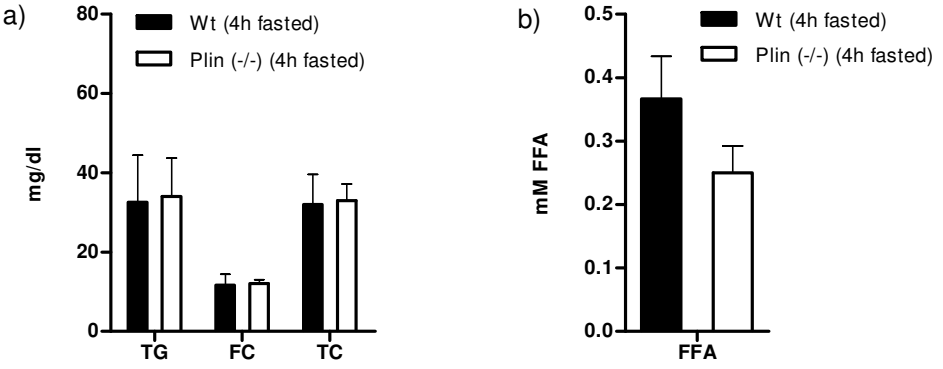

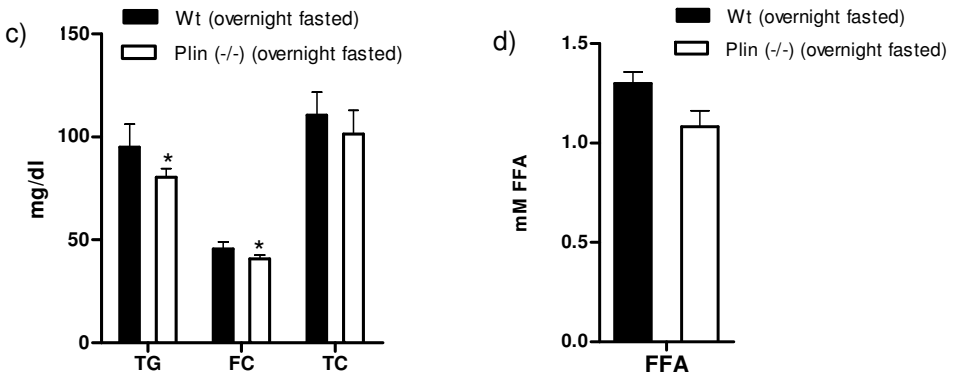

Fig.34: Plasma lipid parameters of male mice after (a, b) 4 hours and (c, d) overnight fasting. Blood was taken from female wild type (n=6) and Plin (-/-) (n=10) mice on chow diet. Lipid parameters were determined enzymatic ally. Values represent mean ± SD. *($p<0.05$).

7.6. THE IMPACT OF PLIN DEFICIENCY ON HEPATIC LIPID METABOLISM

It was reported that Plin (-/-) mice are resistant to diet-induced obesity. Thus I fed wild type and Plin (-/-) mice for 6 months with western-type diet (WTD) (21% fat and 0.2% cholesterol) and examined the consequences on diet-induced liver steatosis. Body weights, liver weights and hepatic lipid parameters of wild type and Plin (-/-) mice were determined. To investigate the development of steatosis within the liver, cry sections from the lobos dextral were cut and stained with eosin and hemotoxylin, a classical method to visualize different tissue structures in histological preparations. This was done in collaboration with Dagmar Silbert from the university hospital of gastroenterology and hepatology in Graz. Histological sections were analyzed with a digital microscope.

After 6 month WTD, male Plin (-/-) mice had a slightly increased mean body weight (36.1g) compared to wild type mice (33.1g), however the difference did not reach statistical significance (Fig.35). Male Plin (-/-) mice had 60% reduced TG plasma concentrations compared to wild type mice, TC, FC and FFA concentrations were not different (Fig.36a,b). Hepatic TG concentrations were increased 1.5-fold, TC and FC concentrations were lowered (33% and 31%, respectively) and CE concentrations were unaltered in Plin (-/-) mice, however the differences failed to reach statistical significance (Fig.37a). Plin (-/-) mice had 1.6-fold increased liver weights compared to wild type littermates (Tab.10). In cardiac muscle, TG concentrations were increased by 44.4% in Plin (-/-) mice whereas TC, FC and CE concentrations were unaltered compared to wild type mice (Fig.37b).

Male and female wild type mice had only mild lipid deposits in the liver after 6 month WTD feeding. On the contrary, massive steatosis could be observed in Plin (-/-) mice of both sexes, which differed in their appearance (Fig.38a, b). Male Plin (-/-) mice displayed a kind of coarse steatosis with big LD within hepatocytes. In female Plin (-/-) mice, lipids were

dispersed in smaller LD and the overall lipid content was lower compared to male Plin (-/-) mice. Two of the three female wild type mice died during the WTD feeding, but none of the male mice. There were two mice which did not fit to the others. One of the male wild type mice had massive steatosis and one of the female Plin (-/-) mice had no steatosis.

			mg/dl			
Genotype	**Sex**	**weight (g)**	**TC**	**FC**	**TG**	**FFA [mM]**
Plin (-/-)	**m**	27,5	217,5	166,5	43,5	0,5
Plin (-/-)	**m**	25,55	175,3	77,4	77,9	0,7
Plin (-/-)	**m**	24,2	187,2	74,4	88,2	0,7
Plin (-/-)	**m**	27,25	150,2	60,6	56,7	0,6
Plin (-/-)	**m**	27,25	170,9	78,7	87,7	0,6
Wt	**m**	26,39	159,7	62	66,1	1,31
Wt	**m**	21,79	172,5	70,3	67,1	0,97
Wt	**m**	22,45	160,1	71,8	69,5	0,98
Wt	**m**	25	177,3	71,7	87,7	0,66

Tab.9: Weight and plasma lipid parameters of male mice before feeding WTD. Blood was taken from wild type (n=4) and Plin (-/-) (n=5) mice after overnight fasting. Plasma was obtained by centrifuging the blood 10 minutes at 8000 rpm, 4℃ and lipid parameters were determined enzymatically.

					mg/dl			
Genotype	**Sex**	**weight (g)**	**Li (g)**	**CM (g)**	**TC**	**FC**	**TG**	**FFA [mM]**
Plin (-/-)	**m**	42,8	2,38	0,14	179	91,6	1526,6	0,73
Plin (-/-)	**m**	41,95	1,63	0,15	94,9	58,1	967,5	0,73
Plin (-/-)	**m**	30,71	2,18	0,12	130,1	75	1250	0,51
Plin (-/-)	**m**	31,44	1,91	0,15	127,2	67,2	1120,5	0,46
Plin (-/-)	**m**	33,84	2,61	0,17	118,3	64,4	1073,4	0,38
Wt	**m**	28,56	1,27	0.13	66,1	44,3	96	0,27
Wt	**m**	28,3	1,09	0,12	117,5	70,1	100	0,79
Wt	**m**	37,21	1,68	0,15	152,7	76,4	110,5	0,63
Wt	**m**	38,42	1,2	0,16	149,1	80,6	127,1	0,45

Tab.10: Weight of male mice, their livers and cardiac muscles as well as plasma lipid parameters after 6 month WTD feeding. Male wild type and Plin (-/-) mice were fed WTD for 6 month. Mice were weighed, were fasted overnight and blood was taken. Plasma was obtained by centrifuging the blood 10 minutes at 8000 rpm, 4℃ and lipid parameters were determined enzymatically. Mice were sacrificed and perfused. Liver and heart were collected and weighed.

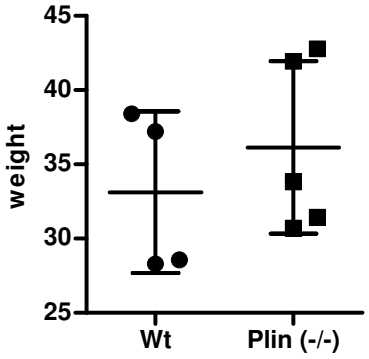

Fig.35: Weights of male mice after 6 month WTD

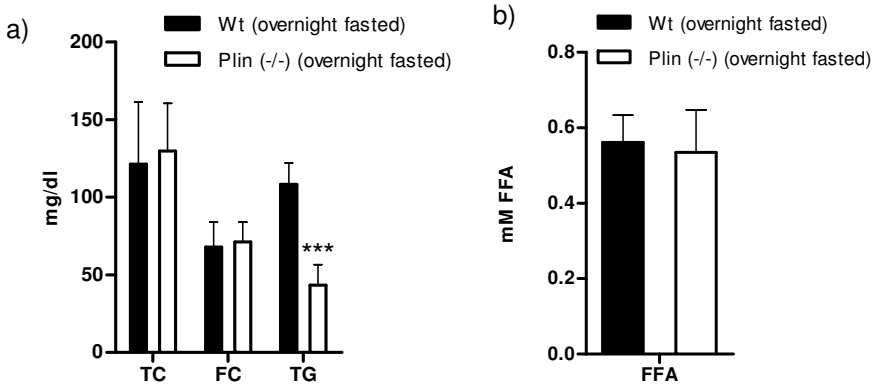

Fig.36: Plasma lipid parameters after 6 month WTD. Male wild type and Plin (-/-) mice were fed WTD for 6 month. Mice were fasted overnight and blood was taken. Plasma was obtained by centrifuging the blood 10 minutes at 8000 rpm, 4°C and lipid parameters were determined enzymatically. Values represent mean (n=4 for wild type and n=5 for Plin (-/-) ± SD. *** ($p<0.001$).

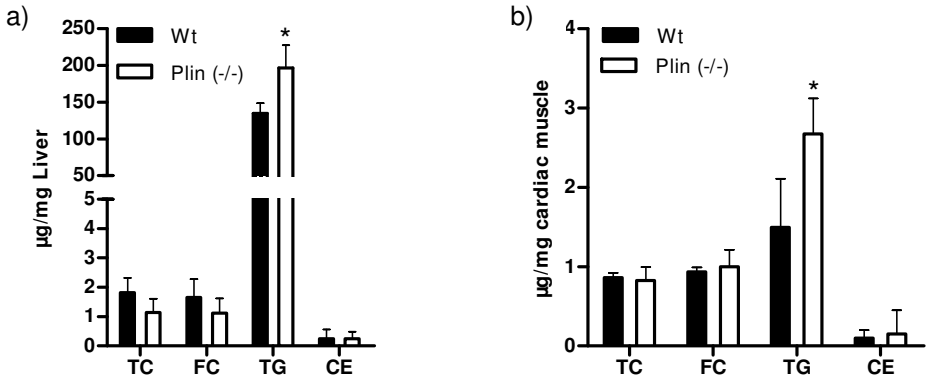

Fig.37: Hepatic and cardiac muscle lipid parameters of male mice. Male wild type and Plin (-/-) mice were fed WTD for 6 month. Mice were fasted overnight, sacrificed and the heart was perfused. Liver and heart were collected, lipids from tissues were extracted with $CHCl_3$:MeOH (2:1) and lipid parameters were determined enzymatically. Values represent mean (n=4 for wild type and n=5 for Plin (-/-)) ±SD. * ($p<0.05$)

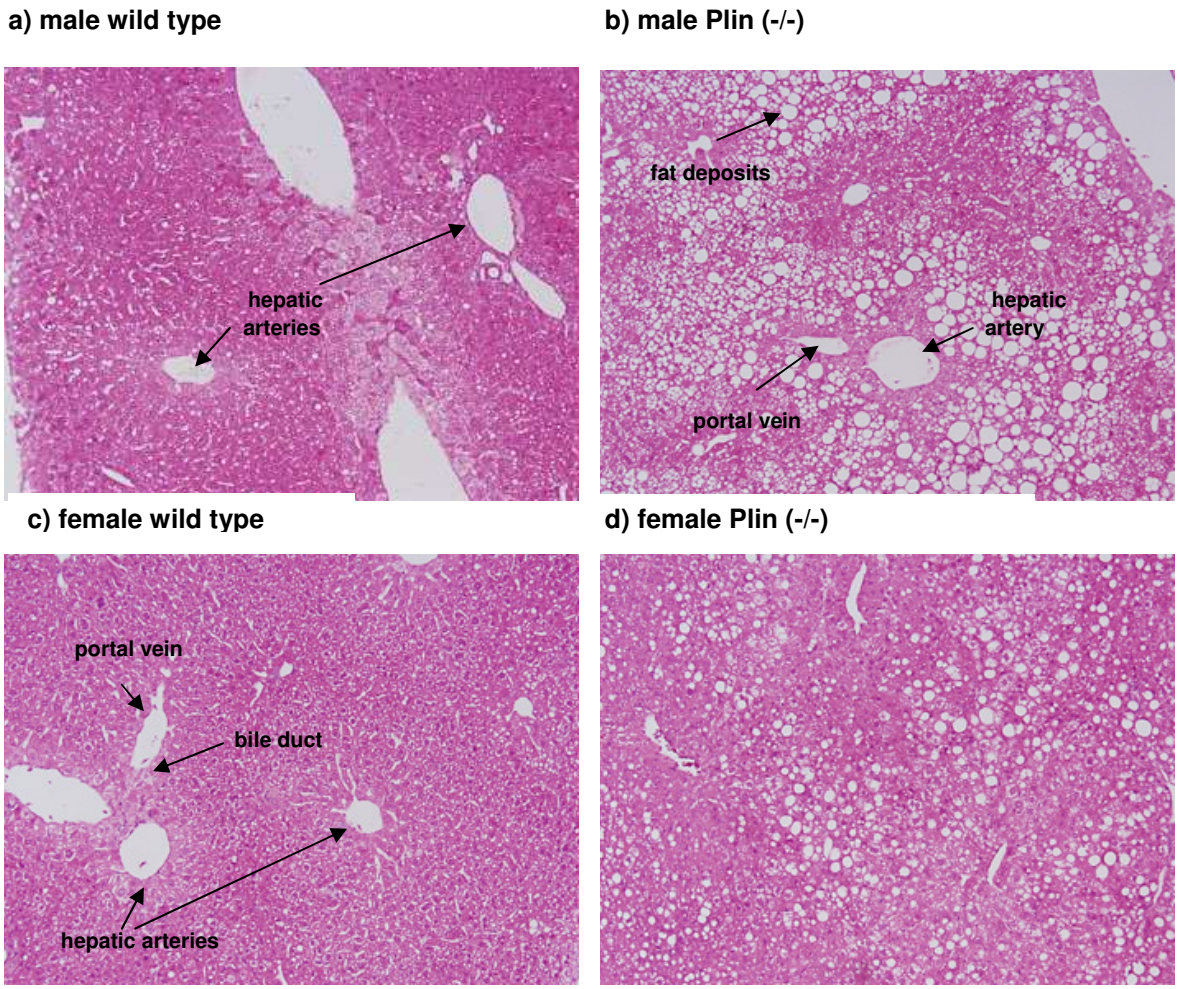

Fig.38: H&E stained histological liver sections of the lobus dextra of wild type and Plin (-/-) mice. Male and female wild type and Plin (-/-) mice were fed WTD for 6 month. Thereafter, mice were perfused, livers were collected, weighed, and sections of the lobus dextra were preserved in 4% formaldehyde until they were stained with hemotoxylin and eosin. Acidic/basophile structures are stained blue (hemotoxylin) and alkaline structures are stained red (eosin). The formerly lipid-containing vacuoles appear white due to the dissolving of the lipids during the histological fixation. Pictures were taken with the digital microscope Leica DM6000B, equipped with a motorized stage and a digital camera (OlympusDP72). Original magnification was 10-fold. n=4 (male wild type), n=5 (male Plin (-/-)), n=1 (female wild type), n=5 (female Plin (-/-)).

To find out whether Plin (-/-) mice had developed diet-induced glucose intolerance during the high fat diet feeding, I performed a glucose tolerance test. Plin (-/-) mice and control littermates were gavaged with 2mg/kg glucose and blood glucose levels were measured after 15, 30, 60 and 120 minutes. , wild type and Plin (-/-) mice reacted with an appropriate response curve to the glucose administration whereas the maximum blood glucose concentration was reached at different time points in wild type (after 30 minutes) and Plin (-/-) mice (after 15 minutes). Wild type and Plin (-/-) showed similar glucose concentrations at their respective maximum glucose levels indicating the same glucose tolerance (Fig.41).

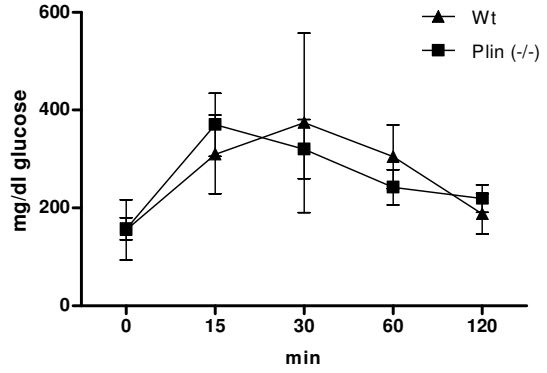

Fig.39: Glucose tolerance test of male mice fed WTD for 6 month. Mice were fasted overnight. Thereafter mice were gavaged with 2mg/kg glucose. Blood was taken from the tail tip while mice were shortly anesthesized with isofuran. Blood glucose concentrations were measured at the indicated time points with an "AccuCheck active" glucometer.

7.7. The impact of Plin deficiency on atherosclerosis in aortic root sections

To examine whether Plin deficiency influences atherosclerosis, I bred Plin(-/-)/apoE(-/-) mice and fed them WTD for 8 weeks. Plasma lipid parameters and plasma lipoprotein profile of wild type and Plin (-/-) mice were investigated. Hepatic lipid parameter determination and histological analysis of aortic roots were performed as well. Plin (-/-) and apoE (-/-) mice were taken as control.

7.7.1. Weights of Plin (-/-), apoE (-/-) and Plin(-/-)/apoE (-/-) mice

After 8 weeks WTD female apoE (-/-) and Plin(-/-)/apoE(-/-) had an increased mean body weight compared to Plin (-/-) mice (14.3% and 13.3%, respectively) (Fig.40a). Male Plin (-/-), apoE (-/-) and Plin(-/-)/apoE(-/-) mice had an equal mean body weight after 8 weeks WTD (Fig.40b).

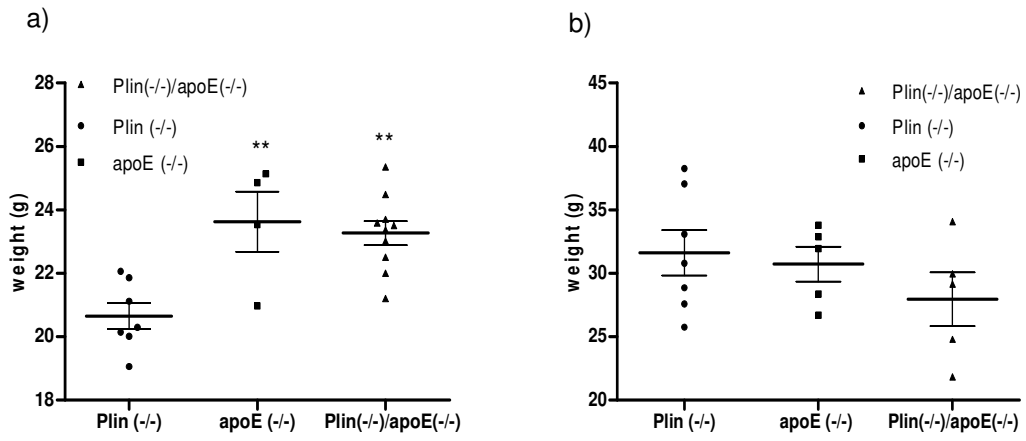

Fig.40: Weights of Plin (-/-), apoE (-/-) and Plin(-/-)/apoE(-/-) mice. (a) female and (b) male mice were fed WTD for 8 weeks. Values represent mean (n=4-9) ± SD. ** ($p<0.01$)

7.7.2. Plasma lipid parameters of Plin (-/-), apoE (-/-) and Plin(-/-)/apoE(-/-) mice

Female apoE (-/-) and Plin(-/-)/apoE(-/-) mice displayed increased TC (4.5-fold and 4.6-fold (4 hours fasted) and 8.7-fold and 9.4-fold (overnight fasted)), FC (13.1-fold and 9.9-fold (4 hours fasted state) and 15.6-fold and 14.4-fold (overnight fasted)) and TG (4.6-fold and 2.8-fold (4 hours fasted) and 7.9-fold and 6.1-fold (overnight fasted)) concentrations compared to Plin (-/-) mice (Fig.41a,c). In the 4 hours fasted state, plasma FC and TG concentrations were decreased by 24% and 38% in female Plin(-/-)/apoE(-/-) mice compared to apoE (-/-) mice while TC concentrations were not different. In the overnight fasted state, only TG were lowered by 23% but without reaching statistical significance. TC and FC concentrations were the same. FFA concentrations were increased in female apoE (-/-) and Plin(-/-)/apoE(-/-) mice (3.6-fold and 3.0-fold (4 hours fasted state) and unaltered and 2.7-fold (overnight fasted)) compared to control mice (Fig.41b, d).

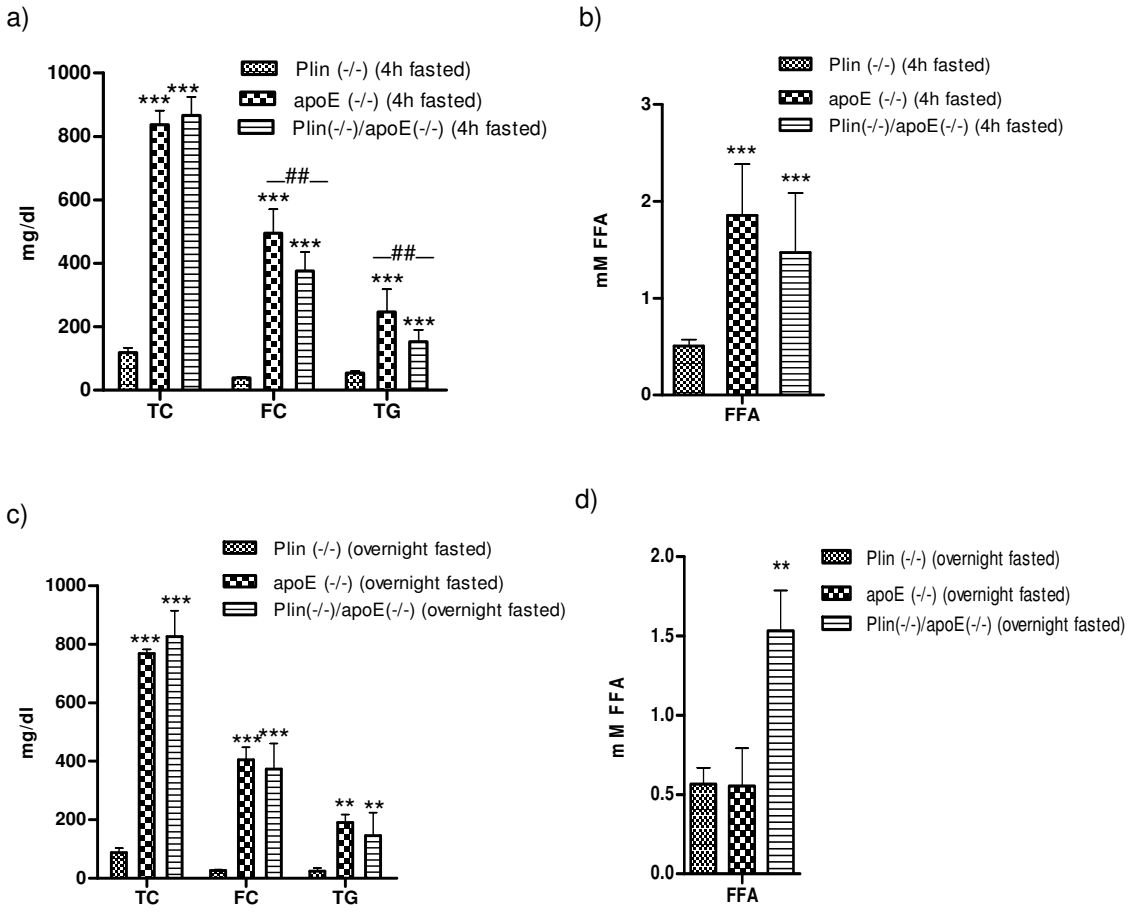

Fig.41: Plasma lipid parameters of female Plin (-/-), apoE (-/-) and Plin(-/-)/apoE(-/-) mice. Female mice were fed WTD for 8 weeks. Blood was taken after mice were fasted 4 hours (a, b) or overnight(c, d) and lipid parameters were determined enzymatically. Values represent mean (n=4-9) ± SD. ** (0.01), *** (0.001)

Like females, male apoE(-/-) and Plin(-/-)/apoE(-/-) mice had increased TC (6.1-fold and 5.2-fold (4 hours fasted) and 6.5-fold and 8.2-fold (overnight fasted)) and FC (7.0-fold and 5.6-fold (4 hours fasted) and 5.2-fold and 7.4-fold higher (without statistical significance) (overnight fasted)) concentrations compared to Plin (-/-) mice (Fig.42a,c). Different to female mice, in male apoE (-/-) and Plin(-/-)/apoE(-/-) mice, TG concentrations were only modestly increased (2.3-fold and 1.8-fold) in the 4 hours fasted state and were unaltered in male apoE(-/-) and 1.3-fold (25.4%) higher in Plin(-/-)/apoE(-/-) mice, however the differences in the TG concentrations were not statistically significant (Fig.42a,c). TC (14.7%), FC (19.1%) and TG (19.1%) concentrations were decreased in Plin(-/-)/apoE(-/-) mice compared to apoE (-/-) mice. Plasma FFA concentrations were increased in male apoE (-/-) and Plin(-/-)/apoE(-/-) mice (4.0-fold and 2.7-fold (4 hours fasted) and 2.2-fold and 2.8-fold (overnight fasted) (Fig.42c, d).

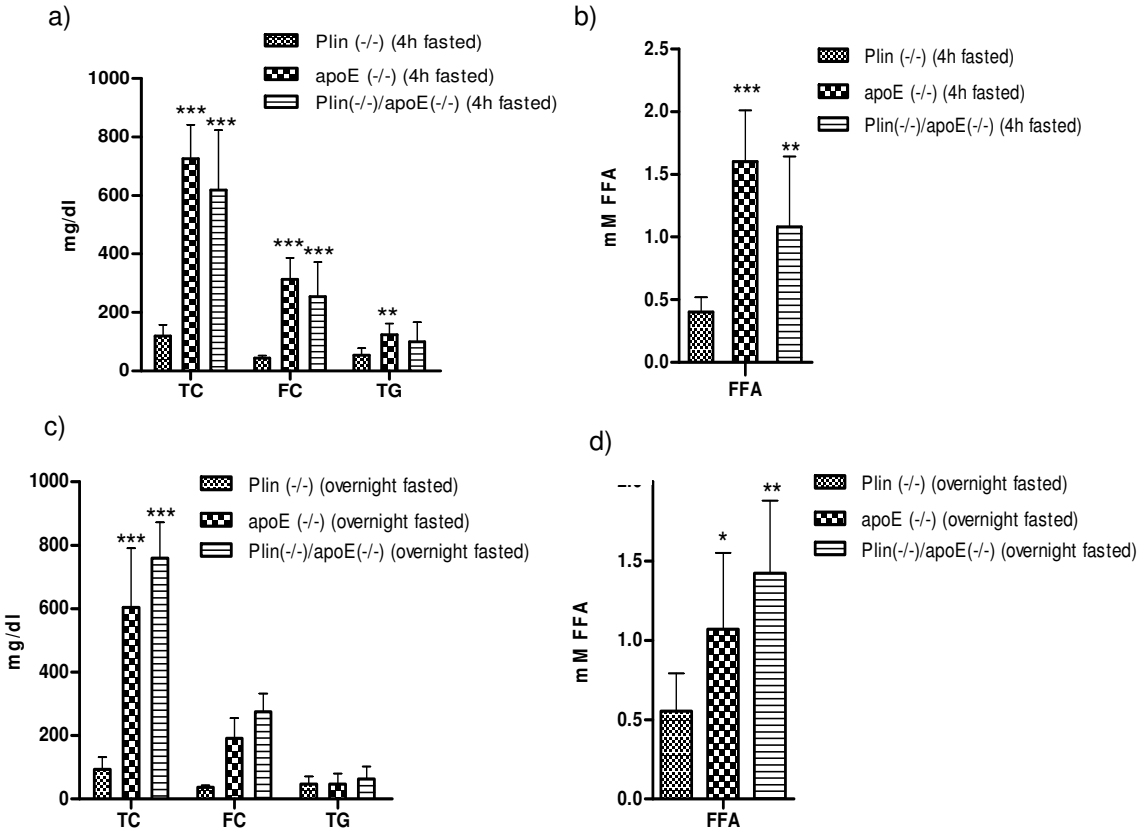

Fig.44: Plasma lipid parameters of male Plin (-/-), apoE (-/-) and Plin(-/-)/apoE(-/-) mice. Male mice were fed WTD for 8 weeks. Blood was taken after mice were fasted 4 hours (a, b) or overnight (c, d) and lipid parameters were determined enzymatically. Values represent mean (n=4-9) ± SD. * ($p<0.05$), ** (0.01), *** (0.001)

7.7.3. Plasma lipoprotein profile of Plin (-/-), apoE (-/-) and Plin(-/-)/apoE(-/-) mice after 8 weeks WTD

To investigate the content of total cholesterol in the different lipoprotein subclasses, pooled plasma from overnight fasted mice was analyzed using FPLC.

After separation of the lipoprotein classes by FPLC, female apoE (-/-) and Plin(-/-)/apoE(-/-) mice had markedly increased TC (62-fold and 61-fold, respectively) content in the VLDL-TC fraction and increased LDL cholesterol (7.2-fold and 5.8-fold, respectively) but markedly reduced HDL cholesterol (91,8% and 95%, respectively) compared to Plin (-/-) mice (Fig.45a) Female Plin(-/-)/apoE(-/-) mice had similar VLDL cholesterol, reduced LDL (20%) and HDL (36% reduced) cholesterol compared to apoE (-/-) mice (Fig.43a). Markedly increased TC in the VLDL fraction (43-fold and 59-fold, respectively), increased LDL cholesterol (5.3-fold and 7-fold, respectively) and markedly reduced HDL cholesterol (95% and 95%, respectively) were also observed in male apoE(-/-) and Plin(-/-)/apoE(-/-) mice compared to Plin (-/-) mice (Fig.43b). Cholesterol content of the VLDL fraction was decreased by 27% and LDL cholesterol was decreaed by 25% in male apoE (-/-) mice compared to Plin(-/-)/apoE (-/-) mice.

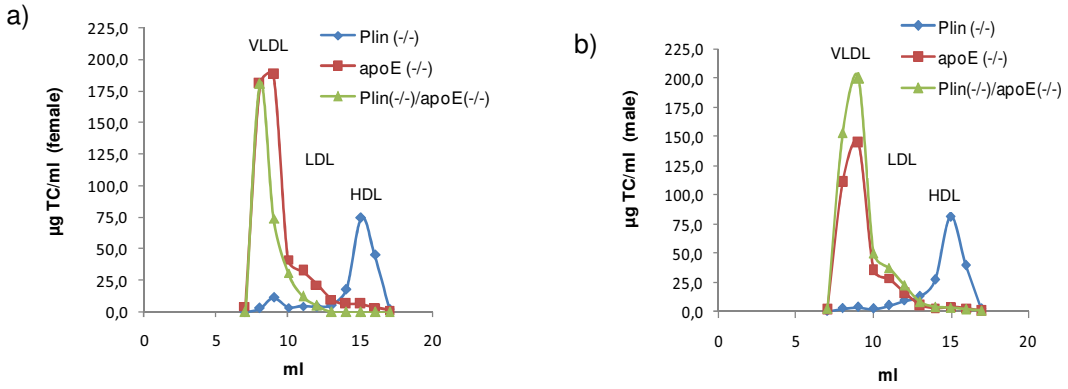

Fig.43: Lipoprotein profile of Plin (-/-), apoE (-/-) and Plin(-/-)/apoE(-/-) mice. Female and male mice were fed WTD for 8 weeks. Mice were sacrificed and lipoproteins were isolated by fast protein liquid chromatography (FPLC) using a Pharmacia FPLC system (Pfizer Pharma, Karlsruhe, Germany) equipped with a Superose 6 column (Amersham Biosciences, Piscataway, NJ). 200 µl pooled plasma from overnight fasted (a) female and (b) male mice were subjected to FPLC analysis and were eluted with 10mM Tris-HCl (in PBS), 1mM EDTA, 0.9% NaCl and 0.02% NaN_3, pH 7.4 with a flow of 0.5 ml/min. Fractions of 0.5 ml were collected and 50µl of each fraction were used for enzymatic TC determination Sodium-3,5-dichloro-2-hydroxybenzenesulfonate (DHBS) (Sigma-Aldrich, Vienna, Austria) was added to the TC reagent to enhance sensitivity.

7.7.4. Hepatic lipid parameters of Plin (-/-), apoE (-/-) and Plin(-/-)/apoE(-/-) mice

Hepatic TC, FC, TG and CE concentration were the same in female Plin (-/-), apoE (-/-) and Plin(-/-)/apoE(-/-) mice after 8 weeks WTD (Fig.44a). Hepatic TG concentrations were decreased by 46% in Plin(-/-)/apoE(-/-) mice compared to apoE (-/-) mice. In male apoE (-/-) and Plin(-/-)/apoE(-/-) mice, hepatic TC, FC, TG and CE concentrations were not different compared to Plin (-/-) mice and were not different comparing apoE (-/-) and Plin (-/-) mice.
Liver weights were similar comparing female and male Plin (-/-), apoE (-/-) and Plin(-/-)/apoE(-/-) mice. (Fig46a, b)

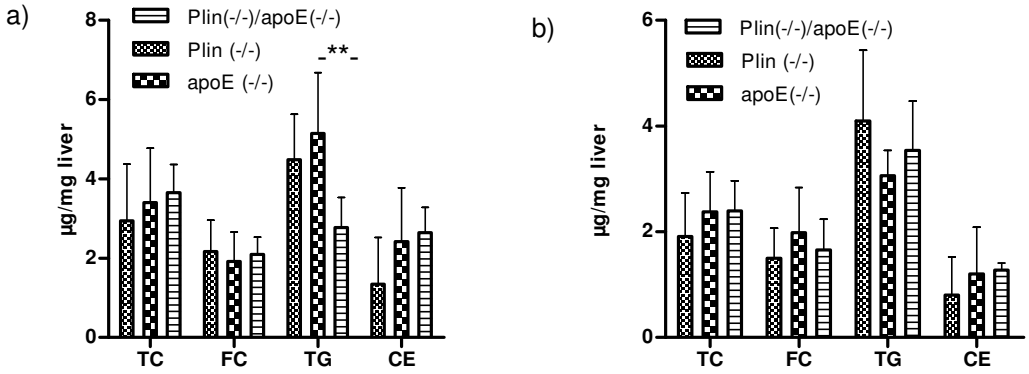

Fig.44: Hepatic lipid parameters of (a) female and (b) male mice after 8 weeks WTD. Female and male mice were fed WTD for 8 weeks. Mice were fasted overnight, perfused with PBS and about 100mg liver tissue were collected. Lipids from the livers were extracted with $CHCl_3$:MeOH (2:1) for 20 minutes on a rotating wheel. Lipid parameters were determined enzymatically. Values represent mean (n=4-9) ±SD. p<** (0.01).

a)

Sex	Plin	apoE	weight (g)	Liver (g)
f	ko	Wt	22,06	1,05
f	ko	Wt	21,86	0,79
f	ko	Wt	21,12	1,09
f	ko	Wt	19,06	0,85
f	ko	Wt	20,15	0,83
f	ko	Wt	20,30	0,77
f	ko	Wt	20,01	0,6
f	Wt	ko	20,97	0,97
f	Wt	ko	23,54	1,06
f	Wt	ko	25,14	1,45
f	Wt	ko	24,86	1,2
f	ko	ko	23,01	1,0
f	ko	ko	24,49	1,0
f	ko	ko	25,35	0,9
f	ko	ko	23,36	1,0
f	ko	ko	22,51	1,0
f	ko	ko	23,59	1,0
f	ko	ko	23,5	1,2
f	ko	ko	22,0	1,1
f	ko	ko	21,2	0,9
f	ko	ko	23,7	0,8

b)

Sex	Plin	apoE	weight (g)	Liver (g)
m	ko	Wt	33,10	1,71
m	ko	Wt	25,76	1,35
m	ko	Wt	37,05	2,0
m	ko	Wt	38,25	1,8
m	ko	Wt	27,60	0,9
m	ko	Wt	30,80	1,2
m	ko	Wt	28,87	1,0
m	Wt	Ko	31,94	1,27
m	Wt	Ko	32,89	1,2
m	Wt	Ko	28,36	1,3
m	Wt	Ko	33,80	1,4
m	Wt	Ko	26,69	1,0
m	ko	Ko	34,07	1,8
m	ko	Ko	29,15	1,2
m	ko	Ko	21,84	1,7
m	ko	Ko	29,96	1,1
m	ko	Ko	24,8	0,9

Fig.45: Body and liver weights of Plin (-/-), apoE (-/-) and Plin(-/-)/apoE(-/-) mice after 8 weeks WTD. (a) female and (b) male Plin (-/-), apoE (-/-) and Plin(-/-)/apoE(-/-) mice were fed WTD for 8 weeks. Mice were weighed, sacrificed, perfused and livers were weighed after perfusion.

7.7.5. Aortic root section analysis of atherosclerosis in Plin (-/-), apoE (-/-) and Plin(-/-)/apoE(-/-) mice

Neither female nor male Plin (-/-) mice developed plaques in their aortic root sections after 8 weeks WTD (Fig.46.a, b). Quantification of Oil red O stained aortic valve sections showed that lesion area in female Plin(-/-)/apoE(-/-) mice was reduced by 42% compared to apoE (-/-) mice (Fig.46c). Male apoE (-/-) and Plin(-/-)/apoE(-/-) mice did not show a difference in the lesion areas (Fig.46d).

a)

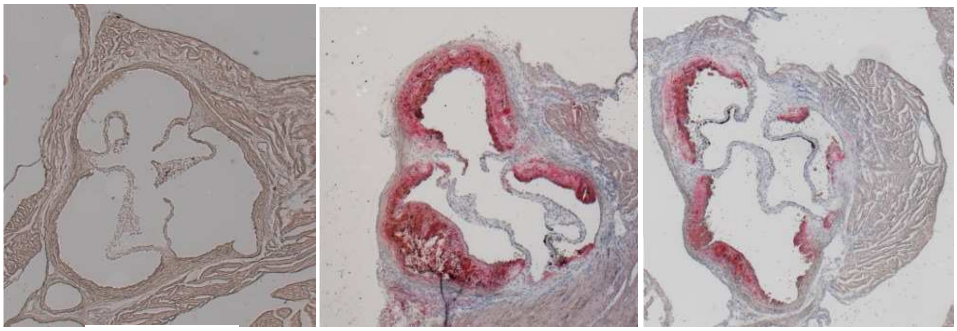

f Plin (-/-) **f apoE (-/-)** **f Plin(-/-)/apoE (-/-)**

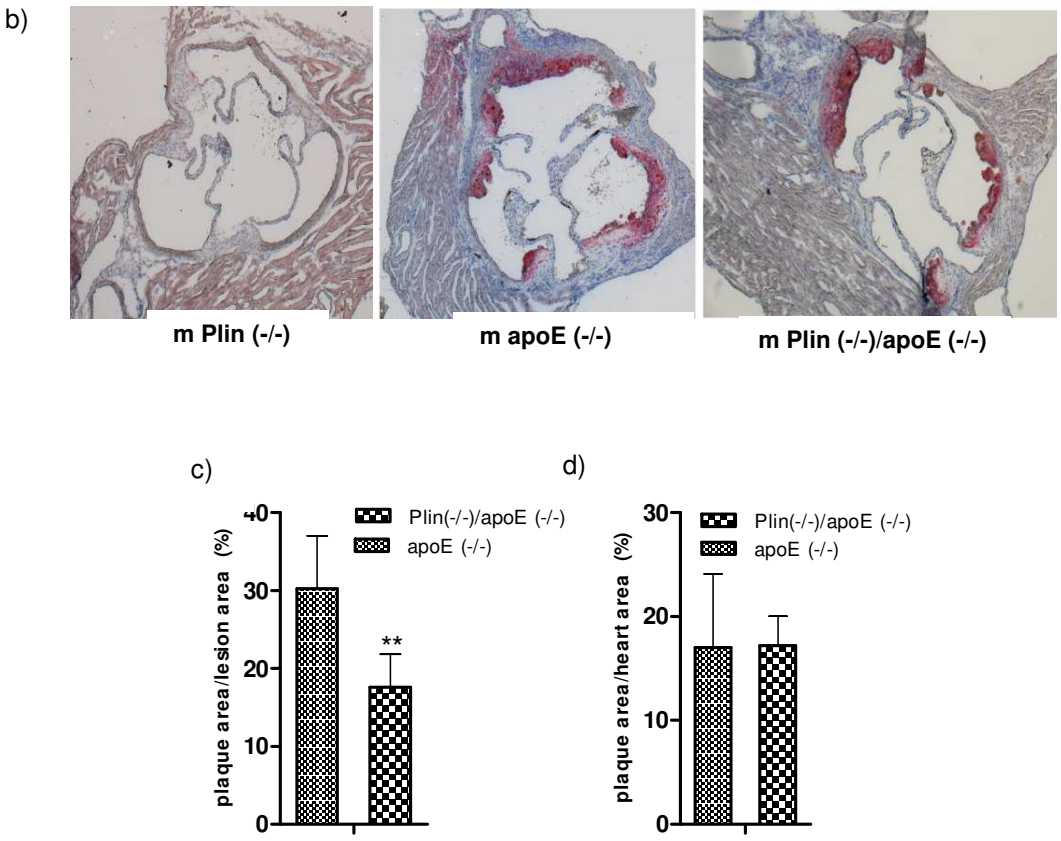

Fig.46: Aortic root section analysis of atherosclerosis in (arc) female and (bad) male Plin (-/-), apoE (-/-) and Plin(-/-)/apoE (-/-) mice. Mice were fed WTD for 8 weeks. Mice were sacrificed and hearts were perfused with PBS. Hearts were embedded in TissueTEK and 8 µm cryosections of the aortic root were cut. Lipid-rich regions were stained with Oil Red O and counterstained with hemotoxylin. (a, b) Shown are representative stained sections of the aortic valves. (c, d) Mean lesion areas in the aortic roots were analyzed in at least 10 consecutive heart sections of each mouse using ImageJ. Values represent mean (n=4-7) ±SD. ** (0.01).

8. DISCUSSION

Excess storage of lipids in cytosolic LD in non-adipose tissue under hyperlipidemic conditions is the starting point and cause of several metabolic disorders like obesity, diabetes and atherosclerosis. The family of PAT proteins are the predominant LD-associated proteins and through their tissue and time-dependent expression they finally determine the management of lipid storage in cells of all tissues (155).

The role of Plin in macrophages

Analogous to adipocytes and preadipocytes, LD-associated proteins could have similar roles in LD formation and their metabolism in macrophages. In the last years increasing interest has focused on the role of PAT proteins in macrophages. Adrp mRNA was shown to be present in human atherosclerotic lesions with macrophages being the predominant source of Adrp mRNA (174). The expression of Plin in macrophages has long been controversial, but recently the finding that Plin is also expressed in human atherosclerotic plaques (176, 177) has drawn new attention to its role in macrophage lipid metabolism and foam cell formation.
Using microscopy I could show that male and female Plin (-/-) foam cells, loaded with VLDL for 24 hours, had significantly smaller LD, one of the key findings of this thesis. Ectopic expression of Plin A in fibroblasts resulted in uniformly sized, Plin coated LD that were clustered (aggregated) in some areas of the cytosol (158). Adrp coated LD were dispersed throughout the cytosol. Incubation with the PKA activators forskolin and isobutylmethylxanthine resulted in dispersion of Plin coated LD, whereas the distribution of Adrp-coated LD was unaltered (199). Ectopic Plin A obviously potentially replaces Adrp to provide a better barrier against LD hydrolysis (180). It can be speculated that over-expression of Plin in macrophages could reconstitute LD size of that found in wild type macrophages. Adrp is the rate limiting protein for lipid accumulation in macrophages since lipid storage in LD was impaired in Adrp (-/-) macrophages (173). However, Adrp is obviously not protective enough to protect LD from hydrolysis. After incubation with oleate in the presence of triacsin C to avoid reincorporation of oleate into TG, no difference in the TG content was found between wild type and Adrp over-expressing THP1 cells (173). These results are in contrast to others (200) who showed elevated TG in Adrp expressing HEK293 cells after oleate treatment in the presence of triacsin C. Livers from Adrp (-/-) mice showed smaller LD compared to high-fat diet fed wild type mice (201). While TG concentrations were decreased in the cytosol, they were increased in the ER indicating a different cellular lipid distribution in the absence of Adrp due to impaired LD formation. Less LD were also observed in macrophages from Adrp(-/-)/apoE (-/-) mice in atherosclerotic lesions (175). The

inability of Adrp compensation thus possibly also influences lipid distribution in macrophages in the same way as in Adrp (-/-) hepatocytes (173).

The down-regulation of Adrp and Tip47 protein in macrophages and foam cells in the absence of Plin was a surprising result. Since Plin is not the predominant LD-associated protein in macrophages, I would have assumed that Plin deficiency does not have an impact on the expression of the other PAT proteins or if, leads to a compensatory up-regulation of Adrp and/or Tip47. An increased Tip47 expression was reported in mouse embryonic fibroblasts from Adrp (-/-) mice (202) indicating functional replacement. Others (200) reported a reduced expression of Tip47 and other unidentified proteins in the presence of Adrp in HEK293 cells. Interestingly, the absence of Adrp in macrophages and hepatocytes did not change Tip47 protein expression or the expression of other PAT proteins (201). The controversial results obtained in different cell models indicate that Adrp deficiency has diverse effects in different cell types and maybe also different tissues. While it promotes lipid accumulation in some tissues (like the liver or macrophages) it promotes lipid efflux in other tissues (like the muscle) to prevent those tissues from lipotoxic effects (193). In AML12 cells, the down-regulation of Adrp with a specific siRNA did not have an impact on LD size or number whereas Tip47 repression led to more, but smaller LD (203) resembling my results obtained in Plin (-/-) macrophages. The absence of both gave rise to a few large LD, which probably reflects fusion of LD in order to reduce the relation between surface area and the aqueous cytosol (203). Similar results were obtained in Huh7 cells (189). The relative expression of Adrp (and Plin) determines the capacity of a cell (or a tissue) to store TG (155). The repression of Adrp should therefore lead to a reduction in the total LD number. The fact that it does not can maybe be explained by its efficient replacement by Tip47 (203) and/or other exchangeable PAT proteins. In addition, Adrp was not completely silenced in the siRNA approach and remaining Adrp protein was possibly fulfilling its function to an adequate extent. Tip47 (like the other exchangeable PAT proteins) mediates the delivery of nascent TG to LD for their ultimate storage (155) and its absence should lead to disturbance in LD formation. To conclude, the repression of Adrp and Tip47 per se influences LD size and number. Since both are also down-regulated in the absence of Plin, this could explain the altered LD morphology in Plin (-/-) foam cells. Nevertheless, lipid accumulation in macrophages possibly depends on the total amount of the LD-surrounding PAT proteins, which is constantly lower in Adrp (-/-) macrophages compared to wild type cells (175). This possibility was not investigated in our experiments. However our observations of Adrp and Tip47 protein down-regulation in the absence of Plin indicate that the total PAT protein content could also be reduced in Plin (-/-) macrophages. Proteomic analysis of LD of basal and stimulated adipocytes has revealed a structural reorganization of LD going hand in hand

with an increase in mass of several proteins and the new recruitment of others upon stimulation (204). The possibility should be taken into account that other LD-associated proteins are up-regulated during deficiency of one PAT protein, also if these proteins occur in lower concentration and also if their up-regulation is probably insufficient to restore the normal ability of macrophages to form LD (175).

In macrophages Adrp protein was shown to be up-regulated, while Plin was not regulated (178), which is consistent with our own observations, or even down-regulated (205), showing a different regulation of the two proteins compared to adipocytes. In adipocytes, the functions of Adrp and Plin are not completely the same (178) and this could also be the case in macrophages. Similar to adipocytes, Plin could compete with Adrp in times of storage of large amounts of lipids since Plin over-expression led to TG accumulation in THP1 macrophages (178). Alternatively the conclusion might be drawn that Plin expression in macrophages is induced only under certain metabolic conditions like the presence of an inflammatory milieu, which was already shown to drive LD formation (206), and/or lipid mediators, which are present in atherosclerotic plaques (Letter to the editor from Larigauderie in Atherosclerosis 2007, Vol.190 “Towards the elucidation of the role of plin in human macrophages”).

Dispersion of Plin-coated LD after PKA activation was shown to be independent of lipolysis since remodeling of the LD was not anticipated by addition of the lipase inhibitor diethylumbelliferyl-phosphate (180). This suggests that the absence of Plin does not necessarily impairs lipase activity. Stimulated PKA-mediated phosphorylation of HSL does not promote enzyme activity but instead phosphorylation of Plin promotes the translocation and docking of HSL to the LD (158) . Moreover, in non-stimulated adipocytes, HSL and Plin are differentially located, HSL in the cytosol, Plin on LD (158, 207, 208). The independency of LD dispersion from lipolysis also provides a possible explanation why I could not find a difference in neutral TG and CE hydrolase activities between wild type and Plin (-/-) macrophages, regardless of smaller LD. Neither HSL nor ATGL were differently regulated on the mRNA or the protein level comparing wild type and Plin (-/-) macrophages or foam cells. In adipocytes, HSL activity is predominantly regulated by phosphorylation, promoting the translocation and docking of HSL to the LD (150). It is thus not surprising that no differences could be found in the expression of HSL on the mRNA or protein level since HSL activity is regulated predominantly post-translational. ATGL is now seen as the principal TG hydrolase, at least in mice (193), mediating the initial step in TG hydrolysis. However a direct interaction of Plin, ATGL and its activator CGI-58 on the LD surface of macrophages has not been proven so far. Lipolysis was not different between wild type and Plin (-/-) macrophages.

However, lipolysis is only of minor importance in macrophages. Its stimulation with PKA activators is maybe necessary to boost lipolysis and to see a higher lipolytic rate in Plin (-/-) macrophages compared to wild type cells similar as in adipocytes of Plin (-/-) mice (178).

FC, TG or CE content in female macrophages was not different between wild type and Plin (-/-) cells. After 6 hours loading with VLDL, TG content was markedly increased in Plin (-/-) foam cells. After 24 hours loading with VLDL, TG content was the same in wild type and Plin (-/-) foam cells. TG and FC content was significantly decreased in Plin (-/-) foam cells after 48 hours loading with aggLDL or VLDL. The difference in the TG content between wild type and Plin (-/-) foam cells was greater after VLDL loading compared to loading with aggLDL. Plin (-/-) foam cells, loaded with VLDL, showed a markedly increase in CPT-1α mRNA expression, indicating an increased β-oxidation. FA could be metabolized more rapidly in Plin (-/-) macrophages, maybe explaining the reduced TG content in Plin (-/-) foam cells. TG-rich particles, like VLDL, can be taken up by macrophages as holoparticles (209). LPL is able to bridge lipoproteins to receptors (SR-BI) (210, 211) or HSPG (212) mediating their uptake. Alternatively and predominantly, TG within the VLDL particle are hydrolyzed by LPL, releasing FFA which are taken up by macrophages (209, 213, 214) via passive diffusion or protein facilitated transport via CD36 (215). Within the cell, FFA are re-esterified into TG leading to TG accumulation. The remaining cholesterol-enriched remnant particles are taken up via binding to apoE-dependent receptors (LDLR, LRP, HSPG) leading to CE accumulation (216). The latter process is maybe also mediated via LPL (217). Adrp (-/-) THP1 macrophages showed a markedly decreased TG content after treatment with siRNA and 48 hours loading with VLDL and a faster uptake of VLDL in those cells was suggested to take place (173). However, I did not observe an increased LPL activity comparing wild type and Plin (-/-) macrophages, indicating that VLDL uptake is not different in both genotypes. However, an increased β-oxidation could potentially balance an increased VLDL uptake in Plin (-/-) foam cells. Both, wild type and Plin (-/-) foam cells had taken up an equivalent amount of oleic acid after 6 and 24 hours loading with [^{3}H]-oleic acid/BSA complex. After 6 hours loading, Plin (-/-) macrophages incorporated more oleic acid into PL. This could indicate that Plin (-/-) macrophages take up FA faster. In addition, the formation of smaller LD observed in Plin (-/-) foam cells would require more PL, which could explain the increased PL concentrations in Plin (-/-) foam cells after 6 hours loading. After 24 hours loading, this effect was not observed any more. The turnover of PL in macrophages is generally very fast (218) together with an increased β-oxidation in Plin (-/-) foam cells, this provides an explanation for this result. Chylomicron remnant-like particles were shown to be metabolized at different rates, depending on their FA constitution (219). Oleic acid was shown to be metabolized

more rapidly than other FA (219). An increased turnover of FA in Plin (-/-) macrophages could aggravate the detection of a difference in the uptake of FA between wild type and Plin (-/-) foam cells.

Peritoneal macrophages from Adrp(-/-)/apoE(-/-) mice showed an increased cholesterol efflux and reduced CE accumulation suggesting that Adrp preferentially delivers cholesterol to the CE pool for storage thereby promoting atherogenesis (175). To determine whether Plin deficiency influences cholesterol efflux similarly, I determined the mRNA expression of ABCA1 as the key transporter mediating cholesterol efflux in macrophages. ABCA1 mRNA was increased (1.9-fold) in Plin (-/-) foam cells after 6 hours loading with VLDL compared to wild type cells. After 24 hours loading this difference was not observed anymore. These data fit with the general increased metabolism that obviously takes place in Plin (-/-) macrophages. However whether cholesterol efflux in Plin (-/-) foam cells is definitively increased remains to be determined.

In adipocytes, LD size changes temporarily and spatially during differentiation as well as oleate loading (220). Olofsson and colleagues showed the existence of Adrp-SNARE (in particular Snap23, syntaxin5 and VAMP4, α-Snap and NSF) complexes on 3T3 adipocytes and linked them with homotypic LD fusion (221). The same group showed the recruitment of Snap23 to LD during oleate loading (222). If the expression of SNAREs is impaired, this also influences LD fusion, maybe resulting in smaller LD. However, SNAP23 and VAMP4 mRNA expression was not different between wild type and Plin (-/-) macrophages or foam cells indicating that fusion is possibly not disturbed in Plin (-/-) foam cells.

Formation of caveolae depends on cholesterol and caveolins are therefore preferentially found in cholesterol-enriched compartments like the Golgi and endosomes or the cytoplasma membrane (223). Caveolins are transported there from the ER via the Golgi by exocytosis. Caveolins were also found on LD (137, 139, 140, 224). N-terminally truncated isoforms of caveolins were shown to be located preferentially on LD (140) whereas full length caveolins were shown to relocate on LD only under conditions with high expression within the ER, like after over-expression, retention in the ER or inhibition of vesicular transport from the ER to the plasma membrane (223). Others (224) reported that caveolins are located on LD also under normal conditions. High levels of truncated caveolin-3 on LD dramatically redistributed cellular FC from the plasma membrane to late endosomes (140). Caveolins were thus proposed to regulate the recycling of cholesterol out of late endosomes thereby maintaining cellular cholesterol balance (223). After 6 hours loading with VLDL, caveolin-1 was markedly (3.7-fold) increased in Plin (-/-) foam cells compared to wild type cells, after 24 hours this

difference was no more observable. Since caveolin-1 expression was only investigated on the mRNA level, it remains to be determined whether protein expression correlates with that of the mRNA and if, where its concentration is definitively increased intracellularly. An increased concentration in the plasma membrane would make cholesterol more accessible for efflux, thereby lowering cholesterol content. On the other hand, an increase in endosomes or the ER would favor lipid accumulation.

The effect of Plin deficiency on plasma lipid parameters

By controlling adipocyte TG hydrolysis, Plin plays a central role in the regulation of whole body TG metabolism. This is also reflected by the phenotype of Plin (-/-) mice. They are lean, though they consume equal amounts of food compared to wild type mice (160). I also found reduced plasma TG concentrations in female and male Plin (-/-) after overnight fasting. TC concentrations were the same in wild type and Plin (-/-) mice. In male Plin (-/-) mice, TG were not reduced to the same extent as in female Plin (-/-) mice and failed to reach statistical significance. These results are in contrast to other reports (160) showing modestly increased TC and TG concentrations in Plin (-/-) mice when they were fasted overnight. The authors suggested that the increased plasma insulin levels present in fed Plin (-/-) mice might be responsible for the relatively balanced plasma lipid concentrations (160). The same group showed that in the fed state, Plin (-/-) mice had equivalent (in males) or lower (in females) plasma FFA concentrations (160). Our data are in accordance with these data but it has to be pointed out that they reflect FFA concentrations in the fasted state. In the fasted state, plasma lipid parameters reflect endogenously synthesized lipids and lipids which are mobilized from adipose tissue. While having a normal body weight, adipose tissue mass is reduced in Plin (-/-) mice to 30% of that in wild type mice and their muscle mass is increased by 10% (160). Abundant Adrp protein was found in adipose tissue of Plin (-/-) mice (160). They also have an increased metabolic rate in muscle and liver (225) reflected by a 16% higher oxygen consumption but an unaltered 24 hour respiratory exchange ratio compared to wild type mice (160). The increased β-oxidation may be the consequence of an increased adiponectin level (226, 227), which was found in Plin (-/-) mice (225). An increased β-oxidation is often linked with an increased insulin sensitivity (160) as it is the case in aged Plin (-/-) mice, but not young mice (225). It can be hypothesized that a reduced VLDL secretion together with an increased metabolism of FA in the liver leads to a reduced lipid distribution to adipose tissue and less FA can be found in the plasma during fasting. Adipocytes from Plin (-/-) mice had an increased basal lipolysis but released FA could be balanced by the increased metabolic rate in the muscle (225). One could argue that Plin (-/-) mice have a priori a reduced capacity to store nutritional lipids due to their reduced adipose

tissue mass, which should lead to elevated plasma TG and FFA concentrations. However this increase could again be counterbalanced by their increased metabolism in muscle and the liver. Plasma leptin levels are normally adapted to the adipose tissue mass. Surprisingly, fed Plin (-/-) mice had increased plasma leptin levels per fat mass although a correlation between leptin levels and the fat mass were preserved (160).

Loss of adipose tissue mass was causally linked with insulin resistance in different mouse models (mice over-expressing SREBP1c in adipose tissue (228) or mice lacking white adipose tissue (229)) leading to glucose intolerance. Regardless of increased insulin concentrations in fed Plin (-/-) mice, glucose tolerance test revealed no difference between Plin (-/-) mice and wild type mice with a body weight up to 30g. In accordance with others, who showed a sluggish glucose response after high fat diet (55% fat) feeding in wild type and Plin (-/-) mice (160), I could not find a significant difference in the glucose tolerance between wild type and Plin (-/-) mice after 6 month WTD (21% fat, 0.2% cholesterol). The ability to keep blood glucose at balanced levels may be due to elevated resistin levels, which regulate fasting blood glucose levels, and which are increased in Plin (-/-) mice. This leads to reduced hepatic glucose production (230) or elevated adiponectin levels which increase with decreasing Plin (225).

The impact of Plin deficiency on hepatic lipid metabolism

A differential expression and subcellular localization of PAT proteins (Adrp, Tip47 and Plin) in human steatotic livers was reported (231). Additionally, studies with full-length knockout mice and antisense oligonucleotide-treated mice revealed the important role for PAT proteins in the management of fat in non-adipose tissue. PAT protein composition on the LD surface of hepatocytes was shown to influence LD size (231) and their absence to induce cellular insulin resistance due to impaired LD utilization (203). The important role for Adrp in the liver was supported by the fact that Adrp (-/-) mice did not develop liver steatosis (201). Adipocyte differentiation, lipolysis and VLDL secretion were unaltered in those mice, blood lipid, glucose and insulin concentrations were normal. However, hepatic TG content was reduced to 40% of that in wild type mice and hepatic steatosis was attenuated after high-fat diet feeding (201). Adrp repression by an antisense oligonucleotide in C57BL/6J mice on high fat diet and $Lep^{ob/ob}$ mice led to a reduced hepatic TG content (without affecting cholesterol content), an attenuated hepatic TG secretion and decreased serum TG concentrations. Moreover, those mice displayed an improved glucose homeostasis (232). On the contrary, apoE (-/-) mice developed profound fat accumulation, macrophage proliferation and

inflammation within the liver after WTD feeding (233). The effects of the diet thereby depended on the type of fat administrated.

Plin is normally not expressed in hepatocytes or hepatocyte cell lines, but it was shown to be de novo expressed in human steatotic livers (231). This indicates again a supporting role for Plin in times of excess lipid accumulation similar as it was proposed for macrophages. The up-regulation of both Adrp and Plin in hepatocytes during high fat diet feeding suggests that both are important in hepatic LD maturation and maintenance (116). In wild type mice, de novo expression of Plin would therefore favour hepatic lipid accumulation, while the impact of its absence remains elusive. Plin (-/-) mice should basically be protected against liver steatosis due to their dramatically reduced fat mass and their increased muscle mass together with an increased metabolism of lipids in adipose tissue, muscle and the liver (225). In discrepancy with this hypothesis I observed massive lipid accumulation in the livers of Plin (-/-) mice after 6 months WTD feeding consistent with an increased (1.6-fold) liver weight. However hepatic TG concentrations were not increased to an adequate, although significant, extent. A possible explanation is that, although I considered to avoid this, samples from different liver sections (for example the center and the border) were used for the histological analysis and the determination of the lipid parameters which would explain this discrepancy. Lipid content of hepatocytes is regulated by integrated lipid uptake, synthesis, oxidation and export. Hepatic FA synthesis and β-oxidation can be imbalanced by diet (234). During insulin resistance, insulin does not adequately inhibit lipolysis within adipose tissue, leading to an increased flow of FA to the liver. Simultaneous elevated glucose concentrations additionally promote de novo hepatic FA synthesis thereby inhibiting β-oxidation at the same time (235). Both could have an effect in Plin (-/-) mice under conditions like WTD feeding.

Plin deficiency and its impact on the development of atherosclerosis

Mouse models for atherosclerosis are based on an altered lipoprotein metabolism, which is the result of diets in combination with the deficiency of enzymes that are implicated in lipoprotein metabolism (35). The most prominent models are the apoE (-/-) and the LDLR (-/-) model. More complex genetic models based on LDLR deficiency exist, like the apoB transgenic mouse or the apobec1 (-/-) mouse, which lacks apoB48. Another mouse, the apoE3L mouse has a rare dominant mutation in the apoE3 gene (236). Unlike in humans, HDL is the predominant lipoprotein in mice, effectively protecting wild type mice from atherogenesis (237). ApoE influences lipoprotein clearance and exerts anti-inflammatory and immune-modulating properties. It is thus suggested to be anti-atherogenic (35). Chylomicron and VLDL particles were increased in the plasma of apoE (-/-) mice and FPLC analysis showed that most of the plasma cholesterol was eluted in the VLDL range (238). I also

observed markedly increased plasma cholesterol concentrations in apoE (-/-) and Plin(-/-)/apoE(-/-) mice compared to Plin (-/-) mice after 8 weeks WTD (21% fat and 0.2% cholesterol) feeding, which were predominantly found in the VLDL fraction. apoA-I on chylomicrons and VLDL particles is exchanged with HDL only when apoE is present. In that way apoE restricts HDL production. In apoE (-/-) mice, apoA-I was mainly found in the chylomicron and VLDL fraction (238) leading to undetectable HDL levels. I also detected only low cholesterol quantities within the HDL fraction of apoE (-/-) and Plin/apoE (-/-) mice, whereas Plin (-/-) mice had markedly increased HDL levels compared to the other two genotypes. Chylomicrons and VLDL can maybe not enter the arterial wall as easy as the smaller LDL particles due to their size and one could argue that they are therefore less atherogenic. However, their delayed clearance in the absence of apoE may lead to oxidation, which causes their increased uptake by macrophages via scavenger receptors. ApoE (-/-) mice develop spontaneous atherosclerosis throughout the microvasculature on normal chow diet which is markedly accelerated by high-fat diet feeding (239). As expected, male and female apoE (-/-) developed marked atherosclerotic plaques in aortic root sections after 8 weeks WTD feeding. On the contrary, I did not detect any plaques in Plin (-/-) mice (as expected), which was a sex-independent effect. As expected, Plin(-/-)/apoE (-/-) mice also developed atherosclerosis but, interestingly, lesion area over several aortic root sections was reduced by 42% in female Plin(-/-)/apoE (-/-) mice compared to apoE (-/-) mice. This indicates that the absence of Plin is atheroprotective. In male mice, this difference was not observed. Besides its allele specific effects, apoE has also sex-specific effects on RCT, platelet aggregation and oxidative processes (reviewed in (240)) thus influencing atherogenesis differently in males and females. In consistence with this, male apoE (-/-) mice on a C57BL/6J background developed atherosclerotic plaques later than female apoE (-/-) mice (241). Due to protective mechanisms mentioned above, male mice are better protected against atherosclerosis and a longer feeding is necessary until these mechanisms fail.

To sum up, Plin deficiency in macrophages led to smaller LD after VLDL loading. The exact underlying mechanisms remain so far unclear and to be resolved. The physiological role of Plin in macrophages could be a supporting one in times of excess lipid accumulation. Alternatively Plin could be expressed only under certain metabolic conditions which occur in atherosclerotic plaques. Plin deficiency was atheroprotective in female Plin(-/-)/apoE(-/-) mice after 8 weeks WTD, which showed 42% reduced atherosclerotic plaque areas compared to apoE (-/-) mice and 50% decreased hepatic TG levels. Plin (-/-) mice had massive liver steatosis compared to wild type mice after 6 months WTD feeding, whereas female mice were better protected from steatosis compared to male mice. Further experiments are necessary to unscramble the pathophysiological mechanisms that underlie

the observed steatotic liver phenotype of Plin (-/-) mice. A possible mechanism could be a lowered hepatic lipoprotein secretion which would favour hepatic lipid accumulation and lack of Plin could impair hepatic lipid mobilization.

1. Harder, T., P. Scheiffele, P. Verkade, and K. Simons. 1998. Lipid domain structure of the plasma membrane revealed by patching of membrane components. *J Cell Biol* **141**: 929-942.
2. Guo, Y., K. R. Cordes, R. V. Farese, Jr., and T. C. Walther. 2009. Lipid droplets at a glance. *J Cell Sci* **122**: 749-752.
3. Ross, R. 1999. Atherosclerosis is an inflammatory disease. *Am Heart J* **138**: S419-420.
4. Libby, P. 2002. Inflammation in atherosclerosis. *Nature* **420**: 868-874.
5. Glass, C. K., and J. L. Witztum. 2001. Atherosclerosis. the road ahead. *Cell* **104**: 503-516.
6. Davignon, J., and P. Ganz. 2004. Role of endothelial dysfunction in atherosclerosis. *Circulation* **109**: III27-32.
7. Pantos, J., E. Efstathopoulos, and D. G. Katritsis. 2007. Vascular wall shear stress in clinical practice. *Curr Vasc Pharmacol* **5**: 113-119.
8. Papaioannou, T. G., E. N. Karatzis, M. Vavuranakis, J. P. Lekakis, and C. Stefanadis. 2006. Assessment of vascular wall shear stress and implications for atherosclerotic disease. *Int J Cardiol* **113**: 12-18.
9. Smith, E. B., I. B. Massie, and K. M. Alexander. 1976. The release of an immobilized lipoprotein fraction from atherosclerotic lesions by incubation with plasmin. *Atherosclerosis* **25**: 71-84.
10. Leake, D. S., and S. M. Rankin. 1990. The oxidative modification of low-density lipoproteins by macrophages. *Biochem J* **270**: 741-748.
11. van Hinsbergh, V. W., M. Scheffer, L. Havekes, and H. J. Kempen. 1986. Role of endothelial cells and their products in the modification of low-density lipoproteins. *Biochim Biophys Acta* **878**: 49-64.
12. Lamb, D. J., G. M. Wilkins, and D. S. Leake. 1992. The oxidative modification of low density lipoprotein by human lymphocytes. *Atherosclerosis* **92**: 187-192.
13. Aviram, M. 1992. Low density lipoprotein modification by cholesterol oxidase induces enhanced uptake and cholesterol accumulation in cells. *J Biol Chem* **267**: 218-225.
14. Aviram, M. 1993. Modified forms of low density lipoprotein and atherosclerosis. *Atherosclerosis* **98**: 1-9.
15. Aviram, M., and I. Maor. 1992. Phospholipase A2-modified LDL is taken up at enhanced rate by macrophages. *Biochem Biophys Res Commun* **185**: 465-472.
16. Buton, X., Z. Mamdouh, R. Ghosh, H. Du, G. Kuriakose, N. Beatini, G. A. Grabowski, F. R. Maxfield, and I. Tabas. 1999. Unique cellular events occurring during the initial interaction of macrophages with matrix-retained or methylated aggregated low density lipoprotein (LDL). Prolonged cell-surface contact during which ldl-cholesteryl ester hydrolysis exceeds ldl protein degradation. *J Biol Chem* **274**: 32112-32121.
17. Nievelstein, P. F., A. M. Fogelman, G. Mottino, and J. S. Frank. 1991. Lipid accumulation in rabbit aortic intima 2 hours after bolus infusion of low density lipoprotein. A deep-etch and immunolocalization study of ultrarapidly frozen tissue. *Arterioscler Thromb* **11**: 1795-1805.
18. Hoff, H. F., and R. E. Morton. 1985. Lipoproteins containing apo B extracted from human aortas. Structure and function. *Ann N Y Acad Sci* **454**: 183-194.
19. Steinberg, D., S. Parthasarathy, T. E. Carew, J. C. Khoo, and J. L. Witztum. 1989. Beyond cholesterol. Modifications of low-density lipoprotein that increase its atherogenicity. *N Engl J Med* **320**: 915-924.
20. Witztum, J. L., and D. Steinberg. 1991. Role of oxidized low density lipoprotein in atherogenesis. *J Clin Invest* **88**: 1785-1792.
21. Esterbauer, H., M. Dieber-Rotheneder, G. Striegl, and G. Waeg. 1991. Role of vitamin E in preventing the oxidation of low-density lipoprotein. *Am J Clin Nutr* **53**: 314S-321S.
22. Gordon, S. 2007. Macrophage heterogeneity and tissue lipids. *J Clin Invest* **117**: 89-93.
23. Swirski, F. K., P. Libby, E. Aikawa, P. Alcaide, F. W. Luscinskas, R. Weissleder, and M. J. Pittet. 2007. Ly-6Chi monocytes dominate hypercholesterolemia-associated monocytosis and give rise to macrophages in atheromata. *J Clin Invest* **117**: 195-205.

24. Swirski, F. K., R. Weissleder, and M. J. Pittet. 2009. Heterogeneous In Vivo Behavior of Monocyte Subsets in Atherosclerosis. *Arterioscler Thromb Vasc Biol*.
25. Navab, M., J. A. Berliner, A. D. Watson, S. Y. Hama, M. C. Territo, A. J. Lusis, D. M. Shih, B. J. Van Lenten, J. S. Frank, L. L. Demer, P. A. Edwards, and A. M. Fogelman. 1996. The Yin and Yang of oxidation in the development of the fatty streak. A review based on the 1994 George Lyman Duff Memorial Lecture. *Arterioscler Thromb Vasc Biol* **16**: 831-842.
26. Kleemann, R., S. Zadelaar, and T. Kooistra. 2008. Cytokines and atherosclerosis: a comprehensive review of studies in mice. *Cardiovasc Res* **79**: 360-376.
27. Moulton, K. S., E. Heller, M. A. Konerding, E. Flynn, W. Palinski, and J. Folkman. 1999. Angiogenesis inhibitors endostatin or TNP-470 reduce intimal neovascularization and plaque growth in apolipoprotein E-deficient mice. *Circulation* **99**: 1726-1732.
28. Galis, Z. S., G. K. Sukhova, M. W. Lark, and P. Libby. 1994. Increased expression of matrix metalloproteinases and matrix degrading activity in vulnerable regions of human atherosclerotic plaques. *J Clin Invest* **94**: 2493-2503.
29. Croce, K., and P. Libby. 2007. Intertwining of thrombosis and inflammation in atherosclerosis. *Curr Opin Hematol* **14**: 55-61.
30. Husmann, M., and M. Barton. 2007. Therapeutical potential of direct thrombin inhibitors for atherosclerotic vascular disease. *Expert Opin Investig Drugs* **16**: 563-567.
31. Brookes, Z. L., C. C. McGown, and C. S. Reilly. 2009. Statins for all: the new premed? *Br J Anaesth* **103**: 99-107.
32. Nicholls, S. J., E. M. Tuzcu, I. Sipahi, A. W. Grasso, P. Schoenhagen, T. Hu, K. Wolski, T. Crowe, M. Y. Desai, S. L. Hazen, S. R. Kapadia, and S. E. Nissen. 2007. Statins, high-density lipoprotein cholesterol, and regression of coronary atherosclerosis. *JAMA* **297**: 499-508.
33. Node, K., M. Fujita, M. Kitakaze, M. Hori, and J. K. Liao. 2003. Short-term statin therapy improves cardiac function and symptoms in patients with idiopathic dilated cardiomyopathy. *Circulation* **108**: 839-843.
34. Tall, A. 1995. Plasma lipid transfer proteins. *Annu Rev Biochem* **64**: 235-257.
35. Zadelaar, S., R. Kleemann, L. Verschuren, J. de Vries-Van der Weij, J. van der Hoorn, H. M. Princen, and T. Kooistra. 2007. Mouse models for atherosclerosis and pharmaceutical modifiers. *Arterioscler Thromb Vasc Biol* **27**: 1706-1721.
36. Yvan-Charvet, L., F. Matsuura, N. Wang, M. J. Bamberger, T. Nguyen, F. Rinninger, X. C. Jiang, C. L. Shear, and A. R. Tall. 2007. Inhibition of cholesteryl ester transfer protein by torcetrapib modestly increases macrophage cholesterol efflux to HDL. *Arterioscler Thromb Vasc Biol* **27**: 1132-1138.
37. Sehayek, E., and S. L. Hazen. 2008. Cholesterol absorption from the intestine is a major determinant of reverse cholesterol transport from peripheral tissue macrophages. *Arterioscler Thromb Vasc Biol* **28**: 1296-1297.
38. Rader, D. J., E. T. Alexander, G. L. Weibel, J. Billheimer, and G. H. Rothblat. 2009. The role of reverse cholesterol transport in animals and humans and relationship to atherosclerosis. *J Lipid Res* **50 Suppl**: S189-194.
39. Chang, C. C., N. Sakashita, K. Ornvold, O. Lee, E. T. Chang, R. Dong, S. Lin, C. Y. Lee, S. C. Strom, R. Kashyap, J. J. Fung, R. V. Farese, Jr., J. F. Patoiseau, A. Delhon, and T. Y. Chang. 2000. Immunological quantitation and localization of ACAT-1 and ACAT-2 in human liver and small intestine. *J Biol Chem* **275**: 28083-28092.
40. Lee, O., C. C. Chang, W. Lee, and T. Y. Chang. 1998. Immunodepletion experiments suggest that acyl-coenzyme A:cholesterol acyltransferase-1 (ACAT-1) protein plays a major catalytic role in adult human liver, adrenal gland, macrophages, and kidney, but not in intestines. *J Lipid Res* **39**: 1722-1727.
41. Chang, T. Y., B. L. Li, C. C. Chang, and Y. Urano. 2009. Acyl-coenzyme A:cholesterol acyltransferases. *Am J Physiol Endocrinol Metab* **297**: E1-9.
42. Llaverias, G., J. C. Laguna, and M. Alegret. 2003. Pharmacology of the ACAT inhibitor avasimibe (CI-1011). *Cardiovasc Drug Rev* **21**: 33-50.

43. Buhman, K. K., M. Accad, S. Novak, R. S. Choi, J. S. Wong, R. L. Hamilton, S. Turley, and R. V. Farese, Jr. 2000. Resistance to diet-induced hypercholesterolemia and gallstone formation in ACAT2-deficient mice. *Nat Med* **6**: 1341-1347.
44. Repa, J. J., K. K. Buhman, R. V. Farese, Jr., J. M. Dietschy, and S. D. Turley. 2004. ACAT2 deficiency limits cholesterol absorption in the cholesterol-fed mouse: impact on hepatic cholesterol homeostasis. *Hepatology* **40**: 1088-1097.
45. Bell, T. A., 3rd, J. M. Brown, M. J. Graham, K. M. Lemonidis, R. M. Crooke, and L. L. Rudel. 2006. Liver-specific inhibition of acyl-coenzyme a:cholesterol acyltransferase 2 with antisense oligonucleotides limits atherosclerosis development in apolipoprotein B100-only low-density lipoprotein receptor-/- mice. *Arterioscler Thromb Vasc Biol* **26**: 1814-1820.
46. Warner, G. J., G. Stoudt, M. Bamberger, W. J. Johnson, and G. H. Rothblat. 1995. Cell toxicity induced by inhibition of acyl coenzyme A:cholesterol acyltransferase and accumulation of unesterified cholesterol. *J Biol Chem* **270**: 5772-5778.
47. Rodriguez, A., and D. C. Usher. 2002. Anti-atherogenic effects of the acyl-CoA:cholesterol acyltransferase inhibitor, avasimibe (CI-1011), in cultured primary human macrophages. *Atherosclerosis* **161**: 45-54.
48. Mahley, R. W., T. L. Innerarity, S. C. Rall, Jr., and K. H. Weisgraber. 1984. Plasma lipoproteins: apolipoprotein structure and function. *J Lipid Res* **25**: 1277-1294.
49. Fainaru, M., R. W. Mahley, R. L. Hamilton, and T. L. Innerarity. 1982. Structural and metabolic heterogeneity of beta-very low density lipoproteins from cholesterol-fed dogs and from humans with type III hyperlipoproteinemia. *J Lipid Res* **23**: 702-714.
50. Harkes, L., A. van Duijne, and T. J. van Berkel. 1989. Interaction of beta-very-low-density lipoproteins with rat liver cells. *Eur J Biochem* **180**: 241-248.
51. Bersot, T. P., T. L. Innerarity, R. W. Mahley, and R. J. Havel. 1983. Cholesteryl ester accumulation in mouse peritoneal macrophages induced by beta-migrating very low density lipoproteins from patients with atypical dysbetalipoproteinemia. *J Clin Invest* **72**: 1024-1033.
52. Tabas, I., S. Lim, X. X. Xu, and F. R. Maxfield. 1990. Endocytosed beta-VLDL and LDL are delivered to different intracellular vesicles in mouse peritoneal macrophages. *J Cell Biol* **111**: 929-940.
53. Rye, K. A., and P. J. Barter. 2004. Formation and metabolism of prebeta-migrating, lipid-poor apolipoprotein A-I. *Arterioscler Thromb Vasc Biol* **24**: 421-428.
54. Brewer, H. B., Jr., A. T. Remaley, E. B. Neufeld, F. Basso, and C. Joyce. 2004. Regulation of plasma high-density lipoprotein levels by the ABCA1 transporter and the emerging role of high-density lipoprotein in the treatment of cardiovascular disease. *Arterioscler Thromb Vasc Biol* **24**: 1755-1760.
55. Lewis, G. F., and D. J. Rader. 2005. New insights into the regulation of HDL metabolism and reverse cholesterol transport. *Circ Res* **96**: 1221-1232.
56. Zambon, A., S. Bertocco, N. Vitturi, V. Polentarutti, D. Vianello, and G. Crepaldi. 2003. Relevance of hepatic lipase to the metabolism of triacylglycerol-rich lipoproteins. *Biochem Soc Trans* **31**: 1070-1074.
57. Wang, X., H. L. Collins, M. Ranalletta, I. V. Fuki, J. T. Billheimer, G. H. Rothblat, A. R. Tall, and D. J. Rader. 2007. Macrophage ABCA1 and ABCG1, but not SR-BI, promote macrophage reverse cholesterol transport in vivo. *J Clin Invest* **117**: 2216-2224.
58. Boucher, J., T. A. Ramsamy, S. Braschi, D. Sahoo, T. A. Neville, and D. L. Sparks. 2004. Apolipoprotein A-II regulates HDL stability and affects hepatic lipase association and activity. *J Lipid Res* **45**: 849-858.
59. Greenow, K., N. J. Pearce, and D. P. Ramji. 2005. The key role of apolipoprotein E in atherosclerosis. *J Mol Med* **83**: 329-342.
60. Goldberg, I. J., C. A. Scheraldi, L. K. Yacoub, U. Saxena, and C. L. Bisgaier. 1990. Lipoprotein ApoC-II activation of lipoprotein lipase. Modulation by apolipoprotein A-IV. *J Biol Chem* **265**: 4266-4272.

61. Kane, J. P. 1983. Apolipoprotein B: structural and metabolic heterogeneity. *Annu Rev Physiol* **45**: 637-650.
62. Segrest, J. P., M. K. Jones, H. De Loof, and N. Dashti. 2001. Structure of apolipoprotein B-100 in low density lipoproteins. *J Lipid Res* **42**: 1346-1367.
63. Stan, S., E. Delvin, M. Lambert, E. Seidman, and E. Levy. 2003. Apo A-IV: an update on regulation and physiologic functions. *Biochim Biophys Acta* **1631**: 177-187.
64. Cohn, J. S., R. Batal, M. Tremblay, H. Jacques, L. Veilleux, C. Rodriguez, O. Mamer, and J. Davignon. 2003. Plasma turnover of HDL apoC-I, apoC-III, and apoE in humans: in vivo evidence for a link between HDL apoC-III and apoA-I metabolism. *J Lipid Res* **44**: 1976-1983.
65. Hasham, S. N., and S. Pillarisetti. 2006. Vascular lipases, inflammation and atherosclerosis. *Clin Chim Acta* **372**: 179-183.
66. Wilson, K., G. L. Fry, D. A. Chappell, C. D. Sigmund, and J. D. Medh. 2001. Macrophage-specific expression of human lipoprotein lipase accelerates atherosclerosis in transgenic apolipoprotein e knockout mice but not in C57BL/6 mice. *Arterioscler Thromb Vasc Biol* **21**: 1809-1815.
67. McCoy, M. G., G. S. Sun, D. Marchadier, C. Maugeais, J. M. Glick, and D. J. Rader. 2002. Characterization of the lipolytic activity of endothelial lipase. *J Lipid Res* **43**: 921-929.
68. Jin, W., G. S. Sun, D. Marchadier, E. Octtaviani, J. M. Glick, and D. J. Rader. 2003. Endothelial cells secrete triglyceride lipase and phospholipase activities in response to cytokines as a result of endothelial lipase. *Circ Res* **92**: 644-650.
69. Maugeais, C., U. J. Tietge, U. C. Broedl, D. Marchadier, W. Cain, M. G. McCoy, S. Lund-Katz, J. M. Glick, and D. J. Rader. 2003. Dose-dependent acceleration of high-density lipoprotein catabolism by endothelial lipase. *Circulation* **108**: 2121-2126.
70. Cohen, J. C. 2003. Endothelial lipase: direct evidence for a role in HDL metabolism. *J Clin Invest* **111**: 318-321.
71. Jin, W., J. S. Millar, U. Broedl, J. M. Glick, and D. J. Rader. 2003. Inhibition of endothelial lipase causes increased HDL cholesterol levels in vivo. *J Clin Invest* **111**: 357-362.
72. Ishida, T., S. Choi, R. K. Kundu, K. Hirata, E. M. Rubin, A. D. Cooper, and T. Quertermous. 2003. Endothelial lipase is a major determinant of HDL level. *J Clin Invest* **111**: 347-355.
73. Ikonen, E. 2008. Cellular cholesterol trafficking and compartmentalization. *Nat Rev Mol Cell Biol* **9**: 125-138.
74. Simons, K., and E. Ikonen. 2000. How cells handle cholesterol. *Science* **290**: 1721-1726.
75. Tabas, I. 1997. Phospholipid metabolism in cholesterol-loaded macrophages. *Curr Opin Lipidol* **8**: 263-267.
76. Yeagle, P. L. 1991. Modulation of membrane function by cholesterol. *Biochimie* **73**: 1303-1310.
77. Papahadjopoulos, D. 1974. Cholesterol and cell membrane function: a hypothesis concerning etiology of atherosclerosis. *J Theor Biol* **43**: 329-337.
78. Puglielli, L., A. Rigotti, A. V. Greco, M. J. Santos, and F. Nervi. 1995. Sterol carrier protein-2 is involved in cholesterol transfer from the endoplasmic reticulum to the plasma membrane in human fibroblasts. *J Biol Chem* **270**: 18723-18726.
79. Smart, E. J., Y. Ying, W. C. Donzell, and R. G. Anderson. 1996. A role for caveolin in transport of cholesterol from endoplasmic reticulum to plasma membrane. *J Biol Chem* **271**: 29427-29435.
80. Cruz, J. C., and T. Y. Chang. 2000. Fate of endogenously synthesized cholesterol in Niemann-Pick type C1 cells. *J Biol Chem* **275**: 41309-41316.
81. Horton, J. D., J. L. Goldstein, and M. S. Brown. 2002. SREBPs: activators of the complete program of cholesterol and fatty acid synthesis in the liver. *J Clin Invest* **109**: 1125-1131.
82. Tabas, I. 2002. Consequences of cellular cholesterol accumulation: basic concepts and physiological implications. *J Clin Invest* **110**: 905-911.
83. Schmitz, G., and M. Grandl. 2008. Lipid homeostasis in macrophages - implications for atherosclerosis. *Rev Physiol Biochem Pharmacol* **160**: 93-125.

84. Porn, M. I., M. P. Ares, and J. P. Slotte. 1993. Degradation of plasma membrane phosphatidylcholine appears not to affect the cellular cholesterol distribution. *J Lipid Res* **34**: 1385-1392.
85. Brown, D. A., and E. London. 1998. Functions of lipid rafts in biological membranes. *Annu Rev Cell Dev Biol* **14**: 111-136.
86. Simons, K., and E. Ikonen. 1997. Functional rafts in cell membranes. *Nature* **387**: 569-572.
87. Nichols, B. J., and J. Lippincott-Schwartz. 2001. Endocytosis without clathrin coats. *Trends Cell Biol* **11**: 406-412.
88. Parton, R. G., and A. A. Richards. 2003. Lipid rafts and caveolae as portals for endocytosis: new insights and common mechanisms. *Traffic* **4**: 724-738.
89. Anderson, R. G. 1998. The caveolae membrane system. *Annu Rev Biochem* **67**: 199-225.
90. Smart, E. J., G. A. Graf, M. A. McNiven, W. C. Sessa, J. A. Engelman, P. E. Scherer, T. Okamoto, and M. P. Lisanti. 1999. Caveolins, liquid-ordered domains, and signal transduction. *Mol Cell Biol* **19**: 7289-7304.
91. Babitt, J., B. Trigatti, A. Rigotti, E. J. Smart, R. G. Anderson, S. Xu, and M. Krieger. 1997. Murine SR-BI, a high density lipoprotein receptor that mediates selective lipid uptake, is N-glycosylated and fatty acylated and colocalizes with plasma membrane caveolae. *J Biol Chem* **272**: 13242-13249.
92. Matveev, S., D. R. van der Westhuyzen, and E. J. Smart. 1999. Co-expression of scavenger receptor-BI and caveolin-1 is associated with enhanced selective cholesteryl ester uptake in THP-1 macrophages. *J Lipid Res* **40**: 1647-1654.
93. Mukherjee, S., R. N. Ghosh, and F. R. Maxfield. 1997. Endocytosis. *Physiol Rev* **77**: 759-803.
94. Lamaze, C., A. Dujeancourt, T. Baba, C. G. Lo, A. Benmerah, and A. Dautry-Varsat. 2001. Interleukin 2 receptors and detergent-resistant membrane domains define a clathrin-independent endocytic pathway. *Mol Cell* **7**: 661-671.
95. Kerr, M. C., and R. D. Teasdale. 2009. Defining macropinocytosis. *Traffic* **10**: 364-371.
96. Caron, E., and A. Hall. 1998. Identification of two distinct mechanisms of phagocytosis controlled by different Rho GTPases. *Science* **282**: 1717-1721.
97. Somsel Rodman, J., and A. Wandinger-Ness. 2000. Rab GTPases coordinate endocytosis. *J Cell Sci* **113 Pt 2**: 183-192.
98. Kruth, H. S., N. L. Jones, W. Huang, B. Zhao, I. Ishii, J. Chang, C. A. Combs, D. Malide, and W. Y. Zhang. 2005. Macropinocytosis is the endocytic pathway that mediates macrophage foam cell formation with native low density lipoprotein. *J Biol Chem* **280**: 2352-2360.
99. Falcone, S., E. Cocucci, P. Podini, T. Kirchhausen, E. Clementi, and J. Meldolesi. 2006. Macropinocytosis: regulated coordination of endocytic and exocytic membrane traffic events. *J Cell Sci* **119**: 4758-4769.
100. Steinberg, D. 2009. The LDL modification hypothesis of atherogenesis: an update. *J Lipid Res* **50 Suppl**: S376-381.
101. van Berkel, T. J., R. Out, M. Hoekstra, J. Kuiper, E. Biessen, and M. van Eck. 2005. Scavenger receptors: friend or foe in atherosclerosis? *Curr Opin Lipidol* **16**: 525-535.
102. Steinberg, D., and J. L. Witztum. 1990. Lipoproteins and atherogenesis. Current concepts. *JAMA* **264**: 3047-3052.
103. Khoo, J. C., E. Miller, P. McLoughlin, and D. Steinberg. 1988. Enhanced macrophage uptake of low density lipoprotein after self-aggregation. *Arteriosclerosis* **8**: 348-358.
104. Goldstein, J. L., Y. K. Ho, M. S. Brown, T. L. Innerarity, and R. W. Mahley. 1980. Cholesteryl ester accumulation in macrophages resulting from receptor-mediated uptake and degradation of hypercholesterolemic canine beta-very low density lipoproteins. *J Biol Chem* **255**: 1839-1848.
105. Klimov, A. N., A. D. Denisenko, A. G. Vinogradov, V. A. Nagornev, Y. I. Pivovarova, O. D. Sitnikova, and V. M. Pleskov. 1988. Accumulation of cholesteryl esters in macrophages incubated with human lipoprotein-antibody autoimmune complex. *Atherosclerosis* **74**: 41-46.
106. Schmidt, A. M., S. D. Yan, S. F. Yan, and D. M. Stern. 2000. The biology of the receptor for advanced glycation end products and its ligands. *Biochim Biophys Acta* **1498**: 99-111.

107. Thornalley, P. J. 1998. Cell activation by glycated proteins. AGE receptors, receptor recognition factors and functional classification of AGEs. *Cell Mol Biol (Noisy-le-grand)* **44**: 1013-1023.
108. Storch, J., and Z. Xu. 2009. Niemann-Pick C2 (NPC2) and intracellular cholesterol trafficking. *Biochim Biophys Acta* **1791**: 671-678.
109. Chang, T. Y., C. C. Chang, S. Lin, C. Yu, B. L. Li, and A. Miyazaki. 2001. Roles of acyl-coenzyme A:cholesterol acyltransferase-1 and -2. *Curr Opin Lipidol* **12**: 289-296.
110. Chen, W., Y. Sun, C. Welch, A. Gorelik, A. R. Leventhal, I. Tabas, and A. R. Tall. 2001. Preferential ATP-binding cassette transporter A1-mediated cholesterol efflux from late endosomes/lysosomes. *J Biol Chem* **276**: 43564-43569.
111. Zha, X., A. Gauthier, J. Genest, and R. McPherson. 2003. Secretory vesicular transport from the Golgi is altered during ATP-binding cassette protein A1 (ABCA1)-mediated cholesterol efflux. *J Biol Chem* **278**: 10002-10005.
112. Puri, V., J. R. Jefferson, R. D. Singh, C. L. Wheatley, D. L. Marks, and R. E. Pagano. 2003. Sphingolipid storage induces accumulation of intracellular cholesterol by stimulating SREBP-1 cleavage. *J Biol Chem* **278**: 20961-20970.
113. Brown, M. S., and J. L. Goldstein. 1999. A proteolytic pathway that controls the cholesterol content of membranes, cells, and blood. *Proc Natl Acad Sci U S A* **96**: 11041-11048.
114. Chawla, A., Y. Barak, L. Nagy, D. Liao, P. Tontonoz, and R. M. Evans. 2001. PPAR-gamma dependent and independent effects on macrophage-gene expression in lipid metabolism and inflammation. *Nat Med* **7**: 48-52.
115. Edvardsson, U., A. Ljungberg, D. Linden, L. William-Olsson, H. Peilot-Sjogren, A. Ahnmark, and J. Oscarsson. 2006. PPARalpha activation increases triglyceride mass and adipose differentiation-related protein in hepatocytes. *J Lipid Res* **47**: 329-340.
116. Motomura, W., M. Inoue, T. Ohtake, N. Takahashi, M. Nagamine, S. Tanno, Y. Kohgo, and T. Okumura. 2006. Up-regulation of ADRP in fatty liver in human and liver steatosis in mice fed with high fat diet. *Biochem Biophys Res Commun* **340**: 1111-1118.
117. Dalen, K. T., K. Schoonjans, S. M. Ulven, M. S. Weedon-Fekjaer, T. G. Bentzen, H. Koutnikova, J. Auwerx, and H. I. Nebb. 2004. Adipose tissue expression of the lipid droplet-associating proteins S3-12 and perilipin is controlled by peroxisome proliferator-activated receptor-gamma. *Diabetes* **53**: 1243-1252.
118. Dalen, K. T., S. M. Ulven, B. M. Arntsen, K. Solaas, and H. I. Nebb. 2006. PPARalpha activators and fasting induce the expression of adipose differentiation-related protein in liver. *J Lipid Res* **47**: 931-943.
119. Langmann, T., G. Liebisch, C. Moehle, R. Schifferer, R. Dayoub, S. Heiduczek, M. Grandl, A. Dada, and G. Schmitz. 2005. Gene expression profiling identifies retinoids as potent inducers of macrophage lipid efflux. *Biochim Biophys Acta* **1740**: 155-161.
120. Kubota, N., Y. Terauchi, H. Miki, H. Tamemoto, T. Yamauchi, K. Komeda, S. Satoh, R. Nakano, C. Ishii, T. Sugiyama, K. Eto, Y. Tsubamoto, A. Okuno, K. Murakami, H. Sekihara, G. Hasegawa, M. Naito, Y. Toyoshima, S. Tanaka, K. Shiota, T. Kitamura, T. Fujita, O. Ezaki, S. Aizawa, T. Kadowaki, and et al. 1999. PPAR gamma mediates high-fat diet-induced adipocyte hypertrophy and insulin resistance. *Mol Cell* **4**: 597-609.
121. Kliewer, S. A., J. M. Lenhard, T. M. Willson, I. Patel, D. C. Morris, and J. M. Lehmann. 1995. A prostaglandin J2 metabolite binds peroxisome proliferator-activated receptor gamma and promotes adipocyte differentiation. *Cell* **83**: 813-819.
122. Nagy, L., P. Tontonoz, J. G. Alvarez, H. Chen, and R. M. Evans. 1998. Oxidized LDL regulates macrophage gene expression through ligand activation of PPARgamma. *Cell* **93**: 229-240.
123. Huang, J. T., J. S. Welch, M. Ricote, C. J. Binder, T. M. Willson, C. Kelly, J. L. Witztum, C. D. Funk, D. Conrad, and C. K. Glass. 1999. Interleukin-4-dependent production of PPAR-gamma ligands in macrophages by 12/15-lipoxygenase. *Nature* **400**: 378-382.
124. Jiang, C., A. T. Ting, and B. Seed. 1998. PPAR-gamma agonists inhibit production of monocyte inflammatory cytokines. *Nature* **391**: 82-86.

125. Ricote, M., A. C. Li, T. M. Willson, C. J. Kelly, and C. K. Glass. 1998. The peroxisome proliferator-activated receptor-gamma is a negative regulator of macrophage activation. *Nature* **391**: 79-82.
126. Marx, N., G. Sukhova, C. Murphy, P. Libby, and J. Plutzky. 1998. Macrophages in human atheroma contain PPARgamma: differentiation-dependent peroxisomal proliferator-activated receptor gamma(PPARgamma) expression and reduction of MMP-9 activity through PPARgamma activation in mononuclear phagocytes in vitro. *Am J Pathol* **153**: 17-23.
127. Tontonoz, P., L. Nagy, J. G. Alvarez, V. A. Thomazy, and R. M. Evans. 1998. PPARgamma promotes monocyte/macrophage differentiation and uptake of oxidized LDL. *Cell* **93**: 241-252.
128. Bartz, R., W. H. Li, B. Venables, J. K. Zehmer, M. R. Roth, R. Welti, R. G. Anderson, P. Liu, and K. D. Chapman. 2007. Lipidomics reveals that adiposomes store ether lipids and mediate phospholipid traffic. *J Lipid Res* **48**: 837-847.
129. Tauchi-Sato, K., S. Ozeki, T. Houjou, R. Taguchi, and T. Fujimoto. 2002. The surface of lipid droplets is a phospholipid monolayer with a unique Fatty Acid composition. *J Biol Chem* **277**: 44507-44512.
130. Ducharme, N. A., and P. E. Bickel. 2008. Lipid droplets in lipogenesis and lipolysis. *Endocrinology* **149**: 942-949.
131. Marchesan, D., M. Rutberg, L. Andersson, L. Asp, T. Larsson, J. Boren, B. R. Johansson, and S. O. Olofsson. 2003. A phospholipase D-dependent process forms lipid droplets containing caveolin, adipocyte differentiation-related protein, and vimentin in a cell-free system. *J Biol Chem* **278**: 27293-27300.
132. Robenek, H., O. Hofnagel, I. Buers, M. J. Robenek, D. Troyer, and N. J. Severs. 2006. Adipophilin-enriched domains in the ER membrane are sites of lipid droplet biogenesis. *J Cell Sci* **119**: 4215-4224.
133. Brown, D. A. 2001. Lipid droplets: proteins floating on a pool of fat. *Curr Biol* **11**: R446-449.
134. Ploegh, H. L. 2007. A lipid-based model for the creation of an escape hatch from the endoplasmic reticulum. *Nature* **448**: 435-438.
135. Walther, T. C., and R. V. Farese, Jr. 2009. The life of lipid droplets. *Biochim Biophys Acta* **1791**: 459-466.
136. Ost, A., U. Ortegren, J. Gustavsson, F. H. Nystrom, and P. Stralfors. 2005. Triacylglycerol is synthesized in a specific subclass of caveolae in primary adipocytes. *J Biol Chem* **280**: 5-8.
137. Fujimoto, T., H. Kogo, K. Ishiguro, K. Tauchi, and R. Nomura. 2001. Caveolin-2 is targeted to lipid droplets, a new "membrane domain" in the cell. *J Cell Biol* **152**: 1079-1085.
138. Fujimoto, Y., J. Onoduka, K. J. Homma, S. Yamaguchi, M. Mori, Y. Higashi, M. Makita, T. Kinoshita, J. Noda, H. Itabe, and T. Takanoa. 2006. Long-chain fatty acids induce lipid droplet formation in a cultured human hepatocyte in a manner dependent of Acyl-CoA synthetase. *Biol Pharm Bull* **29**: 2174-2180.
139. Ostermeyer, A. G., J. M. Paci, Y. Zeng, D. M. Lublin, S. Munro, and D. A. Brown. 2001. Accumulation of caveolin in the endoplasmic reticulum redirects the protein to lipid storage droplets. *J Cell Biol* **152**: 1071-1078.
140. Pol, A., R. Luetterforst, M. Lindsay, S. Heino, E. Ikonen, and R. G. Parton. 2001. A caveolin dominant negative mutant associates with lipid bodies and induces intracellular cholesterol imbalance. *J Cell Biol* **152**: 1057-1070.
141. Cohen, A. W., B. Razani, W. Schubert, T. M. Williams, X. B. Wang, P. Iyengar, D. L. Brasaemle, P. E. Scherer, and M. P. Lisanti. 2004. Role of caveolin-1 in the modulation of lipolysis and lipid droplet formation. *Diabetes* **53**: 1261-1270.
142. Guo, Y., T. C. Walther, M. Rao, N. Stuurman, G. Goshima, K. Terayama, J. S. Wong, R. D. Vale, P. Walter, and R. V. Farese. 2008. Functional genomic screen reveals genes involved in lipid-droplet formation and utilization. *Nature* **453**: 657-661.
143. Bostrom, P., M. Rutberg, J. Ericsson, P. Holmdahl, L. Andersson, M. A. Frohman, J. Boren, and S. O. Olofsson. 2005. Cytosolic lipid droplets increase in size by microtubule-dependent complex formation. *Arterioscler Thromb Vasc Biol* **25**: 1945-1951.

144. Zehmer, J. K., Y. Huang, G. Peng, J. Pu, R. G. Anderson, and P. Liu. 2009. A role for lipid droplets in inter-membrane lipid traffic. *Proteomics* **9**: 914-921.
145. Welte, M. A., S. Cermelli, J. Griner, A. Viera, Y. Guo, D. H. Kim, J. G. Gindhart, and S. P. Gross. 2005. Regulation of lipid-droplet transport by the perilipin homolog LSD2. *Curr Biol* **15**: 1266-1275.
146. Teixeira, L., C. Rabouille, P. Rorth, A. Ephrussi, and N. F. Vanzo. 2003. Drosophila Perilipin/ADRP homologue Lsd2 regulates lipid metabolism. *Mech Dev* **120**: 1071-1081.
147. Welte, M. A. 2007. Proteins under new management: lipid droplets deliver. *Trends Cell Biol* **17**: 363-369.
148. Cermelli, S., Y. Guo, S. P. Gross, and M. A. Welte. 2006. The lipid-droplet proteome reveals that droplets are a protein-storage depot. *Curr Biol* **16**: 1783-1795.
149. Bartz, R., J. K. Zehmer, M. Zhu, Y. Chen, G. Serrero, Y. Zhao, and P. Liu. 2007. Dynamic activity of lipid droplets: protein phosphorylation and GTP-mediated protein translocation. *J Proteome Res* **6**: 3256-3265.
150. Brasaemle, D. L. 2007. Thematic review series: adipocyte biology. The perilipin family of structural lipid droplet proteins: stabilization of lipid droplets and control of lipolysis. *J Lipid Res* **48**: 2547-2559.
151. Kuerschner, L., C. Moessinger, and C. Thiele. 2008. Imaging of lipid biosynthesis: how a neutral lipid enters lipid droplets. *Traffic* **9**: 338-352.
152. Stone, S. J., M. C. Levin, P. Zhou, J. Han, T. C. Walther, and R. V. Farese, Jr. 2009. The endoplasmic reticulum enzyme DGAT2 is found in mitochondria-associated membranes and has a mitochondrial targeting signal that promotes its association with mitochondria. *J Biol Chem* **284**: 5352-5361.
153. Martin, S., and R. G. Parton. 2006. Lipid droplets: a unified view of a dynamic organelle. *Nat Rev Mol Cell Biol* **7**: 373-378.
154. Greenberg, A. S., J. J. Egan, S. A. Wek, N. B. Garty, E. J. Blanchette-Mackie, and C. Londos. 1991. Perilipin, a major hormonally regulated adipocyte-specific phosphoprotein associated with the periphery of lipid storage droplets. *J Biol Chem* **266**: 11341-11346.
155. Wolins, N. E., D. L. Brasaemle, and P. E. Bickel. 2006. A proposed model of fat packaging by exchangeable lipid droplet proteins. *FEBS Lett* **580**: 5484-5491.
156. Blanchette-Mackie, E. J., N. K. Dwyer, T. Barber, R. A. Coxey, T. Takeda, C. M. Rondinone, J. L. Theodorakis, A. S. Greenberg, and C. Londos. 1995. Perilipin is located on the surface layer of intracellular lipid droplets in adipocytes. *J Lipid Res* **36**: 1211-1226.
157. Brasaemle, D. L., T. Barber, A. R. Kimmel, and C. Londos. 1997. Post-translational regulation of perilipin expression. Stabilization by stored intracellular neutral lipids. *J Biol Chem* **272**: 9378-9387.
158. Brasaemle, D. L., B. Rubin, I. A. Harten, J. Gruia-Gray, A. R. Kimmel, and C. Londos. 2000. Perilipin A increases triacylglycerol storage by decreasing the rate of triacylglycerol hydrolysis. *J Biol Chem* **275**: 38486-38493.
159. Martinez-Botas, J., J. B. Anderson, D. Tessier, A. Lapillonne, B. H. Chang, M. J. Quast, D. Gorenstein, K. H. Chen, and L. Chan. 2000. Absence of perilipin results in leanness and reverses obesity in Lepr(db/db) mice. *Nat Genet* **26**: 474-479.
160. Tansey, J. T., C. Sztalryd, J. Gruia-Gray, D. L. Roush, J. V. Zee, O. Gavrilova, M. L. Reitman, C. X. Deng, C. Li, A. R. Kimmel, and C. Londos. 2001. Perilipin ablation results in a lean mouse with aberrant adipocyte lipolysis, enhanced leptin production, and resistance to diet-induced obesity. *Proc Natl Acad Sci U S A* **98**: 6494-6499.
161. Tansey, J. T., A. M. Huml, R. Vogt, K. E. Davis, J. M. Jones, K. A. Fraser, D. L. Brasaemle, A. R. Kimmel, and C. Londos. 2003. Functional studies on native and mutated forms of perilipins. A role in protein kinase A-mediated lipolysis of triacylglycerols. *J Biol Chem* **278**: 8401-8406.
162. Greenberg, A. S., J. J. Egan, S. A. Wek, M. C. Moos, Jr., C. Londos, and A. R. Kimmel. 1993. Isolation of cDNAs for perilipins A and B: sequence and expression of lipid droplet-associated proteins of adipocytes. *Proc Natl Acad Sci U S A* **90**: 12035-12039.

163. Lu, X., J. Gruia-Gray, N. G. Copeland, D. J. Gilbert, N. A. Jenkins, C. Londos, and A. R. Kimmel. 2001. The murine perilipin gene: the lipid droplet-associated perilipins derive from tissue-specific, mRNA splice variants and define a gene family of ancient origin. *Mamm Genome* **12**: 741-749.
164. Servetnick, D. A., D. L. Brasaemle, J. Gruia-Gray, A. R. Kimmel, J. Wolff, and C. Londos. 1995. Perilipins are associated with cholesteryl ester droplets in steroidogenic adrenal cortical and Leydig cells. *J Biol Chem* **270**: 16970-16973.
165. Brasaemle, D. L., T. Barber, N. E. Wolins, G. Serrero, E. J. Blanchette-Mackie, and C. Londos. 1997. Adipose differentiation-related protein is an ubiquitously expressed lipid storage droplet-associated protein. *J Lipid Res* **38**: 2249-2263.
166. Gross, D. N., H. Miyoshi, T. Hosaka, H. H. Zhang, E. C. Pino, S. Souza, M. Obin, A. S. Greenberg, and P. F. Pilch. 2006. Dynamics of lipid droplet-associated proteins during hormonally stimulated lipolysis in engineered adipocytes: stabilization and lipid droplet binding of adipocyte differentiation-related protein/adipophilin. *Mol Endocrinol* **20**: 459-466.
167. Xu, G., C. Sztalryd, X. Lu, J. T. Tansey, J. Gan, H. Dorward, A. R. Kimmel, and C. Londos. 2005. Post-translational regulation of adipose differentiation-related protein by the ubiquitin/proteasome pathway. *J Biol Chem* **280**: 42841-42847.
168. Wolins, N. E., B. K. Quaynor, J. R. Skinner, M. J. Schoenfish, A. Tzekov, and P. E. Bickel. 2005. S3-12, Adipophilin, and TIP47 package lipid in adipocytes. *J Biol Chem* **280**: 19146-19155.
169. Wolins, N. E., J. R. Skinner, M. J. Schoenfish, A. Tzekov, K. G. Bensch, and P. E. Bickel. 2003. Adipocyte protein S3-12 coats nascent lipid droplets. *J Biol Chem* **278**: 37713-37721.
170. Wolins, N. E., B. Rubin, and D. L. Brasaemle. 2001. TIP47 associates with lipid droplets. *J Biol Chem* **276**: 5101-5108.
171. Skinner, J. R., T. M. Shew, D. M. Schwartz, A. Tzekov, C. M. Lepus, N. A. Abumrad, and N. E. Wolins. 2009. Diacylglycerol enrichment of endoplasmic reticulum or lipid droplets recruits perilipin 3/TIP47 during lipid storage and mobilization. *J Biol Chem* **284**: 30941-30948.
172. Wang, X., T. J. Reape, X. Li, K. Rayner, C. L. Webb, K. G. Burnand, and P. G. Lysko. 1999. Induced expression of adipophilin mRNA in human macrophages stimulated with oxidized low-density lipoprotein and in atherosclerotic lesions. *FEBS Lett* **462**: 145-150.
173. Larigauderie, G., C. Cuaz-Perolin, A. B. Younes, C. Furman, C. Lasselin, C. Copin, M. Jaye, J. C. Fruchart, and M. Rouis. 2006. Adipophilin increases triglyceride storage in human macrophages by stimulation of biosynthesis and inhibition of beta-oxidation. *FEBS J* **273**: 3498-3510.
174. Larigauderie, G., C. Furman, M. Jaye, C. Lasselin, C. Copin, J. C. Fruchart, G. Castro, and M. Rouis. 2004. Adipophilin enhances lipid accumulation and prevents lipid efflux from THP-1 macrophages: potential role in atherogenesis. *Arterioscler Thromb Vasc Biol* **24**: 504-510.
175. Paul, A., B. H. Chang, L. Li, V. K. Yechoor, and L. Chan. 2008. Deficiency of adipose differentiation-related protein impairs foam cell formation and protects against atherosclerosis. *Circ Res* **102**: 1492-1501.
176. Faber, B. C., K. B. Cleutjens, R. L. Niessen, P. L. Aarts, W. Boon, A. S. Greenberg, P. J. Kitslaar, J. H. Tordoir, and M. J. Daemen. 2001. Identification of genes potentially involved in rupture of human atherosclerotic plaques. *Circ Res* **89**: 547-554.
177. Forcheron, F., L. Legedz, G. Chinetti, P. Feugier, D. Letexier, G. Bricca, and M. Beylot. 2005. Genes of cholesterol metabolism in human atheroma: overexpression of perilipin and genes promoting cholesterol storage and repression of ABCA1 expression. *Arterioscler Thromb Vasc Biol* **25**: 1711-1717.
178. Larigauderie, G., M. A. Bouhlel, C. Furman, M. Jaye, J. C. Fruchart, and M. Rouis. 2006. Perilipin, a potential substitute for adipophilin in triglyceride storage in human macrophages. *Atherosclerosis* **189**: 142-148.
179. Buers, I., H. Robenek, S. Lorkowski, Y. Nitschke, N. J. Severs, and O. Hofnagel. 2009. TIP47, a Lipid Cargo Protein Involved in Macrophage Triglyceride Metabolism. *Arterioscler Thromb Vasc Biol*.
180. Brasaemle, D. L., V. Subramanian, A. Garcia, A. Marcinkiewicz, and A. Rothenberg. 2009. Perilipin A and the control of triacylglycerol metabolism. *Mol Cell Biochem* **326**: 15-21.

181. Puri, V., S. Konda, S. Ranjit, M. Aouadi, A. Chawla, M. Chouinard, A. Chakladar, and M. P. Czech. 2007. Fat-specific protein 27, a novel lipid droplet protein that enhances triglyceride storage. *J Biol Chem* **282**: 34213-34218.
182. Inohara, N., T. Koseki, S. Chen, X. Wu, and G. Nunez. 1998. CIDE, a novel family of cell death activators with homology to the 45 kDa subunit of the DNA fragmentation factor. *EMBO J* **17**: 2526-2533.
183. Subramanian, V., A. Garcia, A. Sekowski, and D. L. Brasaemle. 2004. Hydrophobic sequences target and anchor perilipin A to lipid droplets. *J Lipid Res* **45**: 1983-1991.
184. Puri, V., S. Ranjit, S. Konda, S. M. Nicoloro, J. Straubhaar, A. Chawla, M. Chouinard, C. Lin, A. Burkart, S. Corvera, R. A. Perugini, and M. P. Czech. 2008. Cidea is associated with lipid droplets and insulin sensitivity in humans. *Proc Natl Acad Sci U S A* **105**: 7833-7838.
185. Zhou, Z., S. Yon Toh, Z. Chen, K. Guo, C. P. Ng, S. Ponniah, S. C. Lin, W. Hong, and P. Li. 2003. Cidea-deficient mice have lean phenotype and are resistant to obesity. *Nat Genet* **35**: 49-56.
186. Garcia, A., A. Sekowski, V. Subramanian, and D. L. Brasaemle. 2003. The central domain is required to target and anchor perilipin A to lipid droplets. *J Biol Chem* **278**: 625-635.
187. Zhang, H. H., S. C. Souza, K. V. Muliro, F. B. Kraemer, M. S. Obin, and A. S. Greenberg. 2003. Lipase-selective functional domains of perilipin A differentially regulate constitutive and protein kinase A-stimulated lipolysis. *J Biol Chem* **278**: 51535-51542.
188. Yamaguchi, T., S. Matsushita, K. Motojima, F. Hirose, and T. Osumi. 2006. MLDP, a novel PAT family protein localized to lipid droplets and enriched in the heart, is regulated by peroxisome proliferator-activated receptor alpha. *J Biol Chem* **281**: 14232-14240.
189. Ohsaki, Y., T. Maeda, M. Maeda, K. Tauchi-Sato, and T. Fujimoto. 2006. Recruitment of TIP47 to lipid droplets is controlled by the putative hydrophobic cleft. *Biochem Biophys Res Commun* **347**: 279-287.
190. Hickenbottom, S. J., A. R. Kimmel, C. Londos, and J. H. Hurley. 2004. Structure of a lipid droplet protein; the PAT family member TIP47. *Structure* **12**: 1199-1207.
191. Bussell, R., Jr., and D. Eliezer. 2003. A structural and functional role for 11-mer repeats in alpha-synuclein and other exchangeable lipid binding proteins. *J Mol Biol* **329**: 763-778.
192. Scherer, P. E., P. E. Bickel, M. Kotler, and H. F. Lodish. 1998. Cloning of cell-specific secreted and surface proteins by subtractive antibody screening. *Nat Biotechnol* **16**: 581-586.
193. Bickel, P. E., J. T. Tansey, and M. A. Welte. 2009. PAT proteins, an ancient family of lipid droplet proteins that regulate cellular lipid stores. *Biochim Biophys Acta* **1791**: 419-440.
194. Kimmel, A. R., D. L. Brasaemle, M. McAndrews-Hill, C. Sztalryd, and C. Londos. 2009. Adoption of PERILIPIN as a unifying nomenclature for the mammalian PAT-family of intracellular, lipid storage droplet proteins. *J Lipid Res*.
195. Pfaffl, M. W. 2001. A new mathematical model for relative quantification in real-time RT-PCR. *Nucleic Acids Res* **29**: e45.
196. Pfaffl, M. W., G. W. Horgan, and L. Dempfle. 2002. Relative expression software tool (REST) for group-wise comparison and statistical analysis of relative expression results in real-time PCR. *Nucleic Acids Res* **30**: e36.
197. Folch, J., M. Lees, and G. H. Sloane Stanley. 1957. A simple method for the isolation and purification of total lipides from animal tissues. *J Biol Chem* **226**: 497-509.
198. Bradford, M. M. 1976. A rapid and sensitive method for the quantitation of microgram quantities of protein utilizing the principle of protein-dye binding. *Anal Biochem* **72**: 248-254.
199. Marcinkiewicz, A., D. Gauthier, A. Garcia, and D. L. Brasaemle. 2006. The phosphorylation of serine 492 of perilipin a directs lipid droplet fragmentation and dispersion. *J Biol Chem* **281**: 11901-11909.
200. Listenberger, L. L., A. G. Ostermeyer-Fay, E. B. Goldberg, W. J. Brown, and D. A. Brown. 2007. Adipocyte differentiation-related protein reduces the lipid droplet association of adipose triglyceride lipase and slows triacylglycerol turnover. *J Lipid Res* **48**: 2751-2761.

201. Chang, B. H., L. Li, A. Paul, S. Taniguchi, V. Nannegari, W. C. Heird, and L. Chan. 2006. Protection against fatty liver but normal adipogenesis in mice lacking adipose differentiation-related protein. *Mol Cell Biol* **26**: 1063-1076.
202. Sztalryd, C., M. Bell, X. Lu, P. Mertz, S. Hickenbottom, B. H. Chang, L. Chan, A. R. Kimmel, and C. Londos. 2006. Functional compensation for adipose differentiation-related protein (ADFP) by Tip47 in an ADFP null embryonic cell line. *J Biol Chem* **281**: 34341-34348.
203. Bell, M., H. Wang, H. Chen, J. C. McLenithan, D. W. Gong, R. Z. Yang, D. Yu, S. K. Fried, M. J. Quon, C. Londos, and C. Sztalryd. 2008. Consequences of lipid droplet coat protein downregulation in liver cells: abnormal lipid droplet metabolism and induction of insulin resistance. *Diabetes* **57**: 2037-2045.
204. Brasaemle, D. L., G. Dolios, L. Shapiro, and R. Wang. 2004. Proteomic analysis of proteins associated with lipid droplets of basal and lipolytically stimulated 3T3-L1 adipocytes. *J Biol Chem* **279**: 46835-46842.
205. Persson, J., E. Degerman, J. Nilsson, and M. W. Lindholm. 2007. Perilipin and adipophilin expression in lipid loaded macrophages. *Biochem Biophys Res Commun* **363**: 1020-1026.
206. Bandeira-Melo, C., P. T. Bozza, and P. F. Weller. 2002. The cellular biology of eosinophil eicosanoid formation and function. *J Allergy Clin Immunol* **109**: 393-400.
207. Brasaemle, D. L., D. M. Levin, D. C. Adler-Wailes, and C. Londos. 2000. The lipolytic stimulation of 3T3-L1 adipocytes promotes the translocation of hormone-sensitive lipase to the surfaces of lipid storage droplets. *Biochim Biophys Acta* **1483**: 251-262.
208. Su, C. L., C. Sztalryd, J. A. Contreras, C. Holm, A. R. Kimmel, and C. Londos. 2003. Mutational analysis of the hormone-sensitive lipase translocation reaction in adipocytes. *J Biol Chem* **278**: 43615-43619.
209. Lindqvist, P., A. M. Ostlund-Lindqvist, J. L. Witztum, D. Steinberg, and J. A. Little. 1983. The role of lipoprotein lipase in the metabolism of triglyceride-rich lipoproteins by macrophages. *J Biol Chem* **258**: 9086-9092.
210. Pagler, T. A., S. Rhode, A. Neuhofer, H. Laggner, W. Strobl, C. Hinterndorfer, I. Volf, M. Pavelka, E. R. Eckhardt, D. R. van der Westhuyzen, G. J. Schutz, and H. Stangl. 2006. SR-BI-mediated high density lipoprotein (HDL) endocytosis leads to HDL resecretion facilitating cholesterol efflux. *J Biol Chem* **281**: 11193-11204.
211. Gianturco, S. H., S. A. Brown, D. P. Via, and W. A. Bradley. 1986. The beta-VLDL receptor pathway of murine P388D1 macrophages. *J Lipid Res* **27**: 412-420.
212. MacArthur, J. M., J. R. Bishop, K. I. Stanford, L. Wang, A. Bensadoun, J. L. Witztum, and J. D. Esko. 2007. Liver heparan sulfate proteoglycans mediate clearance of triglyceride-rich lipoproteins independently of LDL receptor family members. *J Clin Invest* **117**: 153-164.
213. Ishibashi, S., N. Mori, T. Murase, H. Shimano, T. Gotohda, M. Kawakami, Y. Akanuma, F. Takaku, and N. Yamada. 1989. Enhanced lipoprotein lipase secretion from human monocyte-derived macrophages caused by hypertriglyceridemic very low density lipoproteins. *Arteriosclerosis* **9**: 650-655.
214. Bates, S. R., P. L. Murphy, Z. C. Feng, T. Kanazawa, and G. S. Getz. 1984. Very low density lipoproteins promote triglyceride accumulation in macrophages. *Arteriosclerosis* **4**: 103-114.
215. Abumrad, N., C. Harmon, and A. Ibrahimi. 1998. Membrane transport of long-chain fatty acids: evidence for a facilitated process. *J Lipid Res* **39**: 2309-2318.
216. Evans, A. J., C. G. Sawyez, B. M. Wolfe, P. W. Connelly, G. F. Maguire, and M. W. Huff. 1993. Evidence that cholesteryl ester and triglyceride accumulation in J774 macrophages induced by very low density lipoprotein subfractions occurs by different mechanisms. *J Lipid Res* **34**: 703-717.
217. Goldberg, I. J., R. H. Eckel, and N. A. Abumrad. 2009. Regulation of fatty acid uptake into tissues: lipoprotein lipase- and CD36-mediated pathways. *J Lipid Res* **50 Suppl**: S86-90.
218. Calder, P. C., J. A. Bond, D. J. Harvey, S. Gordon, and E. A. Newsholme. 1990. Uptake and incorporation of saturated and unsaturated fatty acids into macrophage lipids and their effect upon macrophage adhesion and phagocytosis. *Biochem J* **269**: 807-814.

219. De Pascale, C., M. Avella, J. S. Perona, V. Ruiz-Gutierrez, C. P. Wheeler-Jones, and K. M. Botham. 2006. Fatty acid composition of chylomicron remnant-like particles influences their uptake and induction of lipid accumulation in macrophages. *FEBS J* **273**: 5632-5640.
220. Nagayama, M., T. Uchida, and K. Gohara. 2007. Temporal and spatial variations of lipid droplets during adipocyte division and differentiation. *J Lipid Res* **48**: 9-18.
221. Olofsson, S. O., P. Bostrom, L. Andersson, M. Rutberg, M. Levin, J. Perman, and J. Boren. 2008. Triglyceride containing lipid droplets and lipid droplet-associated proteins. *Curr Opin Lipidol* **19**: 441-447.
222. Bostrom, P., L. Andersson, M. Rutberg, J. Perman, U. Lidberg, B. R. Johansson, J. Fernandez-Rodriguez, J. Ericson, T. Nilsson, J. Boren, and S. O. Olofsson. 2007. SNARE proteins mediate fusion between cytosolic lipid droplets and are implicated in insulin sensitivity. *Nat Cell Biol* **9**: 1286-1293.
223. van Meer, G. 2001. Caveolin, cholesterol, and lipid droplets? *J Cell Biol* **152**: F29-34.
224. Robenek, M. J., N. J. Severs, K. Schlattmann, G. Plenz, K. P. Zimmer, D. Troyer, and H. Robenek. 2004. Lipids partition caveolin-1 from ER membranes into lipid droplets: updating the model of lipid droplet biogenesis. *FASEB J* **18**: 866-868.
225. Saha, P. K., H. Kojima, J. Martinez-Botas, A. L. Sunehag, and L. Chan. 2004. Metabolic adaptations in the absence of perilipin: increased beta-oxidation and decreased hepatic glucose production associated with peripheral insulin resistance but normal glucose tolerance in perilipin-null mice. *J Biol Chem* **279**: 35150-35158.
226. Yamauchi, T., J. Kamon, H. Waki, Y. Imai, N. Shimozawa, K. Hioki, S. Uchida, Y. Ito, K. Takakuwa, J. Matsui, M. Takata, K. Eto, Y. Terauchi, K. Komeda, M. Tsunoda, K. Murakami, Y. Ohnishi, T. Naitoh, K. Yamamura, Y. Ueyama, P. Froguel, S. Kimura, R. Nagai, and T. Kadowaki. 2003. Globular adiponectin protected ob/ob mice from diabetes and ApoE-deficient mice from atherosclerosis. *J Biol Chem* **278**: 2461-2468.
227. Pajvani, U. B., M. Hawkins, T. P. Combs, M. W. Rajala, T. Doebber, J. P. Berger, J. A. Wagner, M. Wu, A. Knopps, A. H. Xiang, K. M. Utzschneider, S. E. Kahn, J. M. Olefsky, T. A. Buchanan, and P. E. Scherer. 2004. Complex distribution, not absolute amount of adiponectin, correlates with thiazolidinedione-mediated improvement in insulin sensitivity. *J Biol Chem* **279**: 12152-12162.
228. Shimomura, I., R. E. Hammer, J. A. Richardson, S. Ikemoto, Y. Bashmakov, J. L. Goldstein, and M. S. Brown. 1998. Insulin resistance and diabetes mellitus in transgenic mice expressing nuclear SREBP-1c in adipose tissue: model for congenital generalized lipodystrophy. *Genes Dev* **12**: 3182-3194.
229. Moitra, J., M. M. Mason, M. Olive, D. Krylov, O. Gavrilova, B. Marcus-Samuels, L. Feigenbaum, E. Lee, T. Aoyama, M. Eckhaus, M. L. Reitman, and C. Vinson. 1998. Life without white fat: a transgenic mouse. *Genes Dev* **12**: 3168-3181.
230. Banerjee, R. R., S. M. Rangwala, J. S. Shapiro, A. S. Rich, B. Rhoades, Y. Qi, J. Wang, M. W. Rajala, A. Pocai, P. E. Scherer, C. M. Steppan, R. S. Ahima, S. Obici, L. Rossetti, and M. A. Lazar. 2004. Regulation of fasted blood glucose by resistin. *Science* **303**: 1195-1198.
231. Straub, B. K., P. Stoeffel, H. Heid, R. Zimbelmann, and P. Schirmacher. 2008. Differential pattern of lipid droplet-associated proteins and de novo perilipin expression in hepatocyte steatogenesis. *Hepatology* **47**: 1936-1946.
232. Imai, Y., G. M. Varela, M. B. Jackson, M. J. Graham, R. M. Crooke, and R. S. Ahima. 2007. Reduction of hepatosteatosis and lipid levels by an adipose differentiation-related protein antisense oligonucleotide. *Gastroenterology* **132**: 1947-1954.
233. Tous, M., N. Ferre, J. Camps, F. Riu, and J. Joven. 2005. Feeding apolipoprotein E-knockout mice with cholesterol and fat enriched diets may be a model of non-alcoholic steatohepatitis. *Mol Cell Biochem* **268**: 53-58.
234. Koteish, A., and A. M. Diehl. 2001. Animal models of steatosis. *Semin Liver Dis* **21**: 89-104.
235. Postic, C., and J. Girard. 2008. Contribution of de novo fatty acid synthesis to hepatic steatosis and insulin resistance: lessons from genetically engineered mice. *J Clin Invest* **118**: 829-838.
236. Getz, G. S., and C. A. Reardon. 2006. Diet and murine atherosclerosis. *Arterioscler Thromb Vasc Biol* **26**: 242-249.

237. Breslow, J. L. 1996. Mouse models of atherosclerosis. *Science* **272**: 685-688.
238. Zhang, S. H., R. L. Reddick, B. Burkey, and N. Maeda. 1994. Diet-induced atherosclerosis in mice heterozygous and homozygous for apolipoprotein E gene disruption. *J Clin Invest* **94**: 937-945.
239. Nakashima, Y., A. S. Plump, E. W. Raines, J. L. Breslow, and R. Ross. 1994. ApoE-deficient mice develop lesions of all phases of atherosclerosis throughout the arterial tree. *Arterioscler Thromb* **14**: 133-140.
240. Davignon, J. 2005. Apolipoprotein E and atherosclerosis: beyond lipid effect. *Arterioscler Thromb Vasc Biol* **25**: 267-269.
241. Maeda, N., L. Johnson, S. Kim, J. Hagaman, M. Friedman, and R. Reddick. 2007. Anatomical differences and atherosclerosis in apolipoprotein E-deficient mice with 129/SvEv and C57BL/6 genetic backgrounds. *Atherosclerosis* **195**: 75-82.

SUPPLEMENTARY

Plasma lipid parameters of all mice used at the end of the WTD

Tab.11: Plasma lipid parameters of 4 hours fasted female mice at the end of WTD feeding.

mouse	gender	Plin	apoE	mgTC/dl	mgFC/dl	mgTG/dl
9669	f	ko	Wt	120,0	39,65	64,3
9670	f	ko	Wt	129,6	38,61	50,4
9671	f	ko	Wt	125,0	38,96	50,9
10615	f	ko	Wt	113,4	32,75	54,7
10617	f	ko	Wt	120,0	39,30	59,0
10632	f	ko	Wt	134,6	44,48	53,8
11924	f	ko	Wt	97,2	38,5	641,0
9673	f	Wt	ko	785,8	462,01	215,2
9683	f	Wt	ko	817,9	530,33	293,0
10608	f	Wt	ko	853,5	581,40	318,3
11444	f	Wt	ko	343,9	125,2	2086,2
11913	f	ko	ko	324,6	110,7	1845,4
11916	f	ko	ko	361,3	126,1	2101,8
11922	f	ko	ko	356,4	126,1	2101,8
11926	f	ko	ko	468,2	138,2	2303,8
11934	f	ko	ko	501,0	148,5	2474,7
11935	f	ko	ko	501,0	162,9	2715,6
13589	f	ko	ko	255,4	83,0	76,0
13618	f	ko	ko	396,9	120,8	69,0
13606	f	ko	ko	267,9	79,4	102,5
13584	f	ko	ko	150,8	68,0	51,8

Tab.12: Plasma lipid parameters of overnight fasted female mice at the end of WTD feeding.

mouse	**gender**	**Plin**	apoE	**mgTC/dl**	**mgFC/dl**	**mgTG/dl**
9669	f	ko	Wt	83,3	23,95	31,2
9670	f	ko	Wt	98,2	25,67	12,0
9671	f	ko	Wt	108,7	32,92	43,0
10615	f	ko	Wt	87,7	26,02	29,7
10617	f	ko	Wt	81,6	21,19	23,8
10632	f	ko	Wt	95,4	25,67	16,9
11924	f	ko	Wt	61,1	27,1	15,0
9673	f	Wt	ko	771,3	360,04	176,7
9683	f	Wt	ko	753,6	444,58	222,4
10608	f	Wt	ko	780,2	410,42	172,3
11444	f	Wt	ko	396,1	171,0	22,1
11913	f	ko	ko	861,5	307,6	33,5
11916	f	ko	ko	704,7	205,7	13,8
11922	f	ko	ko	695,4	335,0	166,8
11926	f	ko	ko	908,9	427,5	222,7
11934	f	ko	ko	858,7	453,2	176,9
11935	f	ko	ko	902,8	463,5	185,8
13589	f	ko	ko	849,2	312,0	106,6
13606	f	ko	ko	913,3	432,7	235,1
13584	f	ko	ko	738,7	425,8	173,6

Tab.13: Plasma lipid parameters of 4 hours fasted male mice at the end of WTD feeding.

mouse	gender	Plin	apoE	mgTC/dl	mgFC/dl	mgTG/dl
10607	m	ko	Wt	176,4	57,25	75,7
10624	m	ko	Wt	165,2	52,07	46,6
11432	m	ko	Wt	78,8	35,7	594,4
11449	m	ko	Wt	97,2	45,0	749,8
11918	m	ko	Wt	116,4	42,2	703,2
11946	m	ko	Wt	96,7	44,1	734,3
11953	m	ko	Wt	119,3	43,6	726,5
10606	m	Wt	ko	773,9	368,84	131,6
11427	m	Wt	ko	403,7	149,4	2490,3
11430	m	Wt	ko	457,2	175,5	2925,4
11446	m	Wt	ko	276,0	123,8	2062,9
11955	m	Wt	ko	295,7	114,9	1915,3
11455	m	ko	ko	357,4	149,0	2482,5
11910	m	ko	ko	302,9	121,0	2016,3
11941	m	ko	ko	306,8	138,2	2303,8
11956	m	ko	ko	255,7	102,8	1713,3
13577	m	ko	ko	193,8	74,8	42,5

Tab.14: Plasma lipid parameters of overnight fasted male mice at the end of WTD feeding.

mouse	**gender**	**Plin**	apoE	**mgTC/dl**	**mgFC/dl**	**mgTG/dl**
10607	m	ko	Wt	165,2	49,48	90,7
10624	m	ko	Wt	128,9	37,75	44,0
11432	m	ko	Wt	57,8	32,2	60,2
11449	m	ko	Wt	70,8	33,5	52,5
11918	m	ko	Wt	73,6	35,2	32,9
11946	m	ko	Wt	79,2	35,2	15,6
11953	m	ko	Wt	78,2	35,6	31,1
10606	m	Wt	ko	733,4	240,99	85,7
11427	m	Wt	ko	823,0	213,8	25,7
11430	m	Wt	ko	407,2	117,4	18,0
11446	m	Wt	ko	419,3	127,7	27,5
11955	m	Wt	ko	637,9	256,2	80,5
11455	m	ko	ko	866,6	329,9	53,1
11910	m	ko	ko	790,1	215,5	28,7
11941	m	ko	ko	726,0	209,1	32,3
11956	m	ko	ko	835,5	315,3	126,3
13577	m	ko	ko	580,5	306,1	75,4

H&E stained liver sections of the lobus dextra of male and female wild type and Plin (-/-) mice after 6 month WTD

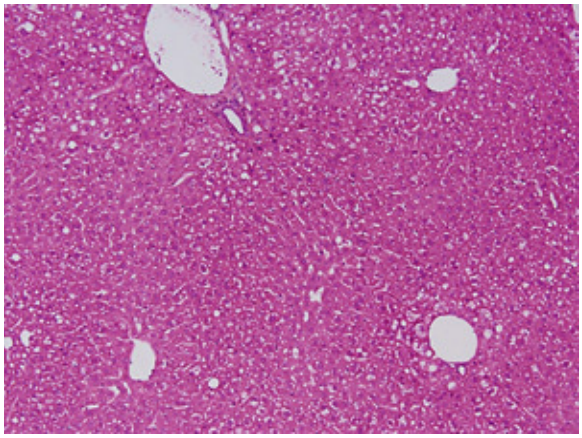

58 Wt m

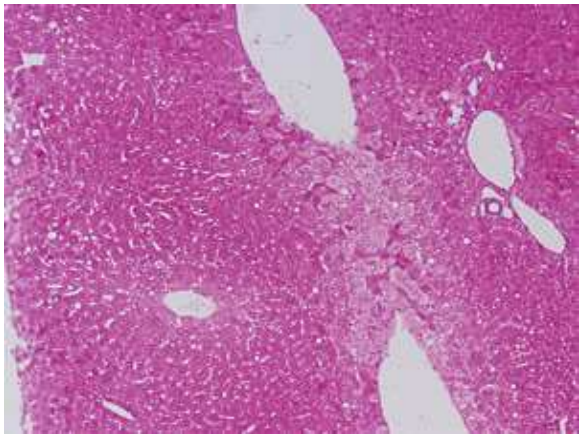

120 Wt m

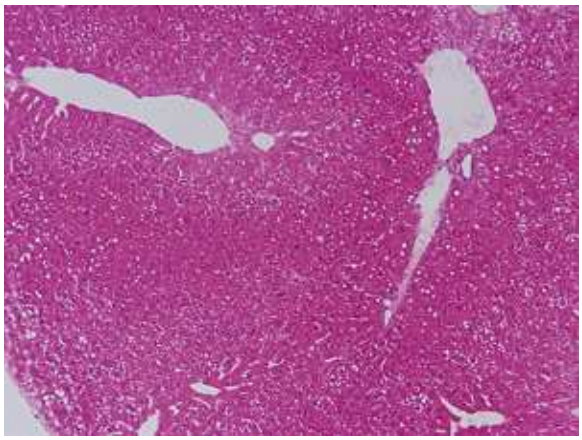

A Wt m

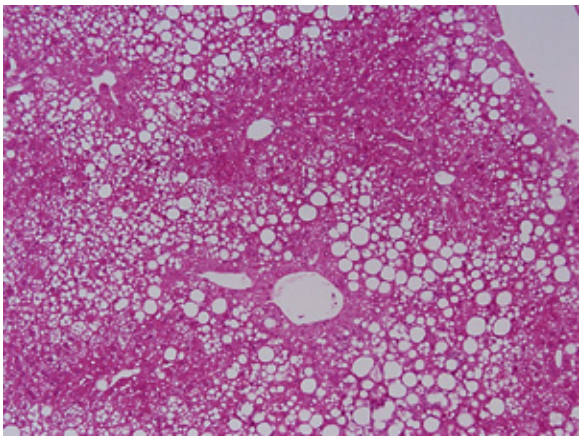

B Wt m

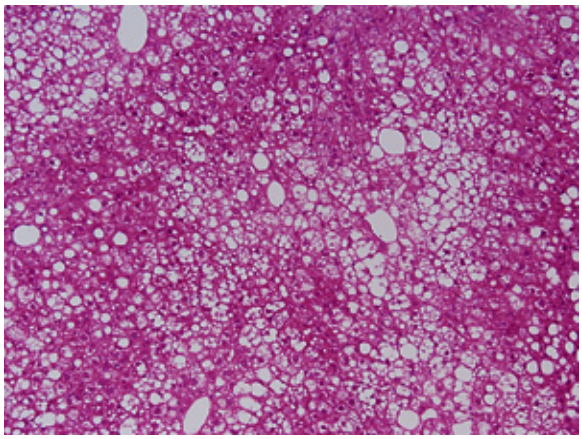

118 Plin (-/-) m

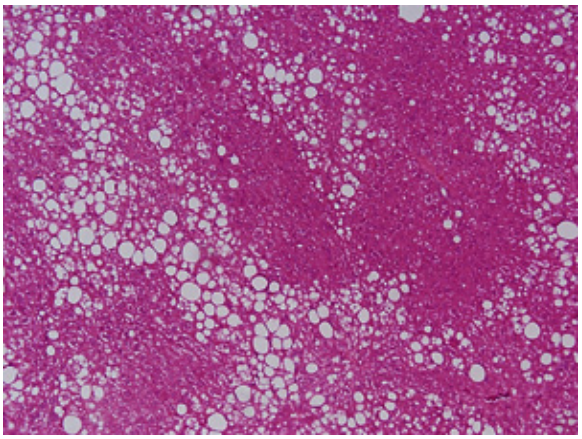

123 Plin (-/-) m

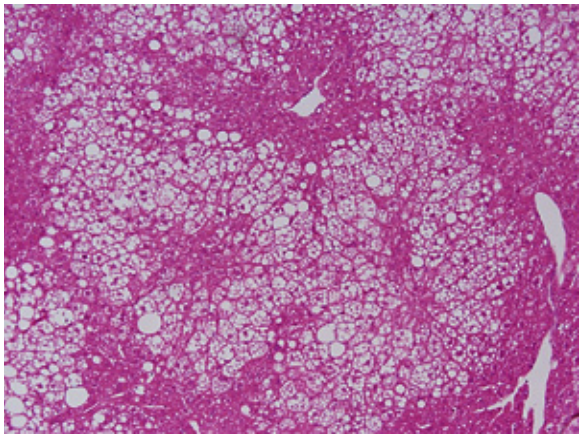

130 Plin (-/-) m

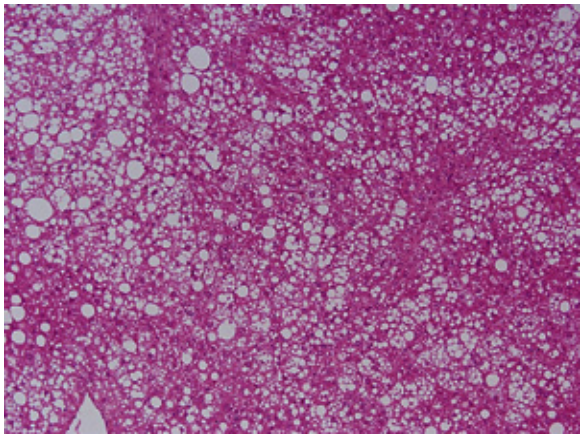

135 Plin (-/-) m

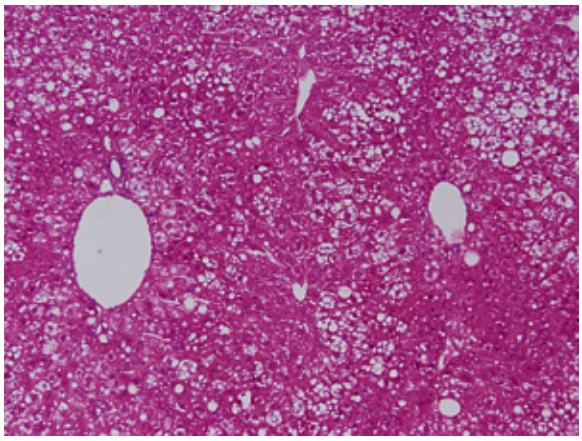

136 Plin (-/-) m

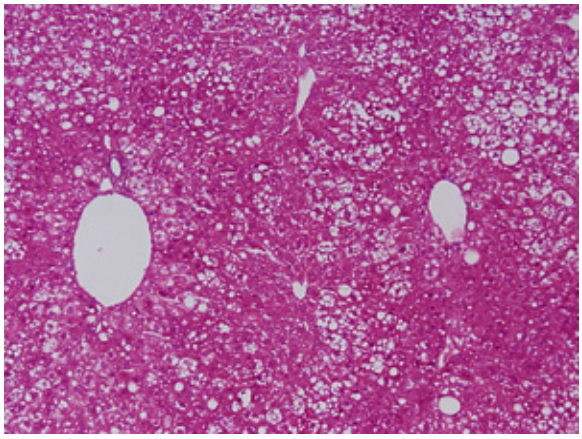

57 Wt f

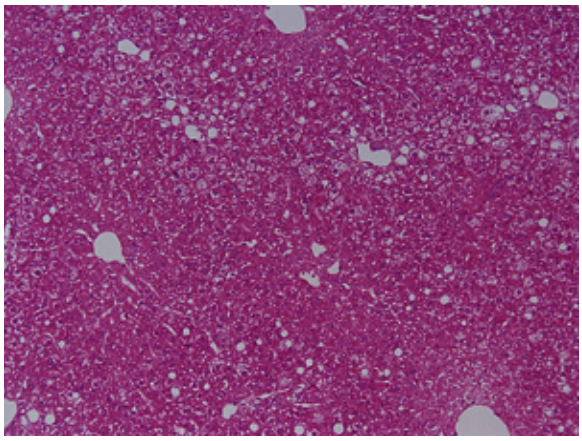

101 Plin (-/-) f

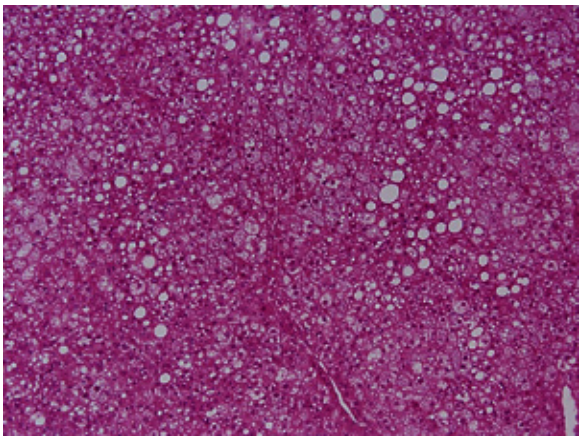

103 Plin (-/-) f

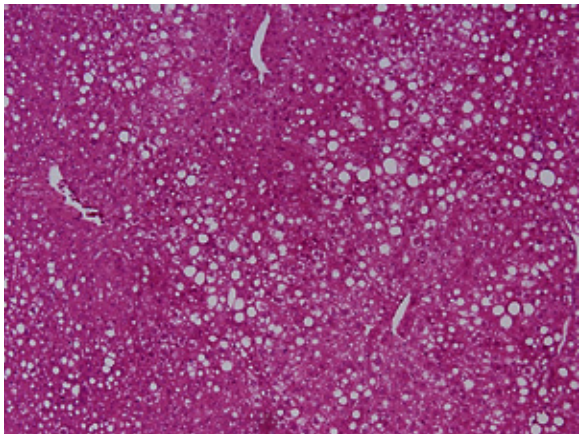

114 Plin (-/-) f

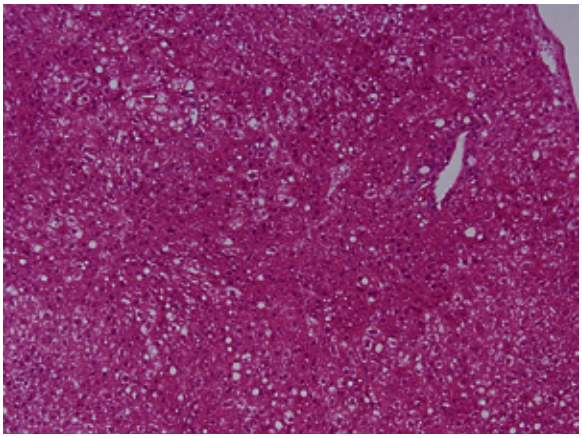

115 Plin (-/-) f

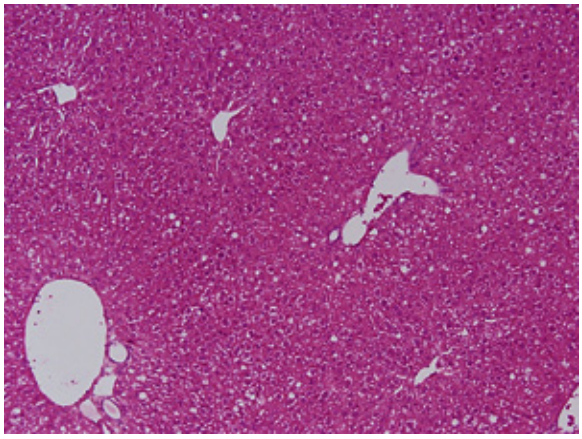

166 Plin (-/-) f